



<https://theses.gla.ac.uk/>

Theses Digitisation:

<https://www.gla.ac.uk/myglasgow/research/enlighten/theses/digitisation/>

This is a digitised version of the original print thesis.

Copyright and moral rights for this work are retained by the author

A copy can be downloaded for personal non-commercial research or study,  
without prior permission or charge

This work cannot be reproduced or quoted extensively from without first  
obtaining permission in writing from the author

The content must not be changed in any way or sold commercially in any  
format or medium without the formal permission of the author

When referring to this work, full bibliographic details including the author,  
title, awarding institution and date of the thesis must be given

Enlighten: Theses

<https://theses.gla.ac.uk/>  
[research-enlighten@glasgow.ac.uk](mailto:research-enlighten@glasgow.ac.uk)

**STRONG INTERACTIONS UP TO MEDIUM ENERGIES**

**by**

**Archibald W. Hendry**

**DEPARTMENT OF NATURAL PHILOSOPHY**

**UNIVERSITY OF GLASGOW**

**Presented to the University of Glasgow, January, 1962,  
as a Thesis for the Degree of Doctor of Philosophy.**

ProQuest Number: 10656294

All rights reserved

INFORMATION TO ALL USERS

The quality of this reproduction is dependent upon the quality of the copy submitted.

In the unlikely event that the author did not send a complete manuscript and there are missing pages, these will be noted. Also, if material had to be removed, a note will indicate the deletion.



ProQuest 10656294

Published by ProQuest LLC (2017). Copyright of the Dissertation is held by the Author.

All rights reserved.

This work is protected against unauthorized copying under Title 17, United States Code  
Microform Edition © ProQuest LLC.

ProQuest LLC.  
789 East Eisenhower Parkway  
P.O. Box 1346  
Ann Arbor, MI 48106 – 1346

CHAPTER I - INTRODUCTION

1

- 1. Single dispersion relations 4
- 2. The Mandelstam representation 12
- 3. Outline of calculations 26

CHAPTER II - PION-NUCLEON SCATTERING

34

- 1. Kinematics 34
- 2. The Mandelstam representation; analytic properties 40
- 3. The single nucleon term 47
- 4. The crossed-physical cut 51
- 5. The  $\pi\pi$  cut 56
- 6. Results 67

CHAPTER III - THE  $\pi + N^*$  CHANNEL

73

- 1. Kinematics 73
- 2. Analytic properties 80
- 3. Partial-wave amplitude 85
- 4. Results 89

	<u>Page</u>
<u>CHAPTER IV - PION PHOTOPRODUCTION</u>	
1. Kinematics	92
2. The Mandelstam representation; analytic properties	101
3. The single nucleon terms	106
4. The crossed-physical photoproduction cut	108
5. The $\Upsilon\pi$ cut	114
6. Results	120

CHAPTER V - DISCUSSION OF RESULTS 128

ACKNOWLEDGMENTS 131

APPENDICES

Appendix A - Useful integrals	132
Appendix B - On the analyticity of partial wave amplitudes for unstable particles in perturbation theory	133
Appendix C - Validity of Legendre polynomial expansions	152

REFERENCES

## CHAPTER I - INTRODUCTION

There is little doubt that, in recent years, the study of dispersion relations has led to a greater understanding of the fundamentals of strong interactions. Since Yukawa's first proposals<sup>1)</sup> for a meson theory, a large variety of methods has certainly been devised to investigate the basic properties of nuclear matter. At present, the dispersion relations approach seems to be very promising, and indeed there is every hope that many of the existing problems of meson physics will be solved in the near future.

Originally, it was thought that most of the answers would be provided by quantum field theory<sup>2),3)</sup>. This theory was found to be extremely successful in describing reactions which involved photons and electrons. The usual procedure was to make expansions in terms of the small photon-electron coupling parameter  $e^2 \approx \frac{1}{137}$ . After removing various divergences by renormalisation, one could in principle calculate quantities to any degree of accuracy required; excellent agreement was obtained with experiment. However, these perturbation methods are completely unsuitable in meson physics: the corresponding coupling constant  $g^2$  has the comparatively large value of 15, with the result that successive terms in the power

series expansions rapidly increase.

In order to circumvent these difficulties, Chew and Low<sup>4)</sup> proposed a simplified model for pion-nucleon scattering. Still working within the framework of field theory, they took the interaction as

$$f_{\pi} \psi^{\dagger} [\underline{\sigma} \cdot \underline{\nabla} (\underline{\tau} \cdot \underline{\phi})] \psi \quad (I.1)$$

where  $\phi$ ,  $\psi$  represent the pion and nucleon fields respectively,  $\underline{\sigma}$  is the Pauli spin matrix, and  $\underline{\tau}$  an operator describing the charge state of the pion.

$f_{\pi}$  is directly related to the more well-known coupling constant  $g_{\pi}$  of the charge-independent, pseudoscalar Kemmer interaction by  $f_{\pi} = \frac{1}{2N} g_{\pi}$ , where  $N$  is the nucleon mass. The low-energy P-wave scattering phase shifts were then calculated, and they were in fact found to be in qualitative agreement with the corresponding experimental values. However, there were two serious objections about the Chew-Low model: the problem was treated non-relativistically (nucleon recoil being neglected completely), and also the use of (I.1) automatically eliminates all anti-nucleon states (which should occur in any complete theory). Divergencies arose in their theory, and it was therefore necessary to

introduce an arbitrary cut-off function to exclude Virtual pions of too high a frequency. As a result of these defects, the state of pion physics continued to remain rather unsatisfactory.

It was about this time that attention was first being drawn to the possibility of investigating strong interactions by using dispersion relation techniques. These do not depend on any power series expansions, but on the analytic properties of the S-matrix elements themselves. At their foundation lies the integral theorem of Cauchy, which allows one to represent a function  $f$  of a complex variable  $z$  as an integral over a simple closed contour  $C$ : if  $f$  is an analytic function in a domain  $D_+$  containing  $C$  and its interior  $D$ , then

$$f(z) = \frac{1}{2\pi i} \int_C \frac{f(z') dz'}{(z' - z)} \quad (I.2)$$

if  $z$  lies in  $D$ . Taking separately the real and imaginary parts of (I.2), we obtain integral relations between  $\text{Re } f$  and  $\text{Im } f$ ; "dispersion relations" are relations just of this type.

We shall now proceed to describe some of the early history of dispersion relations, and trace their rapid development in recent times.

1. Single Dispersion Relations.

The first works of note on dispersion relations were carried out in 1926-27 by Kronig<sup>5)</sup> and Kramers<sup>6)</sup> in their researches dealing with the classical dispersion of light. In particular, the latter showed that a dispersion relation between the real and imaginary parts of the index of refraction (regarded as a function of the frequency  $\omega$ , now allowed to become complex) followed from the requirement that the refractive index was an analytic function in the upper-half  $\omega$ -plane (Cauchy's theorem); and that, for a medium described by such a refractive index, signals could not propagate faster than light. Kramers thus made the vital discovery that dispersion relations were based on the fundamental concept of causality.

Unfortunately, interest in the subject declined for many years until, in 1946, Kronig<sup>7)</sup> suggested that the form of the S-matrix for elementary particle processes might be restricted by causality. Subsequently, many investigations<sup>8)</sup> were carried out to determine general properties of the S-matrix. Dispersion relations also began to be re-applied to problems in electro-dynamics, such as<sup>9)</sup> relating forward scattering of light by a

nuclear Coulomb field to pair production of photons in the same Coulomb field.

A striking advance was made in 1954 by Gell-Mann, Goldberger and Thirring<sup>10)</sup>, who were the first to derive dispersion relations within the formalism of quantum field theory. They considered the forward scattering of light. At the basis of their treatment was a new form of the causality condition: the commutator of two Heisenberg field operators, taken at different space-time points, vanishes if the separation between these points is space-like. This is now known as the principle of "microscopic causality."

Goldberger<sup>11)</sup> later extended these investigations to the case of forward scattering of particles with mass. In doing so, he made use of an important general reduction formula of Lehmann, Symanzik and Zimmermann<sup>12)</sup>. This formula enables one to write the amplitude for an arbitrary transition in terms of the Fourier transform ( $F(q)$ , say) of a matrix element of a commutator of two Heisenberg field operators ( $j, h$  say):

$$F(q) = \int d^4x e^{iqx} \langle p, \alpha | [j(\frac{x}{\lambda}), h(-\frac{x}{\lambda})] | q, \beta \rangle. \quad (1.3)$$

Here the matrix element connects two physical states with

4-momenta  $P, Q$  respectively; the indices  $\alpha, \beta$  specify the other parameters of these states. In (I.3), the energy variable occurs only in the factor  $e^{iqx}$ . The vanishing of the commutator outside the light cone allows one to extend the energy dependence into the complex plane, and a dispersion relation immediately follows.

There were also several interesting applications of these dispersion relations; for example, they were used to distinguish between different sets of phase shifts<sup>13)</sup>, and to deduce a value for the pion-nucleon coupling constant<sup>14)</sup>. Comparison between theory and experiment was facilitated by employing the "optical theorem", which relates the imaginary part of the forward scattering amplitude to the total cross-section:

$$\text{Im } f = \frac{q}{4\pi} \sigma \quad , \quad (\text{I.4})$$

where  $q$  is the magnitude of the centre of mass momentum. Obviously the dispersion integrals may be evaluated from (I.4), provided that the experimental cross-sections are known. It is a significant point that the proof of (I.4) is based on another fundamental property of the S-matrix, its unitarity.

The next development was the generalisation to non-

forward scattering. Many heuristic derivations<sup>15)</sup> were presented, all of them leading to single dispersion relations in the energy variable, the momentum transfer being held fixed. Almost simultaneously, there was a large number of papers investigating the elementary problems of nuclear physics: pion-nucleon scattering<sup>16)</sup>, pion photoproduction<sup>17)</sup>, nucleon-nucleon scattering<sup>18)</sup>, electro-magnetic form factors of nucleons<sup>19)</sup>, K-meson-nucleon scattering<sup>20)</sup>, and decay processes<sup>21)</sup> involving strong as well as weak interactions. Much work was also done for non-relativistic cases<sup>22)</sup>, such as the scattering of a particle by a fixed potential. Each of these subjects is fascinating in itself. However, we shall discuss here only two topics in slightly greater detail: they have been chosen because of their practical consequences for applying the theory to experiment.

The first is sometimes called "poleology", as it concerns the analytic properties of the scattering amplitude  $f$ .  $f$  may be regarded as a function of the two variables  $W$  (the centre of mass energy) and  $Z = \cos \theta$  ( $\theta$  being the scattering angle). Chew<sup>23)</sup> has shown that, for many processes,  $f$  has a real pole in the complex  $z$ -plane at  $z = z_0$ , lying just outside the

physical interval  $-1 \leq z \leq +1$ ; it corresponds to the lowest order perturbation diagram in which a particle is exchanged. Further, the residue at the pole is proportional to the coupling constants involved in the reaction. Obviously, by considering the function

$$(z - z_0)^2 \frac{d\sigma}{d\Omega} \quad \text{for any particular value of the energy } W,$$

and extrapolating outside the physical region to the point  $z = z_0$ , we might be able to determine information about the nature and strength of the interactions taking place in the reaction. This procedure has been carried out for neutron-proton scattering by Cziffra and Moravcsik<sup>24)</sup>, who extrapolated to the "backward" pion pole (at  $z = -1 - \mu^2/2q^2$ ), obtaining a value of the pion-nucleon coupling constant  $g^2$  in reasonable agreement with other estimations. Similar calculations have been considered for pion photoproduction<sup>25)</sup> and K-meson-nucleon scattering<sup>20)</sup>. In the latter case, there were hopes of determining the parity of the K-meson from the sign of the residue; unfortunately, it was impossible to do so due to a lack of experimental data.

The other topic on which we wish to remark at this point is the excellent treatment of pion-nucleon scattering and pion photoproduction by Chew, Goldberger,

Low and Nambu<sup>16),17)</sup>. This formed a considerable improvement on the Chew-Low static nucleon model, because it embodied all of the general principles which any correct theory must have; analytic properties, unitarity, crossing symmetry and the appropriate isotopic spin considerations, as well as Lorentz covariance. Dispersion relations were written down for the invariant amplitudes involved, and the S-, P- and D- partial wave amplitudes projected out. In order to evaluate the dispersion integrals, it was assumed that the integrands were dominated by the  $(\frac{3}{2}, \frac{3}{2})$  pion-nucleon resonance, which seemed very justifiable from the experimental cross-sections. All of the expressions involved were expanded in powers of  $\frac{1}{N}$ , terms up to first order being retained. Chew et al. obtained reasonable agreement with experiment for the P-waves for energies up to the first resonance, but were unable to calculate from their theory the position of the  $(\frac{3}{2}, \frac{3}{2})$  resonance, or the S-wave scattering lengths as they had hoped. However their investigations marked a decided achievement in dispersion theory, and much subsequent work has been dependent on it.

At the same time as all of the dispersion relations

already mentioned in this section were being developed, rigorous proofs were being derived in order to set the theory on a more sound theoretical foundation.

Symanzik<sup>26)</sup> gave the first proof for forward scattering.

Bogoliubov et al.<sup>27)</sup> demonstrated that similar steps could

be carried out for pion-nucleon scattering at a finite angle provided that  $\mu^2$ , the pion mass squared, was taken

sufficiently negative. After a great deal of involved mathematics, they were then able to carry out a

continuation in the auxiliary mass variable up to the real physical value of  $\mu^2$ . However, this method was

soon superseded by the work of Dremermann, Oehme and Taylor<sup>28)</sup> who made use of functions of several complex

variables. The least complicated proof to date is that of Lehmann<sup>29)</sup>, who used Dyson's integral representation<sup>30)</sup>

for the commutator of two Heisenberg fields. Dyson proved that  $F(q)$ , given by (I.3), could be represented in the form

$$F(q) = \int d^4u \int_0^\infty d\kappa^2 \varepsilon(q_0 - u_0) \delta[(q-u)^2 - \kappa^2] \phi(u, \kappa^2). \quad (\text{I.5})$$

Lehmann also deduced that, for fixed energy, the scattering amplitude and its imaginary part were analytic in certain elliptical areas in the complex

momentum transfer plane.

All of these proofs concerned dispersion relations in the energy variable, with the momentum transfer fixed. Apart from being very cumbersome, they were also rather limited, and showed that the dispersion relations were valid provided that the momentum transfer was less than some maximum, and that certain inequalities on the masses of the particles were satisfied.

The next step of great historic importance was made in 1958 by Mandelstam<sup>31)</sup>. Single dispersion relations are obviously restrictive, since one independent variable, usually the momentum transfer, is held fixed in them. They do not give all the singularities of the S-matrix; to do so requires a knowledge of analyticity with respect to the two independent variables. Mandelstam's prescription for extending the energy and momentum transfer variables simultaneously into the complex plane has completely revolutionised modern thinking about the theory of elementary particles.

2. The Mandelstam Representation

Let us consider a reaction involving four particles, two of which are incoming and two outgoing. This is shown in Figure 1, where  $p_1, \dots, p_4$  are the four-momenta

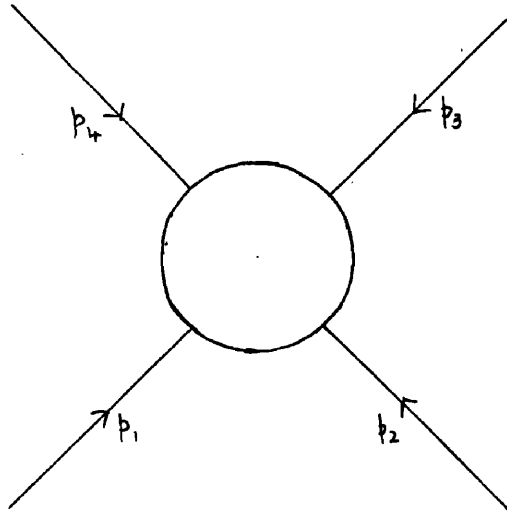


Figure 1

of the particles, all of which are represented as incoming. Obviously there are three distinct ways of taking the reaction. For example, in the system consisting of two nucleons and two pions, the various reactions are  $\pi + N \leftrightarrow \pi + N$ ,  $\pi + N \leftrightarrow \pi + N$  (with the pions interchanged), and  $\pi + \pi \leftrightarrow N + \bar{N}$ .

Energy-momentum conservation gives

$$p_1 + p_2 + p_3 + p_4 = 0$$

It is convenient to introduce three invariants  $s_1, s_2, s_3$

defined by

$$\begin{aligned} s_1 &= (p_4 + p_1)^2 \\ s_2 &= (p_4 + p_2)^2 \\ s_3 &= (p_4 + p_3)^2 \end{aligned} \tag{I.6}$$

Each of them corresponds to the square of the total energy in the barycentric system for the different possible pairings of the particles in Figure 1. They are not linearly independent, but are connected by the equation

$$s_1 + s_2 + s_3 = m_1^2 + m_2^2 + m_3^2 + m_4^2, \tag{I.7}$$

where  $m_i$  ( $i = 1, \dots, 4$ ) are the masses of the particles and are given by  $p_i^2 = m_i^2$ . Only two scalars are needed to specify a four-particle reaction; these may be taken as any two of the invariants  $s_1, s_2, s_3$ . In relativistic dispersion treatments, it is necessary to extend these three variables throughout the whole of the complex plane.

It is a general feature of scattering reactions in elementary particle physics that, after separating off charge and spin dependence, any process can be described by a set of invariant amplitudes  $A^{(i)}$ , say. These

amplitudes are of course functions of  $s_1, s_2, s_3$  (only two of which are independent). Moreover, one can also invoke the substitution law<sup>3)</sup>, which provides the information that all of the three reactions in Figure 1 (of the two-particle type being discussed) can be described by exactly the same set of invariant amplitudes  $A^{(i)}$ . The physical amplitudes for any particular process are the boundary values of the analytic functions  $A^{(i)}$  when the variables  $s_1, s_2, s_3$  approach their physical values for that process. One can further show that the physical regions for the three reactions of Figure 1 are non-overlapping.

The substitution law is obviously very powerful and is of the utmost importance in dispersion relations. It was first discovered in quantum field theory. When there are two or more of the interacting particles identical, the substitution law reduces to "crossing symmetry". Interchanging two like particles leaves the sign of any amplitude unaltered or else changes the sign, depending on whether the particles are bosons or fermions; it also interchanges two of the  $s_i$  variables leaving the third one alone. Obviously if the two like particles occur together in the initial or final state, crossing

symmetry merely corresponds to the Pauli principle.

Mandelstam was the first to propose a general representation for the invariant amplitudes. A typical amplitude may be denoted by  $A(s_1, s_2, s_3)$  where all three variables have been exhibited explicitly. The Mandelstam representation expresses  $A$  in the form:

$$\begin{aligned}
 A(s_1, s_2, s_3) = & \frac{1}{\pi} \int ds'_1 \frac{\rho_1(s'_1)}{(s'_1 - s_1)} + \frac{1}{\pi} \int ds'_2 \frac{\rho_2(s'_2)}{(s'_2 - s_2)} + \frac{1}{\pi} \int ds'_3 \frac{\rho_3(s'_3)}{(s'_3 - s_3)} \\
 & + \frac{1}{\pi^2} \iint ds'_1 ds'_2 \frac{\rho_{12}(s'_1, s'_2)}{(s'_1 - s_1)(s'_2 - s_2)} + \frac{1}{\pi^2} \iint ds'_1 ds'_3 \frac{\rho_{13}(s'_1, s'_3)}{(s'_1 - s_1)(s'_3 - s_3)} \\
 & + \frac{1}{\pi^2} \iint ds'_2 ds'_3 \frac{\rho_{23}(s'_2, s'_3)}{(s'_2 - s_2)(s'_3 - s_3)} \quad (I.8)
 \end{aligned}$$

All the spectral functions  $\rho_i$ ,  $\rho_{ij}$  are real, and the integrations are over the areas in which the spectral functions do not vanish. The boundaries of these areas can be evaluated for any particular reaction, and a general procedure for doing so has also been given by Mandelstam. If the integrals in (I.8) are not sufficiently convergent, they may be made so by the standard method of "subtractions".

One can easily reduce (I.8) to single dispersion relation form. For example, for fixed  $s_3$ ,  $A$  may be

expressed as

$$s_2 = \sum m_i^2 - s_1 - s_3$$

$$A(s_1, s_2, s_3) = \frac{1}{\pi} \int ds'_3 \frac{\rho_3(s'_3)}{(s'_3 - s_3)} + \frac{1}{\pi} \int ds'_1 \frac{A_1(s'_1, s'_2, s_3)}{(s'_1 - s_1)} + \frac{1}{\pi} \int ds'_2 \frac{A_2(s_1, s'_2, s_3)}{(s'_2 - s_2)}, \quad (I.9)$$

where

$$A_1(s_1, s_2, s_3) = \rho_1(s_1) + \frac{1}{\pi} \int ds'_2 \frac{\rho_{12}(s_1, s'_2)}{(s'_2 - s_2)} + \frac{1}{\pi} \int ds'_3 \frac{\rho_{13}(s_1, s'_3)}{(s'_3 - s_3)}, \quad (I.10)$$

with a similar formula for  $A_2$  involving  $\rho_2$ ,  $\rho_{12}$  and  $\rho_{23}$ .

It may be deduced that  $A_1$  is the imaginary part of the amplitude  $A$  when the variables take values in the physical region for the reaction in Figure 1 in which  $s_1$  is the square of the barycentric energy. Outside this region,  $A_1$  becomes complex; (I.10) then constitutes an analytic continuation for  $A_1$ . In general,  $A_1$  is called the absorptive part. Corresponding statements hold for  $A_2$ .

The analytic properties of  $A(s_1, s_2, s_3)$  can be directly deduced from (I.9) and (I.10). Singularities (poles and branch cuts) occur for the vanishing of the various denominators. Chew<sup>32)</sup> has given a physical interpretation of these singularities, and draws an analogy to the problem of finding the Coulomb potential due to point charges and line charges.

The positions of the singularities are determined

by the denominators and the possible energy states. Singularities close to the physical region of the variables are associated with one- and two-particle states, and correspond to "long-range forces"; these will control collisions with high angular momenta. Distant singularities, however, give rise to short-range forces, and are related to multi-particle states. Unfortunately, it is impossible at present to deal with these complicated states; they form a great stumbling block to calculations with the Mandelstam representation.

Also in Chew's picture, the weighting functions  $A_1$  etc. are equivalent to the "strengths" of the "forces", and may be evaluated by using the unitarity condition for the S-matrix. Writing  $S = 1 + 2i T$ , we find that the unitarity of the S-matrix leads to

$$\text{Im} T = T^\dagger T.$$

The invariant amplitude  $A$  is proportional to  $T$ , so that

$$\begin{aligned} A_1(s_1, s_2, s_3) &\propto \text{Im} \langle f | T | i \rangle \\ &\propto \sum_n \langle n | T | f \rangle^\dagger \langle n | T | i \rangle, \end{aligned} \tag{I.11}$$

where the  $|n\rangle$  form a complete set of quantum mechanical

states. Thus in calculating absorptive parts, one soon runs into trouble again with multi-particle states.

When Mandelstam first proposed his two-dimensional representation, it was hoped that, together with unitarity, it would form a framework for complete calculations involving a minimum number of empirical parameters.

The Mandelstam representation could therefore be regarded as the basic postulate of a new theory. Any problem should be capable of solution by starting from it and using only such other general concepts as unitarity and symmetry principles. However, this ideal situation has not so far been achieved in practice. One of the main difficulties is the lack of knowledge about the spectral functions, and in fact, most of the investigations on double dispersion relations have involved only those parts which can be calculated from other simple considerations. There also seems some doubt about the number of basic constants necessary for a complete theory. Further, a generalisation of Mandelstam's ideas is required to handle multi-particle states.

Most of the elementary problems of nuclear physics have been reattacked by means of the Mandelstam representation with renewed vigour, and a vast number of

papers has been published. The general policy is to evaluate as much as can be handled, making use of any helpful experimental information (such as dominant states and resonances), and then to compare with experiment. In this way, many interesting facts have been discovered, as well as gaining much insight into the various problems. It is to be hoped that some day these problems will all be solved by a complete, consistent dynamical theory.

The most fundamental problem is that of pion-pion scattering, and a considerable amount of work has recently been devoted to it. The general formalism has been set up by Chew and Mandelstam<sup>33)</sup> for partial wave amplitudes and only two-pion intermediate states. The singularities in the  $\nu = q^2$  plane ( $q$  being the barycentric momentum) can easily be deduced from the double dispersion relations; they lie on the real  $\nu$ -axis for  $0 \leq \nu \leq \infty$  and  $-\infty \leq \nu \leq -4\mu^2$ . It is also possible to relate the discontinuity across the left-hand cut in terms of that on the right from crossing. As a method of solution, Chew and Mandelstam suggested expressing the partial wave amplitude  $A_\ell$  as  $N_\ell/D_\ell$ , where the numerator function  $N_\ell$  contains the left-hand cut, and

the denominator function the right-hand cut. In this way, they were able to obtain a set of coupled integral equations for the  $N_e$  and  $D_e$ . There is only one parameter  $\lambda$  involved, and this may be interpreted as the  $\pi\pi$  coupling constant; possible values of  $\lambda$  are limited by the condition that there is no  $\pi\pi$  bound state.

Calculations<sup>34)</sup> were carried out with the S- and P-waves being the dominant states. A resonance was obtained for the S-wave in the isotopic  $I = 0$  state at low energies. However for the P-wave, the integral equations became divergent, and to obtain a self-consistent solution, a cut-off (corresponding to a new parameter) had to be introduced.

Cini and Fubini<sup>35)</sup> have also obtained the Chew-Mandelstam equations by using a power series approximation in the double spectral integrals:

$$\iint ds'_1 ds'_2 \frac{\beta_{12}(s'_1, s'_2)}{(s'_1 - s_1)(s'_2 - s_2)} \approx \int ds'_1 \frac{a_0(s'_1)}{(s'_1 - s_1)} + \int ds'_2 \frac{b_0(s'_2)}{(s'_2 - s_2)} \quad (\text{I.12})$$

$$+ s_2 \int ds'_1 \frac{a_1(s'_1)}{(s'_1 - s_1)} + s_1 \int ds'_2 \frac{b_1(s'_2)}{(s'_2 - s_2)} + \dots,$$

keeping as many terms in the expansion as are needed to represent large phase shifts. The advantage of this

method is that the necessary approximations are made at the beginning in a clear-cut manner. The theory is approximately valid at low energies, but for high energies its asymptotic behaviour is inconsistent with unitarity.

Another attack on the  $\pi\pi$  scattering problem was carried out by Bransden and Moffat<sup>36)</sup> using the inverse partial wave amplitudes. The resulting coupled integral equations are more amenable to numerical calculation, and these authors obtained both S- and P-wave low energy resonances, the positions and widths being determined entirely by  $\lambda$ . This result is certainly what might be expected from general considerations<sup>37)</sup>, but many objections have been raised about a method involving inverse amplitudes.

More recently, Chew and Frautschi<sup>38)</sup> have suggested a means of calculating the fringes of the double spectral functions; these regions are likely to control the physical elastic scattering amplitude for arbitrarily high energies at small momentum transfers. This "strip approximation" might well be a step in the right direction. Obviously the evaluation of the spectral functions is of vital importance to the success of a complete theory.

In the meantime, many calculations have been made

to find the effect of a  $\pi\pi$  interaction on various processes. One of the first was the work of Frazer and Fulco<sup>39)</sup>. Making use of their dispersion treatment for  $\pi + \pi \rightarrow N + \bar{N}$ , they were able to obtain reasonable agreement with the experimental data on the electromagnetic isovector form factors of the nucleon, on the assumption that the  $\pi\pi$  interaction was dominated by a resonance in the  $I = 1, J = 1$  state at an energy  $t_R \approx 11.5 \mu^2$ .

The pion-nucleon scattering problem has also been tackled by Frazer and Fulco<sup>40)</sup>, and separately by Frautschi and Walecka<sup>41)</sup>. In both of these papers, the analytic properties of the partial-wave amplitudes are determined. Frautschi and Walecka make calculations for the  $J = 3/2$ , P-wave state by approximating the cuts by a set of judiciously chosen poles; they assume knowledge of the  $\pi\pi$  interaction from the Frazer-Fulco work on nucleon form factors. Using the N/D method of solution, they were able to obtain the general features of experimental data with only this very simple version of the theory.

Processes involving photons,  $\gamma + \pi \rightarrow \pi + \pi$  and  $\gamma + N \rightarrow \pi + N$ , have been examined respectively by Wong<sup>42)</sup> and Ball<sup>43)</sup>. The latter found that the

introduction of a  $\pi\pi$  interaction gave only a small alteration in the Chew, Goldberger, Low and Nambu results<sup>17)</sup>.

All of these reactions have been investigated<sup>44)</sup> too using the Cini-Fubini approximation. On the whole, the results obtained are similar to those from the Chew-Mandelstam programme. By fitting the experimental pion-nucleon phase shifts as well as the nucleon electromagnetic form factors, Bowcock et al. deduced that the  $I = 1 = J$  pion-pion resonance should be at  $t_R \approx 22.4 \mu^2$ , as compared to the much lower Frazer-Fulco value. Recent trends also seem to indicate a much larger resonance energy; it probably has a value<sup>45)</sup> nearer  $t_R \approx 28 \mu^2$ .

Considerable interest has also been paid to strange particle interactions<sup>46)</sup>, for example  $\bar{K}$ -meson-nucleon scattering and absorption. One is greatly handicapped here since there is uncertainty about the parities of the reacting particles, and the values of the coupling constants are unknown. Experiments which could be of help are rather inaccurate and sparse. The consequences of the Mandelstam representation have been examined too in connection with non-relativistic scattering<sup>47)</sup>; double dispersion relations have in fact been proved for

a certain class of potentials.

The Mandelstam representation attributes certain analytic properties to S-matrix elements. It is therefore natural to see whether such a conjecture can be tied up with conventional field theory. Work in this direction was started off by Karplus, Sommerfield and Wickmann<sup>48)</sup> who studied the vertex function and the fourth order Feynman diagram of perturbation theory. Their treatment was soon extended<sup>49)</sup> to a general  $n^{\text{th}}$  order diagram<sup>50), 51)</sup>; and such an examination has gone a long way to justifying the Mandelstam representation. It has also led to the discovery of anomalous thresholds, and has shown that for many reactions a Mandelstam representation certainly does not hold.

One might well ask at this stage what the present position of quantum field theory is, as regards strong interactions. There seems to be a diversity of opinion. Landau<sup>51)</sup> has stated that further work with field theory is a waste of time. Chew<sup>37)</sup> does not adopt such a strong point of view, but asserts that it is "destined just to fade away". On the other hand, many physicists are still actively engaged in research in field theory. Few would deny the extreme importance and value of the

part it has played, for through it have been discovered many of the underlying laws of physics (for example, the symmetry principles). However, grave doubts have been cast on its validity in the realm of strong interactions; it may well be that here the analytic S-matrix plus unitarity is the fundamental theory.

### 3. Outline of Calculations

The problem of pion-nucleon scattering possesses a long history. As mentioned in the previous sections, it has been studied in the Chew-Low model and the single dispersion relations of Chew, Goldberger, Low and Nambu, while recently a more satisfactory treatment has been given in the Mandelstam formalism by Frautschi and Walecka. All these investigations were for low energies only, below the first pion-nucleon resonance which occurs for pion kinetic energies of 200 MeV in the laboratory frame of reference. In particular, by examining explicitly the  $J = 3/2$ , P- partial wave amplitude, Frautschi and Walecka were able to reproduce the general features of the low energy experiments by using only very simple approximations for the more complete double dispersion relation theory.

However, a large amount of data, both experimental<sup>53)</sup> and theoretical<sup>54)</sup>, is now available for pion-nucleon scattering up to several GeV. Of course, for such high energies, inelastic production processes are possible and they become very important, especially  $\pi + N \rightarrow \pi + \pi + N$ . From graphs of the cross-sections, two resonances in the pion-nucleon system have been

found to occur at pion kinetic energies of about 600 MeV and 900 MeV, in addition to the large first resonance at 200 MeV. This latter resonance is known with certainty to occur through a P-wave pion-nucleon state with total isotopic spin  $I = 3/2$  and total angular momentum  $J = 3/2$ . For the two higher resonances, experiment seems to indicate that their corresponding parameters are  $I = 1/2, J = 3/2$ , D-wave and  $I = 1/2, J = 5/2$ , P-wave respectively.

Chapter II of this thesis is concerned with the extension of elastic pion-nucleon scattering up to medium energies (about 750 MeV). The P- and D- partial wave amplitudes are examined using the straightforward approach of Frautschi and Walecka in the hope that, even with this comparatively simple theory, some information will be obtained particularly for energies above the first resonance.

The procedure employed is to deduce the analytic properties of the partial wave amplitudes in the  $s$ -plane ( $s$  is the square of the barycentric energy  $W$ ; Frautschi and Walecka work in the  $W$ -plane) from a Mandelstam representation for the invariant 4-vector amplitudes, and to replace the various cuts by a set of poles.

However, in order to determine these pole positions and the residues there, it is necessary to make use of a certain amount of experimental information: the masses of the reacting particles ( $M \approx 6.72\mu$ ), the pion-nucleon coupling constant ( $g^2 \approx 15$ ), the position of the dominant first resonance ( $\omega_1 \approx 8.9\mu$ ), and the nucleon electromagnetic form factors (via the Frazer-Fulco theory). Of course, if one could handle the Mandelstam representation correctly, no experimental input data would be necessary; the results would be obtained in terms of only one parameter which presumably would define the mass scale.

Above the first resonance, the inelastic process  $\pi + N \rightarrow \pi + \pi + N$  becomes important. From angular distributions and momenta spectra, experiment yields strong evidence<sup>53), 54)</sup> that, in the final state, the nucleon is closely associated with one of the pions, and they appear to be moving relative to each other in a P-wave,  $l = 3/2$ ,  $j = 3/2$  state, that is, with the parameters corresponding to the first pion-nucleon resonance. In Chapter III, an attempt has therefore been made to include explicitly this inelastic channel  $\pi + \pi + N$  by reducing it to a two-particle state  $\pi + N^*$ ,

and treating  $N^*$  as an isobaric nucleon particle of intrinsic isotopic spin  $3/2$ , spin  $3/2$ , even parity and mass corresponding to the barycentric energy of the first pion-nucleon resonance. Some relevant theory of spin  $3/2$  particles is first of all noted, and then the kinematics and analytic properties of the process  $\pi + N \rightarrow \pi + N^*$  discussed. It is found that a Mandelstam representation does not hold for this process, but it is still possible to incorporate the Born terms. The coupling constant  $g^*$  for the  $\pi NN^*$  vertex is estimated by comparison with experiment.

Pion photoproduction  $\gamma + N \rightarrow \pi + N$  is studied in Chapter IV. Experiment reveals three resonances in the cross-sections, for photon laboratory energies of about 350 MeV, 750 MeV and 1050 MeV. It is interesting to note that the laboratory kinetic energies which an incident pion would need to produce the barycentric energies as in these photoproduction cases, are in fact approximately 200 MeV, 600 MeV and 900 MeV, the positions of the resonances in pion-nucleon scattering. This is just another indication of the close connection between photoproduction and pion-nucleon scattering.

The Mandelstam representation has been written down

by Ball, and we use this to obtain the analytic properties of the multipole amplitudes. We have concentrated in particular on the magnetic and electric dipole amplitudes which have total angular momentum  $J = 3/2$ ; these have been suggested<sup>53),54)</sup> as the resonant states. A rough estimation is also made for the effect of the  $\Upsilon + \pi \rightarrow N + \bar{N}$  reaction. The pole approximations for photoproduction are then combined with those already obtained in Chapters II, III, and the photoproduction cross-sections calculated.

The method of solution employed throughout is the  $N/D$  method introduced by Chew and Mandelstam, and which is greatly simplified when the cuts are replaced by poles. A generalisation to multi-channel processes (two particles per channel) has been made by Bjorken<sup>55)</sup>. In the present considerations, we have altogether three channels

$$(1) \Upsilon + N \quad (2) \pi + N \quad (3) \pi + N^*$$

For any specified total isotopic spin and total angular momentum, the scattering amplitudes for the various possible processes can be incorporated into a matrix  $g(s)$ . A typical element  $g_{ij}(s)$  is the transition amplitude from channel  $i$  to channel  $j$ ; for example,  $g_{23}(s)$  represents the process  $\pi + N \rightarrow \pi + N^*$ . It is assumed

that  $g(s)$  can be expressed in the form

$$g(s) = D^{-1}(s) N(s) \quad (I.13)$$

where  $N$  and  $D$  are of course square matrices. The unitarity condition for inverse of  $g(s)$  is

$$I_m (g^{-1})_{ij} = -q_i \theta_i \delta_{ij}, \quad (I.14)$$

where  $q_i$  is the barycentric momentum in the  $i^{\text{th}}$  channel, and  $\theta_i$  is the step function 0 or 1 according as  $W$  is less than or greater than the threshold energy in the  $i^{\text{th}}$  channel.

In any amplitude  $g_{ij}(s)$ , the left-hand cuts are replaced by a set of poles at  $s_{ij}^n$  ( $n=1, \dots$ ) with corresponding residues  $a_{ij}^n$ . In order to satisfy the Riemann-Schwarz reflection principle

$$g^*(s) = g(s^*), \quad (I.15)$$

any complex pole must be accompanied by its complex conjugate pole. These poles  $s_{ij}^n$  are incorporated into  $N(s)$ , and writing

$$N_{ij}(s) = \sum_{k,n} D_{ik}(s_{kj}^n) \frac{a_{kj}^n}{(s-s_{kj}^n)} \quad (I.16)$$

ensures that  $g(s)$  possesses its correct left-hand poles

and residues.

$D(s)$  is taken to include all the right-hand cuts.

From (I.15) and (I.16), we deduce that

$$D^*(s) = D(s^*)$$

and hence obtain the subtracted dispersion relation

$$D_{ij}(s) = D_{ij}(s_0) + \frac{(s-s_0)}{\pi} \int_{s_0}^{\infty} ds' \frac{\text{Im } D_{ij}(s')}{(s'-s)(s'-s_0)} \quad (\text{I.17})$$

The normalisation may be chosen so that

$$D_{ij}(s_0) = \delta_{ij}.$$

It also follows from (I.13) and (I.14) that, for real  $s$ ,

$$\text{Im } D_{ij}(s) = -g_j \theta_j N_{ij}(s).$$

Hence (I.17) becomes

$$D_{ij}(s) = \delta_{ij} - \frac{(s-s_0)}{\pi} \sum_{k,n} D_{ik}(s_{k_j}^n) a_{k_j}^n \int_{s_0}^{\infty} ds' \frac{g_j(s') \theta_j}{(s'-s_0)(s'-s)(s'-s_{k_j}^n)} \quad (\text{I.18})$$

The lower limit of integration is determined by the process being considered and the step function  $\theta_j$ .

Assuming the pole positions and residues are known, we may find the  $D_{ik}(s_{k_j}^n)$  by putting  $s = s_{k_j}^n$  in (I.18) and solving the resulting set of simultaneous equations.

One can then calculate  $N_{ij}(s)$  and  $D_{ij}(s)$  for the physical energy range of interest (the integrals in (I.18) become principal value integrals).

In later work, the above theory will require slight modifications. This is because we shall use redefined amplitudes, as well as consider the special 1 x 1 and 2 x 2 cases. However, these modifications are indicated where necessary.

CHAPTER II - PION-NUCLEON SCATTERING

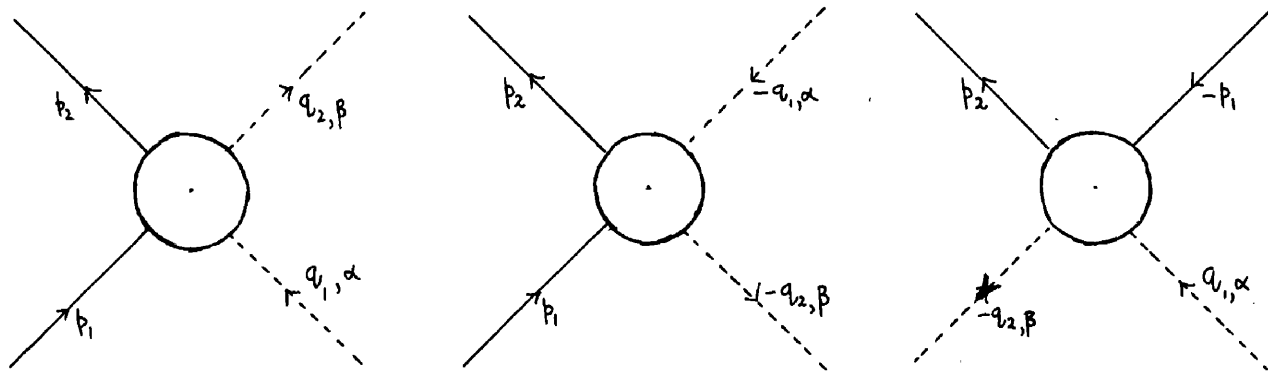
Many of the basic formulae relevant to this chapter have already been presented in the papers of Chew, Goldberger, Low and Nambu<sup>16)</sup>, and Frautsci and Walocka<sup>41)</sup>. The latter authors also give a full discussion of the Mandelstam representation, and the analytic properties of the partial wave amplitudes are derived in the  $W$ -plane; in their calculations, they concentrate on the  $J = 3/2$ ,  $P$ -wave. For the sake of completeness, we shall include these formulae here. Using the same notation, we shall work in the  $s$ -plane, obtaining the corresponding expressions for any partial wave, and later specialising to the  $P$ - and  $D$ -waves.

1. Kinematics.

For pion-nucleon scattering, we denote  $p_1, q_1$  as the incoming nucleon and pion four-momenta respectively, with  $p_2, q_2$  for the corresponding outgoing particles. The Lorentz scalars may be taken as

$$s = -(p_1 + q_1)^2, \quad u = -(p_2 - q_1)^2, \quad t = -(q_1 - q_2)^2. \quad (\text{II.1})$$

$s, u$  and  $t$  are the squares of the energies in the respective



(a)  $\pi + N \rightarrow \pi + N$     (b)  $\pi + N \rightarrow \pi + N$     (c)  $\pi + \pi \rightarrow N + \bar{N}$

Figure 2.

barycentric systems for the three reactions shown in Figure 2 (a,  $\beta$  label the charge states of the pions). They are not linearly independent, but are connected by the equation

$$s + u + t = 2N^2 + 2\mu^2.$$

In the barycentric system of Figure 2(a), we have

$$\begin{aligned} s &= W^2 \\ u &= 2N^2 + 2\mu^2 - W^2 + 2q^2(1 - \cos\theta) \\ t &= -2q^2(1 - \cos\theta), \end{aligned} \tag{II.2}$$

where  $W$  is the total energy,  $\theta$  the scattering angle, and

$q$  the magnitude of the momentum;

$$q^2 = \frac{1}{4W^2} [(W+N)^2 - \mu^2][(W-N)^2 - \mu^2] = \frac{1}{4s} [s - (N+\mu)^2][s - (N-\mu)^2] \quad (\text{II.3})$$

The T-matrix element for the process is defined by

$$S_{fi} = \delta_{fi} - (2\pi)^4 i \delta^4(p_2 + q_2 - p_1 - q_1) \left( \frac{N^2}{4E_1 E_2 \omega_1 \omega_2} \right)^{1/2} \bar{u}_2 T u_1,$$

with  $\bar{u}u = 1$ . T may be expressed in the form

$$T = -A + \frac{1}{2} \gamma \cdot (q_1 + q_2) B, \quad (\text{II.4})$$

where A, B are functions of  $s$ ,  $u$ ,  $t$ .

The decomposition in isotopic spin space is

$$\begin{aligned} A_{\beta\alpha} &= \delta_{\beta\alpha} A^{(+)} + \frac{1}{2} [\tau_\beta, \tau_\alpha] A^{(-)} \\ B_{\beta\alpha} &= \delta_{\beta\alpha} B^{(+)} + \frac{1}{2} [\tau_\beta, \tau_\alpha] B^{(-)} \end{aligned} \quad (\text{II.5})$$

Total isotopic spins of  $3/2$ ,  $1/2$  are allowed, and the corresponding eigenamplitudes are obtained by taking the appropriate combination of the  $(\pm)$  amplitudes:

$$A^{3/2} = A^{(+)} - A^{(-)}, \quad A^{1/2} = A^{(+)} + 2A^{(-)}, \quad (\text{II.6})$$

and similarly for B. The substitution law immediately

yields the following crossing relations:

$$A^{(\pm)}(s,u,t) = \pm A^{(\pm)}(u,s,t), \quad B^{(\pm)}(s,u,t) = \mp B^{(\pm)}(u,s,t). \quad (\text{II.7})$$

These enable us to express the values of A,B for the crossed pion-nucleon scattering case Figure 2(b) in terms of those for Figure 2(a).

We wish to study the partial wave amplitudes  $f_{\ell\pm}^{(s)}$ . They are states of orbital angular momentum  $\ell$ , total angular momentum  $J = \ell \pm \frac{1}{2}$ , and parity  $-(-1)^\ell$ ; and are related to the scattering phase shifts  $\delta_{\ell\pm}$  by

$$f_{\ell\pm}^{(s)} = \frac{1}{q} e^{i\delta_{\ell\pm}} \sin \delta_{\ell\pm}. \quad (\text{II.8})$$

The differential cross-section is

$$\frac{d\sigma}{d\Omega} = \sum_{\text{spins}} \left| \langle f | F_1 + \frac{(\underline{e} \cdot \underline{q}_2)(\underline{e} \cdot \underline{q}_1)}{|\underline{q}_2||\underline{q}_1|} F_2 | i \rangle \right|^2 \quad (\text{II.9})$$

where the matrix element is taken between Pauli spinors, and the summation indicates a sum over the final spin states and an average over the initial ones. An angular momentum decomposition shows that

$$F_1 = \sum_{l=0}^{\infty} f_{l+}^{(s)} P_{l+1}'(x) - \sum_{l=2}^{\infty} f_{l-}^{(s)} P_{l-1}'(x) \quad (\text{II.10})$$

$$F_2 = \sum_{l=1}^{\infty} [f_{l-}^{(s)} - f_{l+}^{(s)}] P_l'(x)$$

with  $x = \cos \theta$ . Inverting these equations, we obtain

$$f_{l\pm}^{(s)} = \frac{1}{2} \int_{-1}^{+1} dx [F_1 P_l(x) + F_2 P_{l\pm 1}(x)]. \quad (\text{II.11})$$

Also, using (II.9) and (II.4), one can deduce that

$$F_1 = \frac{(W+N)^2 - \mu^2}{16\pi W^2} [A + (W-N)B] \quad (\text{II.12})$$

$$F_2 = \frac{(W-N)^2 - \mu^2}{16\pi W^2} [-A + (W+N)B].$$

Combining (II.11) and (II.12), we finally obtain the required expression for the partial wave amplitudes in terms of the invariant amplitudes A, B:

$$f_{l\pm}^{(s)} = \frac{1}{32\pi W^2} \left\{ [(W+N)^2 - \mu^2] [A_l + (W-N)B_l] + [(W-N)^2 - \mu^2] [-A_{l\pm 1} + (W+N)B_{l\pm 1}] \right\}, \quad (\text{II.13})$$

where  $A_l(s) = \int_{-1}^{+1} dx A(s, u, t) P_l(x)$ , and similarly  $B_l(s)$ .

Here  $u, t$  may be regarded as functions of  $s, x$ .

However, it is better to work with the amplitude  $g_{l\pm}^{(\zeta)}$  defined by

$$g_{l\pm}^{(\zeta)} = \frac{s^l}{q^{2l}} f_{l\pm}^{(\zeta)} \quad (\text{II.14})$$

Dividing by  $q^{2l}$  introduces no additional singularities in the  $g_{l\pm}^{(\zeta)}$ , since it is well-known that the phase-shifts  $\delta_{l\pm}$  behave as  $q^{2l+1}$  as  $q^2 \rightarrow 0$ . Thus by working with  $g_{l\pm}^{(\zeta)}$  ensures that our final results will possess the correct threshold behaviour as  $q^2 \rightarrow 0$ . We have also multiplied by  $s^l$ , in order to retain the convergence of certain integrals which occur later in the N/D solution.

2. The Mandelstam representation; analytic properties.

It is assumed that the invariant amplitudes  $A^{(i)}$ ,  $B^{(i)}$  satisfy a Mandelstam representation. Denoting these amplitudes collectively by  $A^{(i)}$  ( $i=1, \dots, 4$ ), we have

$$\begin{aligned}
 A^{(i)}(s, u, t) = & \frac{R_s^{(i)}}{s-N^2} + \frac{R_u^{(i)}}{u-N^2} + \frac{1}{\pi^2} \int_{(N+\mu)^2}^{\infty} ds' \int_{(N+\mu)^2}^{\infty} du' \frac{\rho_{12}^{(i)}(s', u')}{(s'-s)(u'-u)} \\
 & + \frac{1}{\pi^2} \int_{(N+\mu)^2}^{\infty} ds' \int_{\mu^2}^{\infty} dt' \frac{\rho_{13}^{(i)}(s', t')}{(s'-s)(t'-t)} + \frac{1}{\pi^2} \int_{(N+\mu)^2}^{\infty} du' \int_{\mu^2}^{\infty} dt' \frac{\rho_{23}^{(i)}(u', t')}{(u'-u)(t'-t)}
 \end{aligned} \tag{II.15}$$

where

$$R_s^{(i)} = R_u^{(i)} = 0 \quad (i=1, 2)$$

$$R_s^{(3)} = -R_u^{(3)} = R_s^{(4)} = R_u^{(4)} = -4\pi g^2$$

The spectral functions  $\rho_{jk}^{(i)}$  are real, and non-vanishing in regions whose boundaries have been calculated by Mandelstam<sup>31)</sup>; they are asymptotic to the lower limits of integration indicated in (II.15)

One can easily reduce (II.15) to a one-dimensional form; for example, for fixed  $s$ ,

$$A^{(i)}(s, u, t) = \frac{R_s^{(i)}}{s-N^2} + \frac{R_u^{(i)}}{u-N^2} + \frac{1}{\pi} \int_{(N+\mu)^2}^{\infty} du' \frac{A_2^{(i)}(s, u')}{(u'-u)} + \frac{1}{\pi} \int_{\mu^2}^{\infty} dt' \frac{A_3^{(i)}(s, t')}{(t'-t)}, \tag{II.16}$$

where

$$A_2^{(i)}(s, u') = \frac{1}{\pi} \int_{(N+\mu)^2}^{\infty} ds' \frac{P_{12}^{(i)}(s', u')}{(s'-s)} - \frac{1}{\pi} \int_{-\infty}^{2N^2-2\mu^2-u'} ds' \frac{P_{23}^{(i)}(s', t')}{(s'-s)}$$

$$A_3^{(i)}(s, t') = \frac{1}{\pi} \int_{(N+\mu)^2}^{\infty} ds' \frac{P_{13}^{(i)}(s', t')}{(s'-s)} - \frac{1}{\pi} \int_{-\infty}^{(N-\mu)^2-t'} ds' \frac{P_{23}^{(i)}(s', t')}{(s'-s)}$$

This enables us to derive a simple expression for the corresponding partial wave amplitude  $A_{\ell}^{(i)}(s)$ , by projection, we have

$$A_{\ell}^{(i)}(s) = R_s^{(i)} \int_{-1}^{+1} dx \frac{P_{\ell}(x)}{(s-N^2)} + R_u^{(i)} \int_{-1}^{+1} dx \frac{P_{\ell}(x)}{(u-N^2)} \tag{II.17}$$

$$+ \frac{1}{\pi} \int_{(N+\mu)^2}^{\infty} du' A_2^{(i)}(s, u') \int_{-1}^{+1} dx \frac{P_{\ell}(x)}{(u'-u)} + \frac{1}{\pi} \int_{+\mu^2}^{\infty} dt' A_3^{(i)}(s, t') \int_{-1}^{+1} dx \frac{P_{\ell}(x)}{(t'-t)}$$

It is now possible to deduce the analytic properties of the  $g_{\ell\pm}^{(s)}$  in the  $s$ -plane from (I.13), (I.14) and the Mandelstam representation.

(1) The first terms in  $A_2, A_3$  above give rise to a cut for  $(N+\mu)^2 \leq s \leq \infty$ . Since also  $-1 \leq x \leq 1$ , this corresponds to the physical region for pion-nucleon scattering, Figure 2(a), and thus is called the physical cut. The second integrals of  $A_2, A_3$  however do not

produce any singularities; they arise artificially in the reduction of the double dispersion relations to the single dispersion relation form.

(ii) The  $\frac{1}{(s-N^2)}$  term produces a pole at  $s = N^2$ . However,  $(s-N^2)$  is independent of  $\alpha$ , and it follows from the orthogonality properties of the Legendre polynomials that this pole occurs only in the  $J = \frac{1}{2}$ ,  $l = 0$  or  $1$ ,  $I = \frac{1}{2}$  states. Since we shall be concentrating later on the  $J = 3/2$ , P- and D-waves, we shall omit this pole term from further consideration.

The other singularities arising from (II.17) may be easily obtained by writing the other denominators  $(u-N^2)$ ,  $(u'-u)$  and  $(t'-t)$  explicitly in terms of  $s$  and  $\alpha$  (using (II.2)). They are all linear in  $\alpha$ , and therefore the singularities are end-point singularities, that is, the branch points occur for  $\alpha = \pm 1$ . When the denominators vanish, we obtain simple quadratic equations, the roots of which yield the branch cuts in the  $s$ -plane.

(iii) For the  $(u-N^2)$  term, we obtain the quadratic

$$(1+\alpha) s^2 - 2[\mu^2 + (N^2 + \mu^2)\alpha]s - (1-\alpha)(N^2 - \mu^2)^2 = 0,$$

where  $-1 \leq \alpha \leq 1$ . One can immediately show that the roots are real, and the corresponding cuts are a short

cut  $(N - \frac{\mu^2}{N})^2 \leq s \leq (N^2 + 2\mu^2)$  , and a cut along the negative real s-axis  $-\infty \leq s \leq 0$ .

(iv) The quadratic corresponding to the  $(w'-w)$  denominator is

$$(1+x)s^2 + 2[w' - (N^2 + \mu^2)(1+x)]s - (1-x)(N^2 - \mu^2)^2 = 0 ,$$

where  $-1 \leq x \leq 1$  and  $w' \geq (N + \mu)^2$  . Again the roots may be shown to be real for  $w'$  throughout its allowed range, and the resulting cut is  $-\infty \leq s \leq (N - \mu)^2$  . We call this the crossed pion-nucleon cut, because of its close connection with Figure 2(b) (as follows directly from the Mandelstam representation).

(v) The denominator  $(t'-t)$  vanishes for

$$t' + 2a^2(1-x) = 0$$

with  $-1 \leq x \leq 1$  and  $4\mu^2 \leq t' \leq \infty$  ; the roots of the resulting quadratic are

$$s = \frac{1}{(1-x)} \left\{ [-t' + (N^2 + \mu^2)(1-x)] \pm \sqrt{[t' - 2\mu^2(1-x)][t' - 2N^2(1-x)]} \right\} .$$

It follows that these roots are real only for  $t' \geq 4N^2$  , but are complex in the interval  $4\mu^2 \leq t' \leq 4N^2$  . The corresponding cut lies along the negative real axis

$-\infty \leq s \leq 0$  and the circle  $|s| = (N^2 - \mu^2)$  . This cut is

called the  $\pi\pi$  cut, since it is related to the reaction  $\pi + \pi \rightarrow N + \bar{N}$  of Figure 2(c). Later, we shall concentrate only on part of the circle cut: here we have

$$s = (N^2 - \mu^2) e^{i\phi} \tag{II.18}$$

$$-q^2 = N^2 \sin^2 \phi/2 + \mu^2 \cos^2 \phi/2 .$$

It might be added that, for more general reactions in which all the particles have different masses, these denominators give rise to quartic equations in  $s$ , of the form

$$X_{(s)}^2 = Y_{(s)}^2 \chi^2$$

where  $0 \leq \chi^2 \leq 1$ . However, as mentioned above, the branch points are given when  $\chi^2 = 1$ , and the quartic then reduces to a quadratic again plus two additional branch points at  $s = 0$  and  $s = -\infty$ .

(vi) Finally, there is a kinematical cut along the negative real  $s$ -axis, due to the  $W$ -factors in the coefficients of (II.13); this is called the "irrationality cut"<sup>56)</sup>.

All of these cuts are indicated in Figure 3<sup>56)</sup>. A Cauchy integral may now be taken round all of the cuts. We also take the integral round a contour inside the circle even though its value (for a point outside it) is zero; it allows us to work entirely in terms of discontinuities

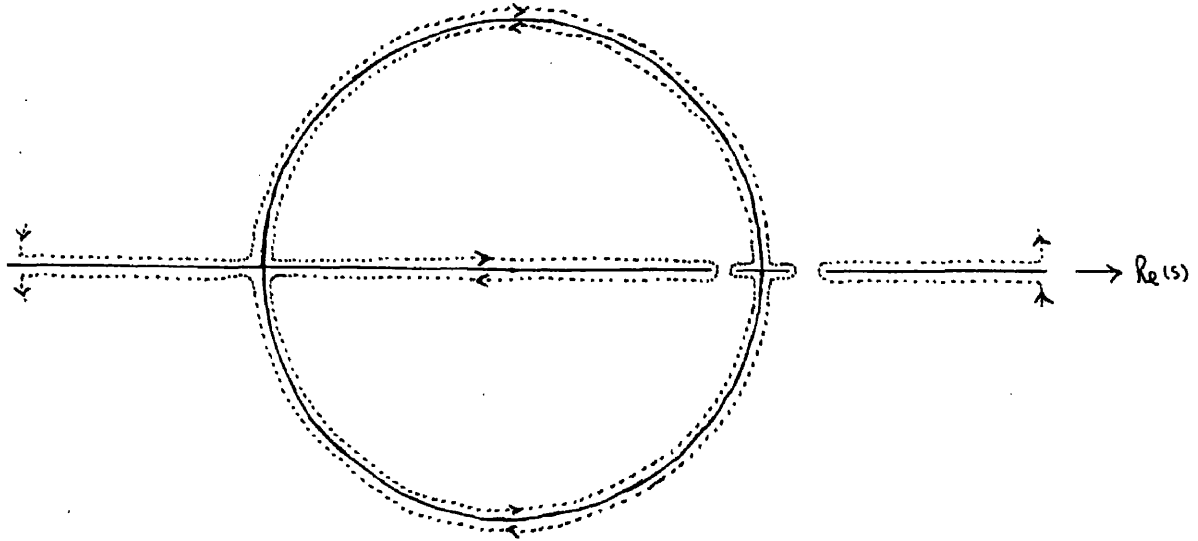


Figure 3.

across the cuts.

The contribution from any particular cut on the left will be of the form

$$\frac{1}{2\pi i} \int_C \frac{g_{l\pm}(s') ds'}{(s'-s)} = \frac{1}{\pi} \int \frac{\text{Abs } g_{l\pm}(s') ds'}{(s'-s)}, \quad (\text{II.19})$$

where C is a (clockwise) contour round the cut, and the absorptive part is just

$$\text{Abs } g_{l\pm}(s) = \frac{1}{2i} [g_{l\pm}(s_+) - g_{l\pm}(s_-)] ; \quad (\text{II.20})$$

$s_+$  refers to one side of the cut, and  $s_-$  to the other

side. As explained in § 3 of the introduction, our policy will be to replace an integral as in (II.19) by a set of pole terms of the form  $\frac{R_p}{(s-s_p)}$ , so that they will be approximately equal to each other when  $s$  takes values in the (physical) energy region we are interested in. Obviously, in order to determine the appropriate pole positions and the corresponding residues, one must evaluate the absorptive parts for the various left-hand cuts.

The general absorptive parts in terms of  $A_2^{(i)}$  and  $A_3^{(i)}$  for the crossed  $\pi N$  cut and the  $\pi\pi$  cut respectively have in fact been derived by Frautschi and Walecka directly from the Mandelstam representation. They also show that, in the positive part  $0 \leq s \leq (N-\mu)^2$  of the crossed  $\pi N$  cut, the variables are in their physical region for the crossed pion-nucleon scattering process Figure 2(b), that is,  $u \geq (N+\mu)^2$  and  $-1 \leq x^* \leq +1$ , where  $x^*$  is the corresponding cosine of the scattering angle. This section is therefore called the crossed physical cut. Thus by using the crossing relations, one can evaluate the absorptive part for the crossed physical cut in terms of physical pion-nucleon scattering; we shall use this important point later.

### 3. The single-nucleon term

The single nucleon term  $\frac{1}{(u-N^2)}$  contributes to all partial waves. Writing

$$u - N^2 = -2q^2 (a + x),$$

where  $a = \left[ \frac{1}{2q^2} (s - N^2 - 2\mu^2) - 1 \right]$ , and substituting into (II.13) and (II.14), we obtain

$$g_{\ell t}^{3/2} (s)^N = - \binom{1}{-1/2} \frac{g^2 W^{2\ell-2}}{8 q^{2\ell+2}} [(W+N)^2 - \mu^2] (W-N) \int_{-1}^{+1} dx \frac{P_{\ell}(x)}{(a+x)} \quad (\text{II.21})$$

$$- \binom{1}{-1/2} \frac{g^2 W^{2\ell-2}}{8 q^{2\ell+2}} [(W-N)^2 - \mu^2] (W+N) \int_{-1}^{+1} dx \frac{P_{\ell \pm 1}(x)}{(a+x)}$$

The integrations with respect to  $x$  may be carried out for any particular angular momentum state. (A number of such integrals has been set out in Appendix A). The integrated result always contains a logarithm term  $\log \left( \frac{a+1}{a-1} \right)$ . It is precisely this logarithm which gives rise to the single nucleon cuts: the argument  $\left( \frac{a+1}{a-1} \right)$  becomes real and negative for  $s$  taking the values  $(N - \frac{\mu^2}{N})^2 \leq s \leq (N^2 + 2\mu^2)$  and  $-\infty \leq s \leq 0$ . The discontinuities across these cuts are therefore easy to find, since a logarithm discontinuity is just  $\pm 2\pi i$ . Nor is it difficult to determine the appropriate sign of the discontinuity: this may be done by finding whether the

denominator acquires a small positive or negative imaginary part as  $s \rightarrow s \pm i\epsilon$  ; use of the identity

$$\frac{1}{x+a \pm i\epsilon} = \mathcal{P} \frac{1}{x+a} \mp \pi i \delta(x+a)$$

then leads to the required answer.

One can immediately determine the absorptive part for the short cut. For  $s \rightarrow s \pm i\epsilon$ , we find  $a \rightarrow a \mp i\epsilon$ . Hence we obtain the following results for the short cut:

$$\frac{1}{\pi} \text{Abs } g_{1+}^{3/2}(s)N = \binom{1}{-1/2} \frac{g^2}{8q^4} \left\{ [(W+N)^2 - \mu^2](W-N)a - [(W-N)^2 - \mu^2](W+N) \frac{1}{2}(3a^2-1) \right\} \quad (\text{II.22})$$

$$\frac{1}{\pi} \text{Abs } g_{2-}^{3/2}(s)N = \binom{1}{-1/2} \frac{g^2 s}{8q^6} \left\{ -[(W+N)^2 - \mu^2](W-N) \frac{1}{2}(3a^2-1) + [(W-N)^2 - \mu^2](W+N)a \right\}$$

These are drawn in Figure 4.

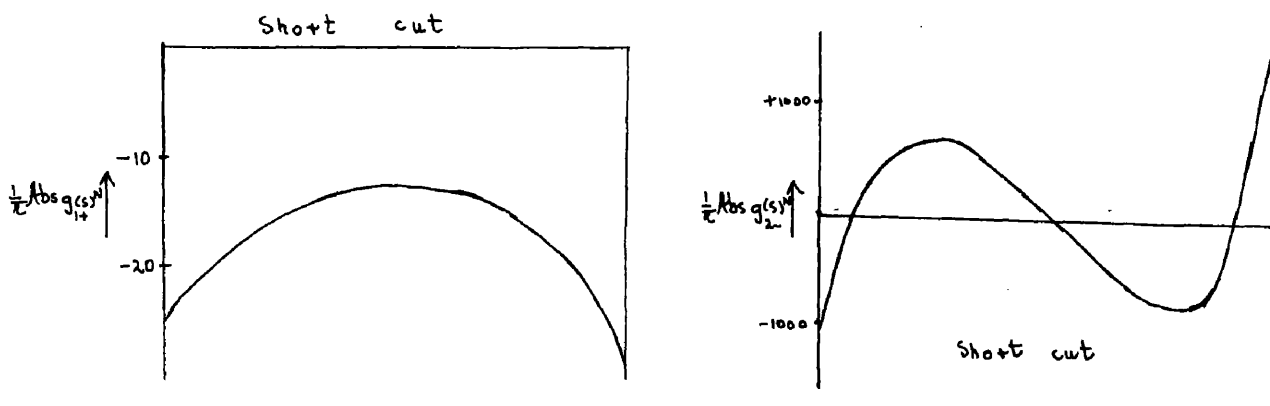


Figure 4.

For the cut along the negative real axis, there is an added complication due to irrationality. Nevertheless, the discontinuity is still reasonably simple to evaluate. We see that, on performing the integration in (II.21), a typical term has the form (remembering 'a' is a function of s)

$$h(W) [d(s) + e(s) \log Z(s)] , \quad (II.23)$$

where the coefficient  $h$  is a function of  $W$ . Writing

$s = -\omega^2$ , and  $h(i\omega) = h_1(\omega) + i h_2(\omega)$ , we can deduce that the corresponding discontinuity is

$$2\pi i \left\{ h_1(\omega) e(s) + \frac{1}{\pi} h_2(\omega) [d(s) + e(s) \log |Z(s)|] \right\} . \quad (II.24)$$

The corresponding absorptive parts for the amplitudes being considered are drawn in Figure 5.

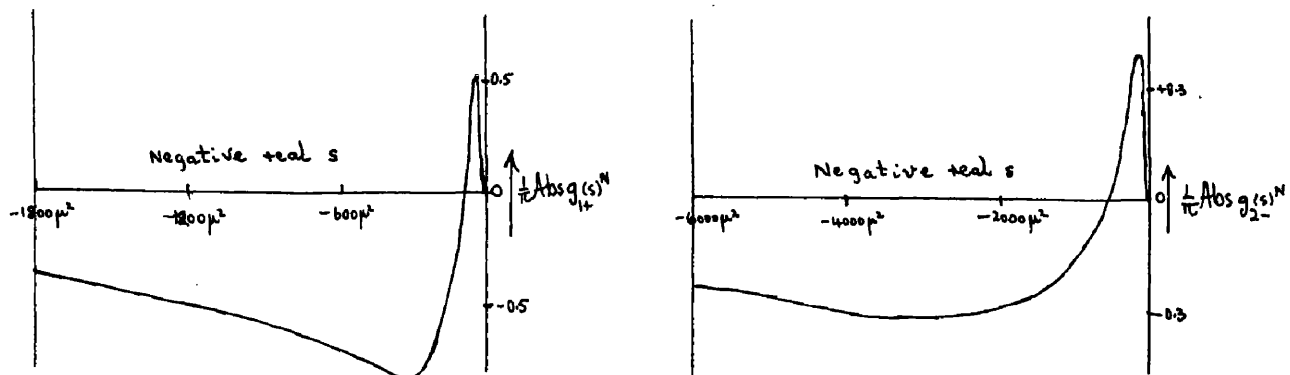


Figure 5.

The integrals (II.19) were computed for a range of  $s$  corresponding to pion kinetic energies in the laboratory system up to 750 MeV. The following pole terms were found to give reasonable approximations (with  $\mu = 1$ )

$$g_{1+}^{3/2, 1/2}(s)N = \begin{pmatrix} 1 \\ -1/2 \end{pmatrix} \left[ \frac{68.4}{s - 45.2} + \frac{350}{s + 140} + \frac{320}{s + 520} \right] \quad (\text{II.25})$$

$$g_{2-}^{3/2, 1/2}(s)N = \begin{pmatrix} 1 \\ -1/2 \end{pmatrix} \left[ \frac{58}{s - 44.1} + \frac{450}{s + 900} \right]$$

A two-pole approximation was taken for the P-wave amplitude along the negative real axis since, as we shall see later, this contribution is a very important one in this partial wave. It turns out that, for the D-wave, the single nucleon terms are not so dominant. The poles at  $s \approx N^2$  correspond to the static nucleon pole of the Chew-Low theory.

4. The crossed physical cut

It has been previously noted that the crossed physical cut  $0 \leq s \leq (N-\mu)^2$  is closely associated with physical pion-nucleon scattering; this follows from the crossing relations. To determine its contribution, we use the simple procedure of Frautschi and Walecka, and introduce the functions

$$A(s, \alpha)^x = \frac{1}{\pi} \int_{(N+\mu)^2}^{\infty} \frac{dw'}{w'-w} \frac{\text{Abs } A(w', s)}{(w'-w)}, \quad B(s, \alpha)^x = \frac{1}{\pi} \int_{(N+\mu)^2}^{\infty} \frac{dw'}{w'-w} \frac{\text{Abs } B(w', s)}{(w'-w)} \quad ; \quad (\text{II.26})$$

they are both analytic in the  $s$ -plane except for a branch cut along the crossed  $\pi N$  cut, across which they have the correct discontinuities.

From (II.12), we have

$$A^{(\pm)}(s, \alpha) = 8\pi W \left\{ \frac{W+N}{[(W+N)^2 - \mu^2]} F_1^{(\pm)} - \frac{W-N}{[(W-N)^2 - \mu^2]} F_2^{(\pm)} \right\} \quad (\text{II.27})$$

$$B^{(\pm)}(s, \alpha) = 8\pi W \left\{ \frac{1}{[(W+N)^2 - \mu^2]} F_1^{(\pm)} + \frac{1}{[(W-N)^2 - \mu^2]} F_2^{(\pm)} \right\}$$

The  $F_1, F_2$  may now be expanded in terms of the partial wave amplitudes  $f_{l\pm}^{(\pm)}(s)$  by (II.10). (Frautschi and Walecka have shown that these Legendre polynomial expansions are in fact valid on the crossed physical cut,

but not on the negative real axis part of the crossed  $\pi N$  cut). Further, assuming the dominance of the resonant  $(\frac{3}{2}, \frac{3}{2})$  state in these expansions, we obtain

$$F_1^{(\pm)}(s, \chi) \approx 3\chi \int_{1+}^{(\pm)}(s) \approx 3\chi \begin{pmatrix} 2/3 \\ -1/3 \end{pmatrix} \int_{1+}^{3/2}(s) \quad (\text{II.28})$$

$$F_2^{(\pm)}(s, \chi) \approx -\int_{1+}^{(\pm)}(s) \approx - \begin{pmatrix} 2/3 \\ -1/3 \end{pmatrix} \int_{1+}^{3/2}(s)$$

The existence of this resonance and its position are experimental results. Great simplification is introduced into our calculations if we take the resonance as a very sharp one. Chew, Goldberger, Low and Nambu have shown that this corresponds to the approximation

$$I_{1+} \int_{1+}^{3/2}(s) = \frac{8\pi W_R}{3} \left(\frac{f}{\mu}\right)^2 g^2 \delta(s - W_R^2), \quad (\text{II.29})$$

where  $f^2 = \left(\frac{\mu}{2N}\right)^2 g^2$ , and  $W_R$  is the barycentric energy of the resonance.

The absorptive parts in the integrands of (II.26) may now be obtained by substituting (II.28), (II.29) into (II.27), and using the crossing relations. Taking the appropriate linear combinations of the isotopic spin amplitudes, we obtain

$$\frac{1}{\pi} \text{Abs } A^{3/2}(u, s) = \binom{1}{4} \frac{64\pi W_R^{x^2}}{9} \left(\frac{f}{\mu}\right)^2 q_R^{x^2} \left\{ \frac{W_R^x + N}{[(W_R^x + N)^2 - \mu^2]} 3x_R^x + \frac{W_R^x - N}{[(W_R^x - N)^2 - \mu^2]} \right\} \delta(u - W_R^{x^2})$$

$$\frac{1}{\pi} \text{Abs } B^{3/2}(u, s) = -\binom{1}{4} \frac{64\pi W_R^{x^2}}{9} \left(\frac{f}{\mu}\right)^2 q_R^{x^2} \left\{ \frac{1}{[(W_R^x + N)^2 - \mu^2]} 3x_R^x - \frac{1}{[(W_R^x - N)^2 - \mu^2]} \right\} \delta(u - W_R^{x^2}),$$

where  $q_R^{x^2} = \frac{1}{4W_R^{x^2}} [W_R^{x^2} - (N + \mu)^2] [W_R^{x^2} - (N - \mu)^2]$ , and  $x_R^x$  is given by  $W_R^{x^2} = 2N^2 + 2\mu^2 - s - 2q_R^{x^2}(1 - x_R^x)$ . Substituting these formulae into the above expressions for  $A(s, x)^x$  and  $B(s, x)^x$ , and performing the integration, we obtain

$$A^{3/2}(s, x)^x = \binom{1}{4} \frac{64\pi W_R^{x^2}}{9} \left(\frac{f}{\mu}\right)^2 q_R^{x^2} \left\{ \frac{W_R^x + N}{[(W_R^x + N)^2 - \mu^2]} 3x_R^x + \frac{W_R^x - N}{[(W_R^x - N)^2 - \mu^2]} \right\} \frac{1}{(u_R - u)} \tag{II.30}$$

$$B^{3/2}(s, x)^x = -\binom{1}{4} \frac{64\pi W_R^{x^2}}{9} \left(\frac{f}{\mu}\right)^2 q_R^{x^2} \left\{ \frac{1}{[(W_R^x + N)^2 - \mu^2]} 3x_R^x - \frac{1}{[(W_R^x - N)^2 - \mu^2]} \right\} \frac{1}{(u_R - u)}$$

It is now simple to deduce  $q_{R\pm}(s)^x$  from (II.30).

Writing  $(u_R - u)$  as

$$u_R - u = 2q^2(b + x),$$

where  $b = \left[ \frac{1}{2q^2} (W_R^{x^2} - 2N^2 - 2\mu^2 + s) - 1 \right]$ , we derive the formula

$$q_{R\pm}^{3/2}(s)^x = \binom{1}{4} \frac{W_R^{x^2} q_R^{x^2} W^{2\ell-2}}{9q^{2\ell+2}} \left(\frac{f}{\mu}\right)^2 \left[ \frac{1}{[(W+N)^2 - \mu^2]} \left\{ \frac{(W_R^x + 2N - W)}{[(W_R^x + N)^2 - \mu^2]} 3x_R^x + \frac{(W_R^x - 2N + W)}{[(W_R^x - N)^2 - \mu^2]} \right\} \int_{-1}^{+1} \frac{P_\ell(x)}{(b+x)} dx \right. \tag{II.31}$$

$$\left. - \frac{1}{[(W-N)^2 - \mu^2]} \left\{ \frac{(W_R^x + 2N + W)}{[(W_R^x + N)^2 - \mu^2]} 3x_R^x + \frac{(W_R^x - 2N - W)}{[(W_R^x - N)^2 - \mu^2]} \right\} \int_{-1}^{+1} \frac{P_{\ell\pm 1}(x)}{(b+x)} dx \right]$$

From an examination of the logarithm term  $\log\left(\frac{b+1}{b-1}\right)$ , it may be shown that the cut lies in the interval

$$2N^2 + 2\mu^2 - W_R^2 \leq s \leq \frac{(N^2 - \mu^2)^2}{W_R^2} \quad (\text{II.32})$$

which is contained in  $0 \leq s \leq (N-\mu)^2$ ; this may be seen immediately from (II.32) by remembering that  $W_R^2 \approx N+2\mu$ . Thus as a result of the sharp resonance approximation, the crossed physical cut has been reduced to (II.32).

In exactly the same way as described in detail in § 3 above for the single nucleon term, one can easily obtain from (II.31) expressions for the partial waves  $q_{1+}^{3/2}(s)^x$  and  $q_{2-}^{3/2}(s)^x$  by performing the appropriate integrations. These immediately give the algebraic formulae for the corresponding absorptive parts for the cut (II.32); the Cauchy integrals round the cut may then be computed for a range of physical values of  $s$ . The following pole approximations were obtained

$$q_{1+}^{3/2}(s)^x = \binom{1}{4} \frac{2.1}{s-25}$$

(II.33)

$$q_{2-}^{3/2}(s)^x = \binom{1}{4} \frac{-10.5}{s-25}$$

We see that these terms are quite small, and consequently

it is found that the crossed physical cut contributions do not have much effect on our final results.

Similar work was carried through with the second and third pion-nucleon scattering resonances included (taking them to be  $I = \frac{1}{2}$ ,  $J = \frac{3}{2}$ , D-wave and  $I = \frac{1}{2}$ ,  $J = \frac{5}{2}$ , F-wave states respectively). Their contributions were likewise found to be small, and so are omitted in further calculations.

It is impossible at present to tackle the negative real axis part of the crossed  $\pi N$  cut. The reason for this is that we can no longer use the Legendre polynomial expansions for  $F_1$  and  $F_2$ , since they now diverge. To calculate the absorptive parts for the negative real axis cut requires a knowledge about the double spectral functions themselves; very little is known about them at the present time.

5. The  $\pi\pi$  cut.

As was found convenient in discussing the crossed physical cut, we introduce new functions  $A^{(s,x)\pi\pi}$ ,  $B^{(s,x)\pi\pi}$  which enable us to calculate very easily the contribution from the  $\pi\pi$  cut. They are defined by

$$A^{(\pm)}(s,x)\pi\pi = \frac{1}{\pi} \int_{4\mu^2}^{\infty} dt' \frac{Abs A^{(\pm)}(t',s)}{(t'-t)}, \quad B^{(\pm)}(s,x)\pi\pi = \frac{1}{\pi} \int_{4\mu^2}^{\infty} dt' \frac{Abs B^{(\pm)}(t',s)}{(t'-t)} \quad (\text{II.34})$$

which have the appropriate analytic properties, namely a branch cut along the  $\pi\pi$  cut with the correct discontinuities across it. It follows from the Mandelstam representation that the absorptive parts in the integrands of (II.34) correspond to the absorptive parts of the amplitudes A,B for the process  $\pi + \pi \rightarrow N + \bar{N}$  (Figure 2(c)). This latter reaction has been studied in detail by Frazer and Fulco, who use it to enable them to investigate the electromagnetic form factors of the nucleon. Here, we shall take the electromagnetic form factors as given, and use them to estimate the necessary absorptive parts.

Let us consider the reaction  $\pi + \pi \rightarrow N + \bar{N}$  in its barycentric system. Let  $p, \xi$  denote the magnitudes of the nucleon and meson momenta respectively; then

$$s = -p^2 - \xi^2 + 2p\xi y$$

$$u = -p^2 - \xi^2 - 2p\xi y$$

(II.35)

$$t = 4(\xi^2 + \mu^2) = 4(p^2 + N^2) = 4\mathcal{E}^2,$$

where  $\mathcal{E}$  is the total nucleon energy, and  $y$  is given by

$$y = \cos \vartheta = \frac{(p_1 \cdot \xi_2)}{p\xi} = \frac{1}{2p\xi} (s + \frac{1}{2}t - N^2 - \mu^2). \quad (\text{II.36})$$

$t$  is of course the square of the energy in this barycentric system.

The S-matrix element for the process is

$$S_{fi} = -2\pi i \delta^4(p_1 + p_2 - q_1 - q_2) \left( \frac{N^2}{4\mathcal{E}_1 \mathcal{E}_2 \omega_1 \omega_2} \right)^{1/2} \bar{u}(p_2) T v(p_1),$$

where the T-matrix can be expressed in the form

$$T = -A + \frac{1}{2} i \gamma \cdot (q_1 - q_2) B.$$

The isotopic spin decomposition is exactly the same as in (II.5) for pion-nucleon scattering, but now total isotopic spins of 0, 1 are the allowed states. It may be shown that the projection operators  $\int_{p\alpha}^I$  for  $I = 0, 1$  are  $\frac{1}{\sqrt{6}} \delta_{\beta\alpha}$  and  $\frac{1}{4} [\tau_\beta, \tau_\alpha]$  respectively; so that

$$A^{(+)} = \frac{1}{\sqrt{6}} A^{\circ}, \quad A^{(-)} = \frac{1}{2} A'$$

$$B^{(+)} = \frac{1}{\sqrt{6}} B^{\circ}, \quad B^{(-)} = \frac{1}{2} B'$$

(II.37)

Frazer and Fulco have shown how A, B may be expressed in terms of helicity amplitudes:

$$A(t, s) = -\left(\frac{8\pi}{p^2}\right) \sum_{J=0}^{\infty} (J+\frac{1}{2}) (p\xi)^J \left[ f_+^J(t) P_J^J(y) - \frac{Ny}{\{J(J+1)\}^{1/2}} f_-^J(t) P_J'(y) \right]$$

(II.38)

$$B(t, s) = 8\pi \sum_{J=1}^{\infty} \frac{J+1/2}{\{J(J+1)\}^{1/2}} (p\xi)^{J-1} f_-^J(t) P_J'(y),$$

where the  $f_+^J(t)$ ,  $f_-^J(t)$  are the redefined helicity amplitudes for  $\pi + \pi \rightarrow N + \bar{N}$ . The isotopic spin indices  $(\pm)$  have been omitted in (II.38). The corresponding expansions for the absorptive parts  $\frac{1}{\pi} \text{Abs } A(t, s)$  and  $\frac{1}{\pi} \text{Abs } B(t, s)$  follow immediately from (II.38).

We wish to use the latter partial wave expansions on the  $\pi\pi$  cut, over part of which  $s$  and hence  $\cos \vartheta$  are complex. It is therefore necessary to determine the region of convergence of these expansions. Since

a function  $f(z)$  which is analytic inside an ellipse with foci at  $z = \pm 1$  can be expanded in a Legendre polynomial series within the ellipse, we must find from the Mandelstam representation which singularities limit the size of the ellipse. They in fact come from the vanishing of the denominators in the expression for  $A_3^{(1)}$  when the two-dimensional spectral functions  $\rho_{ij}$  are non-zero. By considering the regions in which the  $\rho_{ij}$  do not vanish, Frazer and Fulco proved<sup>40)</sup> that the Legendre polynomial expansions were valid over only part of the  $\pi\pi$  cut, namely that section of the circle for which  $|\phi| \leq 66^\circ$ . The contribution from the  $\pi\pi$  cut has therefore been evaluated as far as is possible at present, that is for  $|\phi| \leq 66^\circ$ , using the Frazer-Fulco theory. To treat the remainder would require a knowledge of the double spectral functions.

We now assume that the  $\pi + \pi \rightarrow N + \bar{N}$  reaction is dominated by the  $I = 1, J = 1$  state. From (II.37), this means that

$$A^{(+)}(t,s) = 0 = B^{(+)}(t,s) \quad ; \quad A^{(-)}(t,s) = \frac{1}{2} A^1(t,s) \quad , \quad B^{(-)}(t,s) = \frac{1}{2} B^1(t,s) \quad ,$$

and from (II.38),

$$\frac{1}{\pi} \text{Abs } A^{(\pm)}(t,s) = - \begin{pmatrix} 0 \\ 1 \end{pmatrix} \frac{1254}{P} \left[ \text{Abs } f_+^{1(-)}(t) - \frac{N}{\sqrt{2}} \text{Abs } f_-^{1(-)}(t) \right]$$

$$\frac{1}{\pi} \text{Abs } B^{(\pm)}(t,s) = \begin{pmatrix} 0 \\ 1 \end{pmatrix} 6\sqrt{2} \text{Abs } f_-^{1(-)}(t).$$

(II.39)

Frazer and Fulco have related the helicity amplitudes  $f_+^{1(-)}(t)$ ,  $f_-^{1(-)}(t)$  to the nucleon electromagnetic form factors. For the photon-nucleon vertex

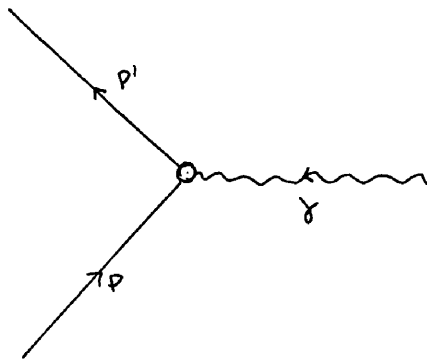


Figure 6.

illustrated in Figure 6, the amplitude has the form

$$\bar{u}(P') \left[ G_1(t) i\gamma_\mu + G_2(t) i\sigma_{\mu\nu} (P'-P)^\nu \right] u(P);$$

$G_1$  describes the charge structure, while  $G_2$  describes the anomalous magnetic moment structure. It is now convenient to introduce the isotopic scalar and vector

splitting

$$G_i(t) = G_i^s(t) + \tau_3 G_i^v(t) \quad (i=1,2) \quad (\text{II.40})$$

For zero momentum transfer, we have that

$$\begin{aligned} G_1^s(0) &= \frac{1}{2}e = G_1^v(0) \\ G_2^s(0) &= \frac{1}{2}(\mu_p + \mu_n) \approx -0.06 \frac{e}{2N} \\ G_2^v(0) &= \frac{1}{2}(\mu_p - \mu_n) \approx 1.85 \frac{e}{2N} \end{aligned} \quad (\text{II.41})$$

It follows from conservation of G-parity that for the isoscalar part, only odd pion states ( $3\mu, 5\mu, \dots$ ) are allowed for  $\Upsilon \rightarrow N\bar{N}$ , but even pion states ( $2\mu, 4\mu, \dots$ ) are allowed for the isovector part.

Regarded as functions of  $t$ , the  $G_i^{s,v}(t)$  are analytic in the  $t$ -plane except for a branch cut  $t \geq 4\mu^2$  or  $9\mu^2$  along the positive real axis. Thus we can write the following dispersion relations for them:

$$\begin{aligned} G_1^v(t) &= \frac{1}{2}e + \frac{t}{\pi} \int_{4\mu^2}^{\infty} dt' \frac{g_1^v(t')}{t'(t'-t)} \quad , \quad G_1^s(t) = \frac{1}{2}e + \frac{t}{\pi} \int_{9\mu^2}^{\infty} dt' \frac{g_1^s(t')}{t'(t'-t)} \\ G_2^v(t) &= \frac{1}{\pi} \int_{4\mu^2}^{\infty} dt' \frac{g_2^v(t')}{(t'-t)} \quad , \quad G_2^s(t) = \frac{1}{\pi} \int_{9\mu^2}^{\infty} dt' \frac{g_2^s(t')}{(t'-t)} \end{aligned} \quad (\text{II.42})$$

where we have used (II.41) to make a subtraction in the charge from factors  $G_1^{S,V}(t)$ .

The next step is to relate the  $q_i^V(t)$  (concentrating now on the isovector form factors for which two-pion intermediate states are allowed) to the pion form factor

$F_\pi(t)$  and the process  $\pi + \pi \rightarrow N + \bar{N}$ , using unitarity for the process  $\gamma \rightarrow N + \bar{N}$  with only a two-pion intermediate state. The result of this is

$$q_i^V(t) = - \frac{e F_\pi^*(t) \xi^3}{2 \xi} \Gamma_i(t), \quad (\text{II.43})$$

where

$$\Gamma_1(t) = - \frac{N}{\beta^2} \left[ \frac{\xi^2}{\sqrt{2} N} f'_-(t) - f'_+(t) \right] \quad (\text{II.44})$$

$$\Gamma_2(t) = - \frac{1}{2\beta^2} \left[ f'_+(t) - \frac{N}{\sqrt{2}} f'_-(t) \right],$$

and  $\xi^2 = (\frac{1}{4}t - \mu^2)$ ,  $\beta^2 = (\frac{1}{4}t - N^2)$ ,  $\xi^2 = \frac{1}{4}t$ .

Solving for the  $f'_+(t)$  and  $f'_-(t)$  in (II.44), and substituting into (II.39), we obtain

$$\frac{1}{\pi} \text{Abs } A^{(\pm)}(t,s) = \begin{pmatrix} 0 \\ 1 \end{pmatrix} 24 \beta \xi \gamma \text{Abs } \Gamma_2(t) \quad (\text{II.45})$$

$$\frac{1}{\pi} \text{Abs } B^{(\pm)}(t,s) = - \begin{pmatrix} 0 \\ 1 \end{pmatrix} 12 \left[ \text{Abs } \Gamma_1(t) + 2N \text{Abs } \Gamma_2(t) \right].$$

It is also reasonable to make the approximation

$$g_i^v(t) \approx |F_\pi(t)|^2 [g_i^v(t)]_0, \quad (\text{II.46})$$

where  $[g_i^v(t)]_0$  is the value of  $g_i^v(t)$  neglecting any pion-pion interaction. From (II.43), we then obtain for  $4\mu^2 \leq t \leq 4N^2$ ,

$$\text{Abs } \Gamma_i^v(t) \approx \left( \frac{2\varepsilon}{\xi^3} \right) \frac{[g_i^v(t)]_0}{e} \text{Abs } F_\pi(t). \quad (\text{II.47})$$

Assuming a  $\pi\pi$  resonance in the  $I = 1, J = 1$  state at an energy  $t_R = 11.5\mu^2$ , one can derive a simple formula for the pion form factor  $F_\pi(t)$ :

$$F_\pi(t) \approx \frac{11.3}{(11.5 - t) - 2.32i}. \quad (\text{II.48})$$

Further simplification is obtained if  $\text{Abs } F_\pi(t)$  is taken to have a very sharp resonance; equivalently,

$$\text{Abs } \Gamma_1^v(t) = \delta_1 \delta(t - t_R), \quad \text{Abs } \Gamma_2^v(t) = \frac{\delta_2}{N} \delta(t - t_R). \quad (\text{II.49})$$

The  $\delta_i$  may be evaluated by using (II.48) which yields

$$\int_{-\infty}^{\infty} \text{Abs } F_\pi(t) dt = 35.5\mu^2.$$

Substituting (II.47) into the integrand, and using the known values

$$[g_1^v(11.5\mu^2)]_0 = 1.85 ef^2, \quad [g_2^v(11.5\mu^2)]_0 = 0.61 \frac{ef^2}{\mu}$$

from Chew, Karplus, Gasiorowicz and Zachariasen<sup>19)</sup>, one finds that

$$\delta_1 = -6.9, \quad \delta_2 = -15.6. \quad (\text{II.50})$$

From (II.45), (II.49) and (II.36), we obtain the expressions

$$\frac{1}{\pi} \text{Abs } A^{(t)}(t,s) = \begin{pmatrix} 0 \\ 1 \end{pmatrix} 12 (s + \frac{1}{2}t_R - N^2 - \mu^2) \frac{\delta_2}{N} \delta(t-t_R)$$

$$\frac{1}{\pi} \text{Abs } B^{(t)}(t,s) = - \begin{pmatrix} 0 \\ 1 \end{pmatrix} 12 (\delta_1 + 2\delta_2) \delta(t-t_R);$$

and putting these into the integrands of (II.34) with the appropriate isotopic spin combinations, we obtain

$$A^{\frac{3}{2}}(s,x)^{\pi\pi} = \begin{pmatrix} -1 \\ 2 \end{pmatrix} 12 \frac{\delta_2}{N} (s + \frac{1}{2}t_R - N^2 - \mu^2) \frac{1}{(t_R - t)} \quad (\text{II.51})$$

$$B^{\frac{3}{2}}(s,x)^{\pi\pi} = - \begin{pmatrix} -1 \\ 2 \end{pmatrix} 12 (\delta_1 + 2\delta_2) \frac{1}{(t_R - t)}$$

We may now finally deduce the formula for the partial

wave amplitude. Writing

$$t_R - t = 2q^2 (d-x),$$

where  $d = (1 + t_R/2q^2)$ , we find

$$q_{R\pm}^{3/2}(s)^{\pi\pi} = \left(\frac{-1}{2}\right) \frac{3W^{2l-2}}{16\pi q^{2l+2}} \left[ \begin{aligned} & [(W+N)^2 - \mu^2] \left\{ \frac{\delta_2}{N} (s + \frac{1}{2}t_R - N^2 - \mu^2) - (\gamma_1 + 2\gamma_2)(W-N) \right\} \int_{-1}^{+1} dx \frac{P_2(x)}{(d-x)} \\ & + [(W-N)^2 - \mu^2] \left\{ -\frac{\delta_2}{N} (s + \frac{1}{2}t_R - N^2 - \mu^2) - (\gamma_1 + 2\gamma_2)(W+N) \right\} \int_{-1}^{+1} dx \frac{P_{2+1}(x)}{(d-x)} \right] \quad (\text{II.52}) \end{aligned}$$

As a result of taking a sharp resonance at  $t_R \approx 11.5\mu^2$ , the  $\pi\pi$  cut is reduced in size, and extends over only part of the circle; it is open at the end near the physical region, and starts at the angles  $\phi = \pm 23\frac{1}{2}^\circ$ . This can again be deduced from the logarithmic term arising after the integration in (II.52) is performed; or else by observing from the quadratic equation discussed in §2(v) above that, for any given  $t'$ , the branch points occur for

$$\cos \phi = \frac{1}{2(N^2 - \mu^2)} (2N^2 + 2\mu^2 - t').$$

By computing the absorptive parts from (II.52) and the corresponding Cauchy integrals, we find that the contributions from  $23\frac{1}{2}^\circ \leq |\phi| \leq 66^\circ$  can be approximated by

$$g_{1+}^{3/2}(s)^{\pi\pi} = \begin{pmatrix} -1 \\ 2 \end{pmatrix} \left[ \frac{-4.8 + 30.9i}{s - (38.6 + 8.8i)} + \frac{-4.8 - 30.9i}{s - (38.6 - 8.8i)} \right]$$

(II.53)

$$g_{2-}^{3/2}(s)^{\pi\pi} = \begin{pmatrix} -1 \\ 2 \end{pmatrix} \left[ \frac{600 - 120i}{s - (39.5 + 26.5i)} + \frac{600 + 120i}{s - (39.5 - 26.5i)} \right]$$

As stated before, we are unable as yet to calculate the effect of the negative real axis and the remaining part of the circle, due to a lack of knowledge about the double spectral functions.

## 6. Results

Having approximated by pole terms (II.25), (II.33), (II.53) all the left-hand cuts which can be handled, we are now in a position to use the  $N/D$  method of solution. Obviously the reaction  $\pi + N \rightarrow \pi + N$  which we are considering at the moment, is a single-channel ( $\pi + N$ ) process; it is a special case of the general discussion given in the Introduction (Chapter I, § 3).

The unitarity condition for the inverse of the partial wave amplitude  $g_{\ell\pm}^{(\zeta)}$  becomes

$$\text{Im} \left( g_{\ell\pm}^{-1(\zeta)} \right) = - \frac{q_{\ell}^{2\ell+1}}{s^{\ell}} \left( \frac{\sigma_{\text{tot}}}{\sigma_{\text{el}}} \right)_{\mathcal{J},\ell}^{\text{I}} \quad (\text{II.54})$$

An extra factor  $q_{\ell}^{2\ell}/s^{\ell}$  arises in (II.54) due to the redefinition (II.14) of the amplitudes.  $\left( \frac{\sigma_{\text{tot}}}{\sigma_{\text{el}}} \right)_{\mathcal{J},\ell}^{\text{I}}$  is the ratio of the total to elastic cross-sections for the particular partial wave being considered. It is this ratio which takes into account the existence of all the other energetically possible channels; this may be deduced by letting the phase shifts become complex. For pure elastic scattering of the partial wave, the ratio is 1; while for its total absorption, it is 2. For strong interactions, in fact,  $\left( \frac{\sigma_{\text{tot}}}{\sigma_{\text{el}}} \right)_{\mathcal{J},\ell}^{\text{I}}$  takes only values between

1 and 2 for all physical  $s \geq (N+\mu)^2$ . It is of course possible to envisage some reaction in which the ratio does become greater than 2, but this does not happen for pion-nucleon scattering.

Writing  $g = D^{-1}N$  as before, we obtain

$$N(s) = \sum_n D(s^n) \frac{a^n}{(s - s^n)} \quad (\text{II.55})$$

and

$$D(s) = 1 - \frac{(s-s_0)}{\pi} \sum_n D(s^n) a^n \int_{(N+\mu)^2}^{\infty} \frac{\rho^{2l+1}(s') ds'}{(s'-s)(s'-s_0)(s'-s^n)(s')^l} \left( \frac{\sigma_{tot}}{\sigma_{el}} \right),$$

where we have omitted the various isotopic spin and angular momentum indices. In order to make the integration in (II.55) simpler, an average value was taken for the ratio of the cross-sections over the whole energy range; we considered values between 1.0 and 1.5. The  $D(s^n)$  were first calculated by solving the appropriate set of simultaneous equations, then  $N(s)$ ,  $D(s)$  and finally the pion-nucleon phase shifts  $\delta_{lt}^I$ . The results of these single-channel considerations are indicated in Figures 7 and 8 for the P- and D-waves respectively.

For the P-wave, our results are similar to those of

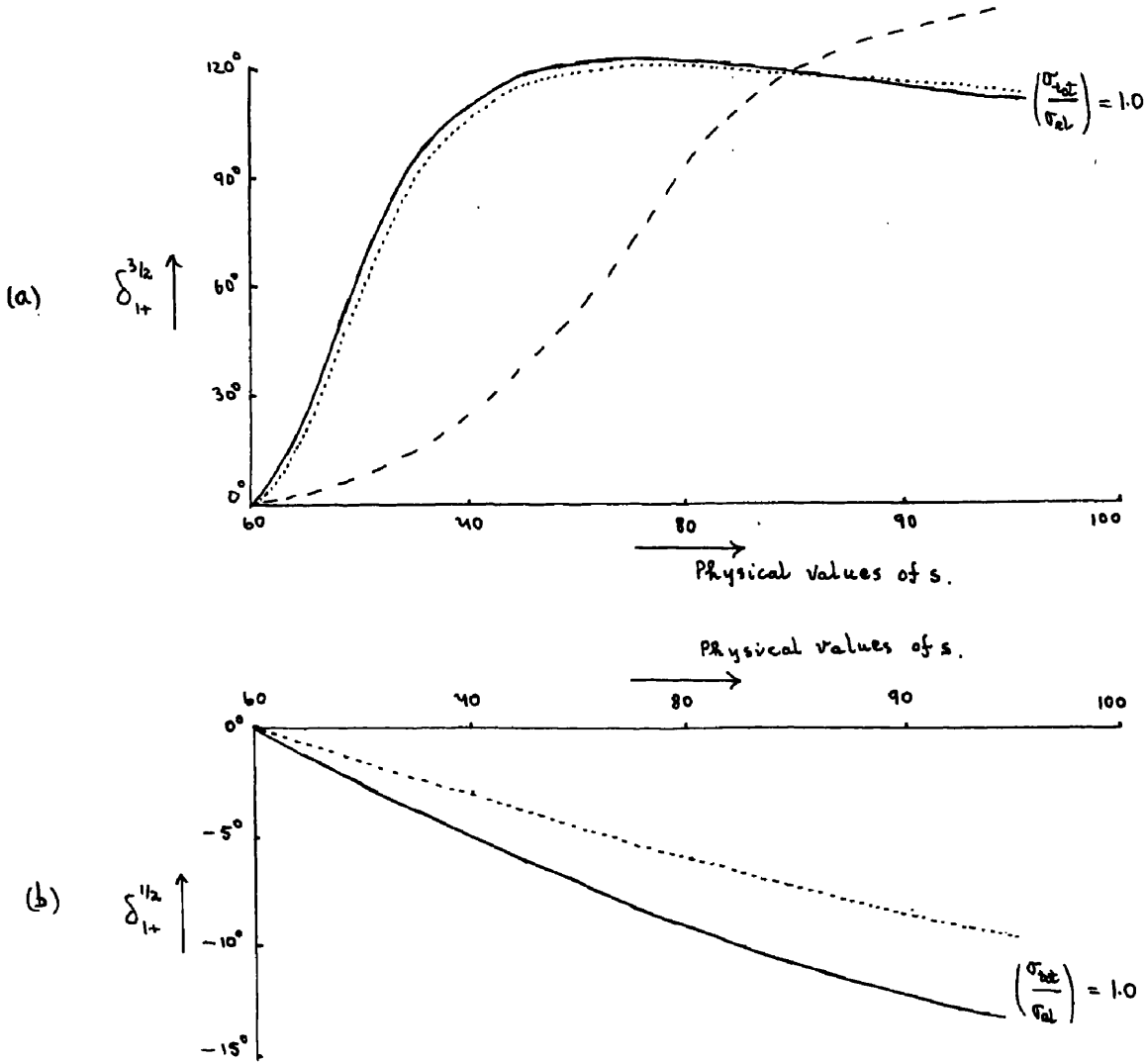


Figure 7. (a) and (b)

..... Single nucleon terms only, ——— All pion-nucleon poles,

- - - - Experiment

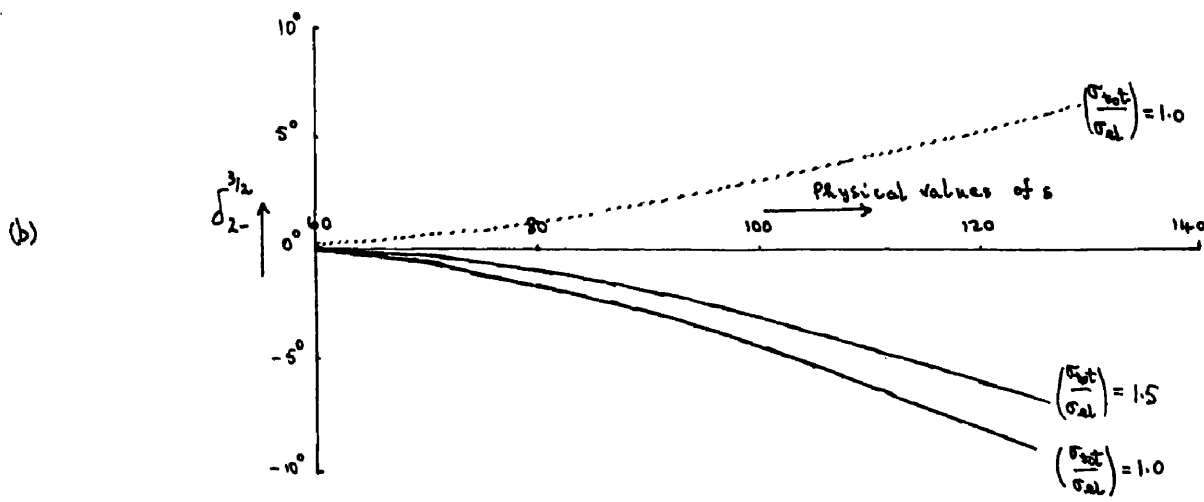
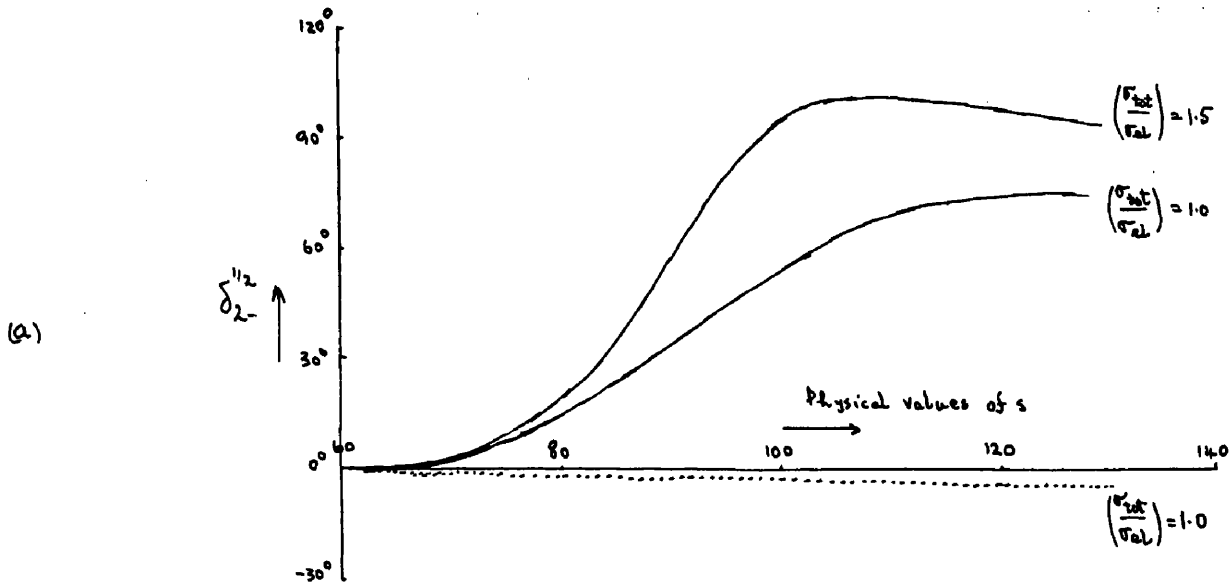


Figure 8, (a) and (b)

..... Single nucleon terms only, — All pion-nucleon poles.

Frautichi and Walecka who worked in the  $W$ -plane. The qualitative features of experiment for both isotopic spin states  $I = 3/2, 1/2$  are certainly reproduced. However, the position of the  $(3/2, 3/2)$  resonance obtained is rather lower than the experimental one. Also, the  $\delta_{1+}^{3/2}$  phase shift starts falling off at higher energies; this is where our pole approximations are not so good. If  $(\sigma_{tot}^{3/2}/\sigma_{el})$  is taken greater than 1.0, the resonance position is lowered even further, but the higher energy phase shifts are increased. The resonance position can be improved however by taking  $g^2$  slightly less than 15. It is significant that the  $\pi\pi$  poles have little effect on the  $I = 3/2$  phase shifts, whereas they alter the  $I = 1/2$  phase shifts by about 30%. The  $I = 3/2$  state is completely dominated by the large poles on the negative real axis for the single nucleon term. (These correspond to poles on the imaginary axis of the  $W$ -plane). The other poles nearer the physical region merely affect the shape of the graph for  $\delta_{1+}^{3/2}$ . It is indeed an important advantage of this simple method of approximating cuts by poles in being able to see clearly the effects of the individual contributions.

A very interesting result is obtained in the  $D$ -wave,

$I = \frac{1}{2}$ ,  $J = \frac{3}{2}$  state. It can be seen from Figure 8(a) that the single nucleon terms alone give small negative phase shifts in contradiction to the experimental values of  $\delta_{2-}^{1/2}$ . As noted earlier, the crossed physical pole gives only a small contribution. It is in fact the  $\pi\pi$  poles which have the dominant effect in this partial wave; they cause the phase shifts  $\delta_{2-}^{1/2}$  to become positive and large, which is what would be expected if it was indeed this state that produced the second resonance.

These same  $\pi\pi$  poles decrease the single nucleon phase shifts in Figure 8(b) for  $\delta_{2-}^{3/2}$ , and are strong enough to make the resulting phase shifts small and negative. Experimentally, the  $\delta_{2-}^{3/2}$  are not very well determined<sup>57)</sup>, but there is a slight indication that they are small and positive. It would therefore appear that we have used too powerful a  $\pi\pi$  interaction. However, even if we were to reduce this so as to keep the  $\delta_{2-}^{3/2}$  still positive, it would not alter the qualitative features of the  $\delta_{2-}^{1/2}$  phase shifts. The conclusion therefore from the D-wave is that a  $\pi\pi$  interaction has a strong influence on the second resonance.

CHAPTER III - THE  $\pi + N^*$  CHANNEL.

As was mentioned in the Introduction, the inelastic process  $\pi + N \rightarrow \pi + \pi + N$  becomes very important above the first resonance. For the present investigations, we have reduced this rather infamous three-particle state  $\pi + \pi + N$  to a two-particle one  $\pi + N^*$ , where  $N^*$  is regarded as a bound pion-nucleon system (isobaric nucleon) which we shall take as having intrinsic isotopic spin  $3/2$ , spin  $3/2$  and even parity, with a mass (also denoted by  $N^*$ ) equal to the barycentric energy of the first pion-nucleon resonance ( $N^* \approx 8.9\mu$ ). If the initial  $\pi + N$  state has  $J = 3/2$  and is D-wave, it follows from the conservation of total angular momentum and parity that the  $N^*$  particle and the other final state pion are in a relative S-wave state. This approximation seems to be well-justified by experiment for energies up to about 750 MeV.

1. Kinematics.

We shall first of all set out some formulae for spin  $3/2$  particles. A spin  $3/2$  particle  $N^*$  can be described <sup>58)</sup> by a wave function  $\Psi_p(x)$  which satisfies the equations

$$(\gamma_\nu \partial_\nu + N^*) \Psi_p(x) = 0, \quad \gamma_\mu \Psi_p(x) = 0$$

with the subsidiary condition

$$\partial_\mu \Psi_\mu(x) = 0.$$

$\Psi_\mu(x)$  is a 4-vector, each component of which is a spinor. Explicit forms of this wave function when the direction of motion of  $N^*$  is along the positive  $z$ -axis have been given by Kusaka<sup>59</sup>). Denoting  $\Psi_\mu(x)$  as  $(\underline{\Phi}, i\phi)$ , we have the four independent positive energy solutions

$$\begin{aligned} \underline{\Phi}^{(1)} &= \underline{e}_1 \psi_{+1} & \phi^{(1)} &= 0 \\ \underline{\Phi}^{(2)} &= \underline{e}_2 \psi_{-1} & \phi^{(2)} &= 0 \\ \underline{\Phi}^{(3)} &= \frac{1}{\sqrt{3}} \underline{e}_1 \psi_{+1} - \sqrt{\frac{2}{3}} \frac{E}{N^*} \underline{e}_3 \psi_{-1} & \phi^{(3)} &= -\sqrt{\frac{2}{3}} \frac{P}{N^*} \psi_{-1} \\ \underline{\Phi}^{(4)} &= \frac{1}{\sqrt{3}} \underline{e}_1 \psi_{-1} + \sqrt{\frac{2}{3}} \frac{E}{N^*} \underline{e}_3 \psi_{+1} & \phi^{(4)} &= +\sqrt{\frac{2}{3}} \frac{P}{N^*} \psi_{+1} ; \end{aligned} \tag{III.1}$$

they correspond to spin projections  $+3/2, -3/2, -1/2, +1/2$  respectively in the  $N^*$  rest frame.  $\underline{e}_1, \underline{e}_2$  and  $\underline{e}_3$  are the usual orthogonal polarisation vectors:

$$\underline{e}_1 = \frac{1}{\sqrt{2}} (1, i, 0), \quad \underline{e}_2 = \frac{1}{\sqrt{2}} (1, -i, 0), \quad \underline{e}_3 = \frac{P}{|P|} = (0, 0, 1).$$

$E$  and  $P$  in (III.1) are the energy and magnitude of the momentum respectively of the  $N^*$  particle;  $\psi_{\pm 1}$  are

the spin  $\frac{1}{2}$  wave functions.

The T-matrix element for  $\pi + N \rightarrow \pi + N^*$  can be written in the form

$$T_{fi} = (Q_1)_\mu \bar{U}_\mu(P_2) \left[ -A + \frac{1}{2} i \gamma \cdot (Q_1 + Q_2) B \right] \gamma_5 u(P_1) \quad (\text{III.2})$$

$$+ (Q_2)_\mu \bar{U}_\mu(P_2) \left[ -C + \frac{1}{2} i \gamma \cdot (Q_1 + Q_2) D \right] \gamma_5 u(P_1)$$

where  $Q_1, Q_2$  are the meson momenta,  $P_1, P_2$  the nucleon and  $N^*$  momenta respectively. In the barycentric system, we shall denote the total energy  $W = \sqrt{s}$  as usual, and the scattering angle by  $\Theta$ . The invariant scalars are

$$s = -(P_1 + Q_1)^2, \quad u = -(P_1 - Q_2)^2, \quad t = -(Q_1 - Q_2)^2, \quad (\text{III.3})$$

where  $s + u + t = N^{*2} + N^2 + 2\mu^2$ . One can easily show that the particle energies are

$$E_1 = \frac{1}{2W} (s + N^2 - \mu^2), \quad E_2 = \frac{1}{2W} (s + N^{*2} - \mu^2) \quad (\text{III.4})$$

$$Q_1^0 = \frac{1}{2W} (s - N^2 + \mu^2), \quad Q_2^0 = \frac{1}{2W} (s - N^{*2} + \mu^2);$$

and the magnitudes of the 3-momenta are

$$q_1 = \frac{1}{2W} \left\{ [(W+N)^2 - \mu^2][(W-N)^2 - \mu^2] \right\}^{1/2}$$

(III.5)

$$q_2 = \frac{1}{2W} \left\{ [(W+N^*)^2 - \mu^2][(W-N^*)^2 - \mu^2] \right\}^{1/2}$$

The  $\Upsilon$ -matrix form (III.2) can be reduced to a 3-vector form by using

$$u(P) = \frac{M - i\gamma \cdot P}{[2M(E+M)]^{1/2}} \chi$$

where  $\chi_{\pm}^{\pm 1/2}$  is a Pauli spinor. From (III.2), we then obtain the expression  $\bar{\chi}_\mu \mathcal{O}_\mu \chi$ , with

$$\mathcal{O}_\mu = (Q_1)_\mu \left[ \gamma_{\mu 1} \frac{(x \cdot Q_1)}{q_1} + \gamma_{\mu 2} \frac{(x \cdot Q_2)}{q_2} \right] + (Q_2)_\mu \left[ \gamma_{\mu 3} \frac{(x \cdot Q_3)}{q_1} + \gamma_{\mu 4} \frac{(x \cdot Q_4)}{q_2} \right]. \quad (\text{III.6})$$

The  $\gamma_{\mu i}$  ( $i=1, \dots, 4$ ) are defined by

$$\gamma_{\mu 1} = -\frac{1}{16\pi W^2} \left\{ [(W-N)^2 - \mu^2][(W+N^*)^2 - \mu^2] \right\}^{1/2} [A + \{W - \frac{1}{2}(N^* - N)\} B]$$

(III.7)

$$\gamma_{\mu 2} = -\frac{1}{16\pi W^2} \left\{ [(W+N)^2 - \mu^2][(W-N^*)^2 - \mu^2] \right\}^{1/2} [-A + \{W + \frac{1}{2}(N^* - N)\} B],$$

and  $\gamma_{\mu 3}, \gamma_{\mu 4}$  have exactly the same form as  $\gamma_{\mu 1}, \gamma_{\mu 2}$

respectively but with  $A, B$  replaced by  $C, D$ .

The next task is to express the partial wave amplitudes  $F_J(s)$  in terms of the invariant amplitudes  $A, B, C, D$ . This can be done by using the general formula

$$F_J(s) = \frac{1}{(2J+1)} \int d\Omega' \int d\Omega \sum_{J_z} \langle f | \mathcal{O}_\mu | i \rangle, \quad (\text{III.8})$$

where the initial and final states are linear combinations of spin and orbital angular momentum. The initial state is

$$|i\rangle = C_{\frac{1}{2}, 2} \left( \frac{3}{2}, J_z; +\frac{1}{2}, J_z - \frac{1}{2} \right) \chi_{\frac{1}{2}}^{+\frac{1}{2}} Y_2^{J_z - \frac{1}{2}}(\theta, \phi) \\ + C_{\frac{1}{2}, 2} \left( \frac{3}{2}, J_z; -\frac{1}{2}, J_z + \frac{1}{2} \right) \chi_{\frac{1}{2}}^{-\frac{1}{2}} Y_2^{J_z + \frac{1}{2}}(\theta, \phi);$$

and the final state ( $J' = 3/2, L' = 0$ ) is

$$|f\rangle = \left( \frac{1}{4\pi} \right)^{\frac{1}{2}} C_{\frac{3}{2}, 0} \left( \frac{3}{2}, J_z; J_z, 0 \right) \left( \Psi_{\pm 3/2}^{J_z} \right)_\mu.$$

As can be seen, the full expansion of (III.8) will contain a large number of Clebsch-Gordon coefficients and spherical harmonics; there is no difficulty involved

in deriving this expansion, but it is laborious. The resulting expressions are rather long and complicated, and need not be reproduced here. However, the work is greatly simplified by observing that the integrand of the  $\Omega$ -integration in (III.8) is rotationally invariant. This allows us to transform to the frame in which  $\theta' = 0$ , that is the one in which  $N^*$  is moving along the positive z-direction. We may therefore use the Kusaka wave functions (III.1) in the final state expansions. Further, the spherical harmonics may be combined by using the theorem<sup>(6)</sup>

$$Y_{\ell}^m(\theta, \phi) Y_{\ell'}^{m'}(\theta, \phi) = \sum_L \sum_M \left[ \frac{(2\ell+1)(2\ell'+1)}{4\pi(2L+1)} \right]^{1/2} C_{\ell\ell'}(L, 0; 0, 0) C_{\ell\ell'}(L, M; m, m') Y_L^M(\theta, \phi)$$

for spherical harmonics at the same angle.

We shall merely quote the final result obtained by the above method for the partial wave which is of interest to us ( $J = 3/2$ , D-wave going to S-wave):

$$F_{3/2}^{(s)} = \frac{\pi}{10\sqrt{3}} \int_{-1}^{+1} dx \left[ \left\{ \frac{q_1}{14} (33 - 56 \frac{E_2}{N^*}) P_4(x) + \frac{5q_1}{21} (16 + 4 \frac{E_2}{N^*}) P_2(x) - \frac{q_1}{6} (34 - 14 \frac{E_2}{N^*}) P_0(x) - \frac{9q_2 Q_1}{N^*} (P_3(x) - P_1(x)) \right\} \gamma_{\ell}^e \right.$$

(III.9)

$$+ 4q_1 (P_3(x) - P_1(x)) \gamma_{\ell}^e + \text{terms in } \gamma_{\ell}^e, \gamma_{\ell}^e \left. \right]$$

where the  $\gamma_i$  are related to the invariant amplitudes  $A, B, C, D$  by (III.7).

For the reaction  $\pi + N \rightarrow \pi + N^*$  with the angular momentum states already stated, we shall use the redefined amplitude

$$g_{23}(s) = \frac{W}{q_1^2} F_{3/2}(s) \quad , \quad (\text{III.10})$$

where channel (2) refers to  $\pi + N$ , and channel (3) to  $\pi + N^*$ .

## 2. Analytic properties

The important question at this stage is: do the invariant amplitudes  $A, B, C, D$  possess a Mandelstam representation? The answer is that they do not. This may be proved by examining the fourth order loop diagram in Figure 9. It is in fact a special case of the more

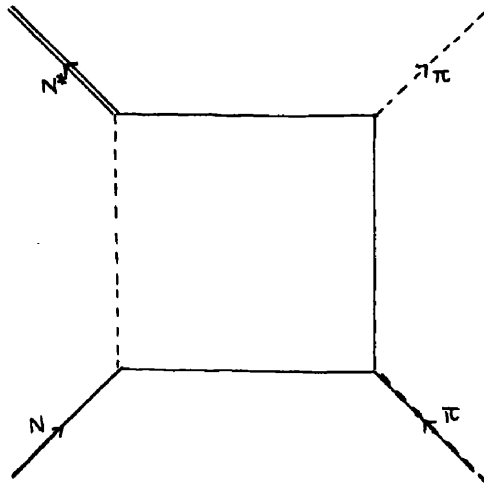


Figure 9

general situation investigated by the author<sup>61)</sup> in which an external stability condition<sup>48),49)</sup> is violated at one of the corners of a Feynman diagram. This paper, apart from a few minor alterations, has been included in Appendix B. It is shown that the scattering amplitude

has complex singularities, and these invalidate a Mandelstam representation.

It is no longer possible to calculate the discontinuities across most of the branch cuts of the partial wave amplitudes in the  $s$ -plane, as we did in Chapter II for pion-nucleon scattering. However, it is still possible to incorporate part of the  $\pi + N \rightarrow \pi + N^*$  reaction into our calculations, namely the contribution from the crossed single nucleon diagram, Figure 10.

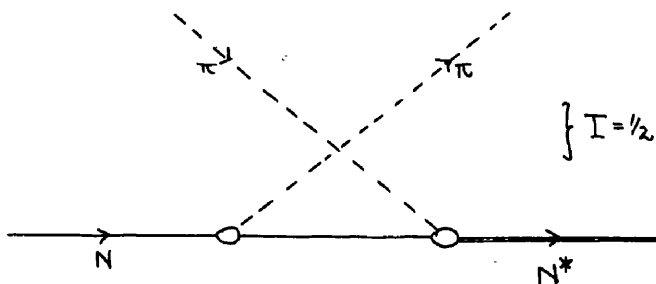


Figure 10.

In analogy to the pion-nucleon scattering case, the corresponding Born term here for  $\pi + N \rightarrow \pi + N^*$  will be of the form  $\frac{1}{(\omega - N^2)}$ . From (III.3) - (III.5), it

follows that

$$u - N^2 = a + b\alpha,$$

where  $\alpha = \cos \Theta$ , and

$$a = -\frac{1}{2s} \left\{ (s+N^2-\mu^2)(s-N^2+\mu^2) - 2\mu^2s \right\}$$

$$b = -\frac{1}{2s} \left\{ [s-(N+\mu)^2][s-(N-\mu)^2][s-(N^2+\mu)^2][s-(N^2-\mu)^2] \right\}^{1/2}. \quad (\text{III.11})$$

The resulting singularities of  $g_{23}(s)$  in the  $s$ -plane may now be deduced. After integration in (III.9) with respect to  $\alpha$ , we will obtain the logarithm term  $\log \left( \frac{a+b}{a-b} \right)$ . The argument becomes real and negative when the condition

$$a^2 = b^2 \alpha^2 \quad (0 \leq \alpha^2 \leq 1) \quad (\text{III.12})$$

is satisfied. The branch points of the corresponding cuts in the  $s$ -plane are given by the roots of (III.12) when  $\alpha^2 = 1$ ; (III.12) then reduces from a quartic equation in  $s$  to a quadratic, plus the two additional roots at  $s = 0$  and  $s = -\infty$ . The roots of the quadratic turn out to be

$$s = N^2 - \frac{\mu^2}{2N^2} (N^2 - N^2 - \mu^2) \pm i \frac{\mu}{N} \left\{ [N^2 - N^2 + \frac{\mu}{2N} (N^2 + 3N^2 - \mu^2)][N^2 - N^2 - \frac{\mu}{2N} (N^2 + 3N^2 - \mu^2)] \right\}^{1/2}.$$

For  $N = 6.72\mu$ ,  $N^* = 8.9\mu$ , these roots are the complex conjugate pair

$$s = 49.55 \pm i 4.6 \quad (\text{III.13})$$

The cuts of the Born amplitude  $g_{23}$  are therefore along the negative real axis  $-\infty \leq s \leq 0$ , and between the points (III.13). These are indicated in Figure 11, as well as the physical cut  $s \geq (N + \mu)^2$ . For the negative real axis, there is also an irrationality cut. Instead of

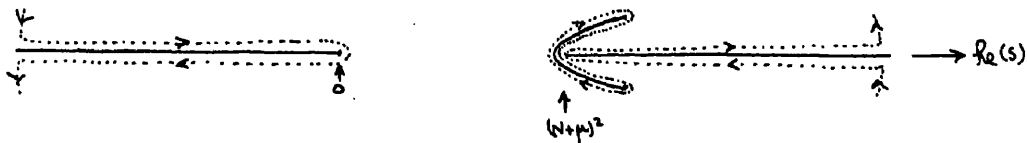


Figure 11.

employing the more accurate complex cut as shown, we took it (for ease of computation) as a straight line between the branch points. The discontinuities over the

unphysical cuts are not difficult to calculate: they are proportional to  $g_+ g_+^*$ , where  $g_+$  is the usual pion-nucleon coupling constant given by  $g_+^2 = 4\pi g^2$  ( $g^2 \approx 15$ ), and  $g_+^*$  is the coupling parameter for the  $\chi NN^*$  vertex.

3. Partial wave amplitude.

From a simple perturbation treatment for Figure 10, we may derive the single nucleon terms for the invariant amplitudes:

$$\begin{aligned}
 A &= 2\sqrt{\frac{2}{3}} \frac{-\frac{i}{2}(N+N^*)}{\omega-N^2} g_+ g_+^* \\
 B &= 2\sqrt{\frac{2}{3}} \frac{-i}{\omega-N^2} g_+ g_+^* \\
 b &= \mathcal{D} = 0.
 \end{aligned}
 \tag{III.14}$$

The  $2\sqrt{\frac{2}{3}}$  factor here is the isotopic spin factor for the state  $I = \frac{1}{2}$ .

The definition of  $g_+^*$  is arbitrary, but we have taken it so that the Hamiltonian for the  $\pi NN^*$  vertex is

$$\begin{aligned}
 g_+^* \left[ \overline{N}_{\frac{3}{2}}^* (\pi_1 N_{\frac{1}{2}}) - \overline{N}_{\frac{1}{2}}^* \left( \sqrt{\frac{2}{3}} \pi_0 N_{\frac{1}{2}} + \sqrt{\frac{1}{3}} \pi_1 N_{\frac{1}{2}} \right) \right. \\
 \left. + \overline{N}_{-\frac{1}{2}}^* \left( -\sqrt{\frac{1}{3}} \pi_{-1} N_{\frac{1}{2}} + \sqrt{\frac{2}{3}} \pi_0 N_{-\frac{1}{2}} \right) - \overline{N}_{-\frac{3}{2}}^* (\pi_{-1} N_{-\frac{1}{2}}) + h.c. \right]
 \end{aligned}$$

In order to find an estimate of  $g_+^*$ , it was assumed that the first pion-nucleon scattering resonance took place through the diagram shown in Figure 12, that is, with the  $N^*$  particle as the intermediate state. The matrix element for this Feynman diagram is

$$g_+^{*2} \bar{u}(p_2) (i q_2)_\mu \mathcal{D}_{\mu\nu}(k) (i q_1)_\nu u(p_1),
 \tag{III.15}$$

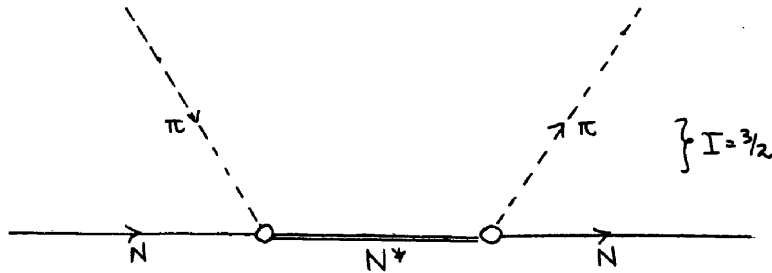


Figure 12.

where  $P_{\mu\nu}$  is the propagator function for the intermediate  $N^*$  particle (momentum  $k$ ), and is<sup>62)</sup>

$$P_{\mu\nu}(k) = \frac{\phi_{\mu\nu}(k)}{k^2 + N^{*2}}$$

with

$$\begin{aligned} \phi_{\mu\nu}(k) = (N^* - i\gamma \cdot k) & \left[ \delta_{\mu\nu} - \frac{1}{3} \gamma_\mu \gamma_\nu + \frac{i}{3N^{*2}} (\gamma_\mu k_\nu - k_\mu \gamma_\nu) + \frac{2}{3N^{*2}} k_\mu k_\nu \right] \\ & + \frac{2}{3N^{*2}} (k^2 + N^{*2}) \left[ i (\gamma_\mu k_\nu - k_\mu \gamma_\nu) - (N^* - i\gamma \cdot k) \gamma_\mu \gamma_\nu \right]. \end{aligned} \quad (\text{III.16})$$

When (III.16) is substituted into (III.15), the resulting

expression must reduce to the T-matrix formula (II.4) for pion-nucleon scattering. On doing this, one can find explicit expressions for A, B in terms of  $W, q, \chi$  and the masses of the interacting particles, as well as  $g_+^{*2}$ . Hence the partial wave amplitude  $g_{1+}^{3/2}(s)$  may be obtained from (II.13) and (II.14). This was compared with the corresponding sharp resonance formula

$$g_{1+}^{3/2}(s) = -\frac{4}{3} f^2 \frac{s(W_R - N)}{(W - N)} \cdot \frac{1}{(W - W_R)}$$

of Chew, Goldberger, Low and Nambu<sup>16)</sup>. Reasonable agreement over a range of values of  $s$  was obtained for  $g_+^{*2} \approx 6$ .

Substitution of (III.14), (III.7) and (III.9) into (III.10) yields the following expanded form for  $g_{23}^{1/2}(s)^N$ :

$$g_{23}^{1/2}(s)^N = 2\sqrt{\frac{2}{3}} \frac{i(W+N)g+g_+^*}{160\sqrt{3}q_1^2W} \left\{ [(W-N)^2 - \mu^2][(W+N^*)^2 - \mu^2] \right\}^{1/2} \\ \times \int_{-1}^{+1} dx \left[ \frac{q_1}{14} (33 - 56 \frac{E_2}{N^*}) P_4(x) + \frac{5q_1}{21} (16 + 4 \frac{E_2}{N^*}) P_2(x) \right. \\ \left. - \frac{q_1}{6} (34 - 14 \frac{E_2}{N^*}) P_0(x) - \frac{9q_2 Q_1^0}{N^*} (P_3(x) - P_1(x)) \right] \frac{1}{(a+bx)} \quad \text{(III.17)}$$

$$+ 2\sqrt{\frac{2}{3}} \frac{i(W+N)g+g_+^*}{160\sqrt{3}q_1^2W} \left\{ [(W+N)^2 - \mu^2][(W-N^*)^2 - \mu^2] \right\}^{1/2} \\ \times \int_{-1}^{+1} dx [4q_1 (P_3(x) - P_1(x))] \frac{1}{(a+bx)}$$

The absorptive parts across the cuts may be evaluated in the usual manner, and pole terms obtained from the Cauchy integrals. It was found that  $g_{23}^{1/2}(s)^N$  could be approximated by:

$$g_{23}^{1/2}(s)^N \approx \frac{14 + 25i}{s - (49.55 + i)} + \frac{14 - 25i}{s - (49.55 - i)} + \frac{-91}{s} \quad (\text{III.18})$$

From (III.18), it will be seen that the contribution from the negative real axis has been replaced simply by a pole at the origin.

#### 4. Results

At the present stage, there are now two channels available,  $\pi + N$  and  $\pi + N^*$ , which we will label as (2) and (3) respectively. They are both  $I = \frac{1}{2}$ ,  $J = \frac{3}{2}$  states. The extended  $N/D$  method of Bjorken (described in Chapter I, § 3) indicates how the two channels are coupled, and it is therefore possible to calculate the amplitude  $g_{22}^{1/2}$  for pion-nucleon scattering with the inelastic channel  $\pi + N^*$  explicitly taken into account.

The pole approximations for the single nucleon cut, the crossed physical cut and the  $\pi\pi$  cut of the pion nucleon scattering amplitude  $g_{22}^{1/2}(s)$  have been stated in (II.25), (II.33) and (II.53). As discussed in the present chapter, we have been able to obtain pole terms (III.18) for the Born amplitude of  $g_{23}^{1/2}$  (and hence also of  $g_{32}^{1/2}$ ). However the reaction  $\pi + N^* \rightarrow \pi + N^*$  is extremely complicated and prohibitively difficult to tackle; it has therefore been omitted completely in our work.

From a knowledge of the pole positions and the residues, one can easily re-calculate the pion-nucleon phase shifts  $\delta_{2-}^{1/2}$  having incorporated the effect of the Born term of the reaction  $\pi + N \leftrightarrow \pi + N^*$ . Our results

for this are presented in Figure 13.

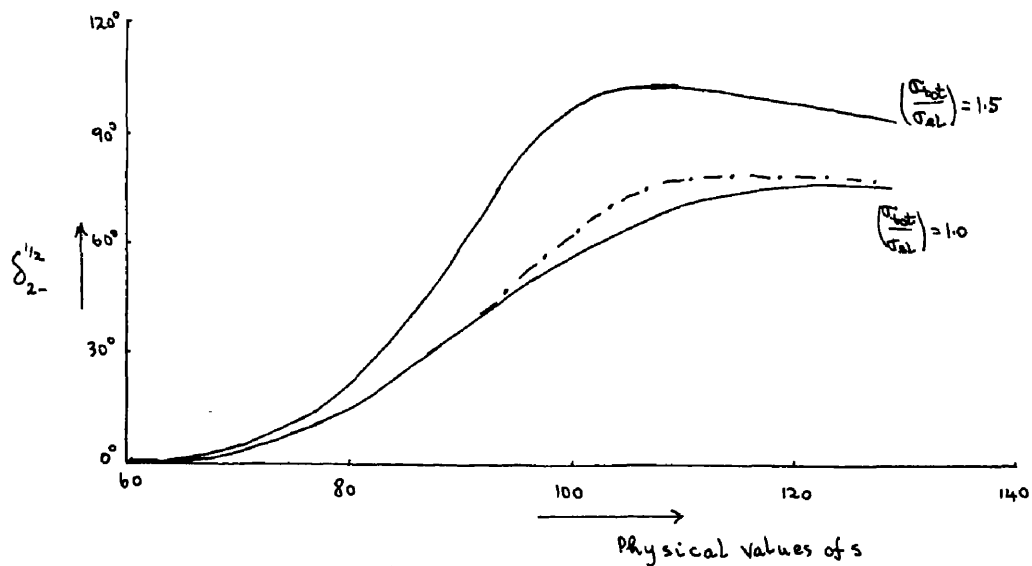


Figure 13

- \_\_\_\_\_ Single channel pion-nucleon scattering  
(all  $\pi N$  poles)
- Pion-nucleon scattering (all  $\pi N$  poles,  
 $\pi N^*$  poles included).

It will be seen that, although the  $\pi + N^*$  channel (as far as we have treated it) does not produce a significant alteration of the phase shifts, it certainly does enhance them above the values obtained for purely elastic pion-nucleon scattering with all other possible reactions neglected. However, the  $\delta_{2-}^{1/2}$  phase shifts remain dominated by the  $\pi\pi$  pole terms of  $g_{22}^{1/2}(s)$ . This result may well be an indication that it is the  $\pi\pi$  interaction which is providing the mechanism for the higher pion-nucleon resonances.

CHAPTER IV - PION PHOTOPRODUCTION

It is well-known that pion photoproduction is strongly dependent on pion-nucleon scattering. The close connection between the two processes is clearly indicated by the  $N/D$  method, which relates their various contributions in a definite manner. Such is the topic considered in the present chapter, and photoproduction is investigated with the knowledge of the results previously obtained for the reactions  $\pi + N \rightarrow \pi + N$  and  $\pi + N \rightarrow \pi + N^*$ . The procedure is similar to that used already in Chapters II and III. Pole approximations are calculated from the analytic properties of the amplitudes, with particular reference to the  $J = 3/2$ , magnetic and electric dipoles, since these are the states which are thought to give rise to the resonances in the photoproduction cross-sections.

1. Kinematics.

Most of the formulae in this section, as well as in the next, are contained in the works of Chew, Goldberger, Low and Nambu<sup>17)</sup>, and Ball<sup>43)</sup>; our notation is similar, though a few alterations have been made.

The 4- momenta of the interacting particles are denoted by  $P_2$ ,  $P_1$ ,  $Q$  and  $K$  corresponding to the outgoing and incoming nucleons, the pion and the photon respectively. The invariant scalars may be taken as

$$s = -(P_1 + K)^2, \quad u = -(P_2 - K)^2, \quad t = -(Q - K)^2; \quad (\text{IV.1})$$

they are the squares of the energies in the barycentric systems of the three reactions indicated in Figure 14.

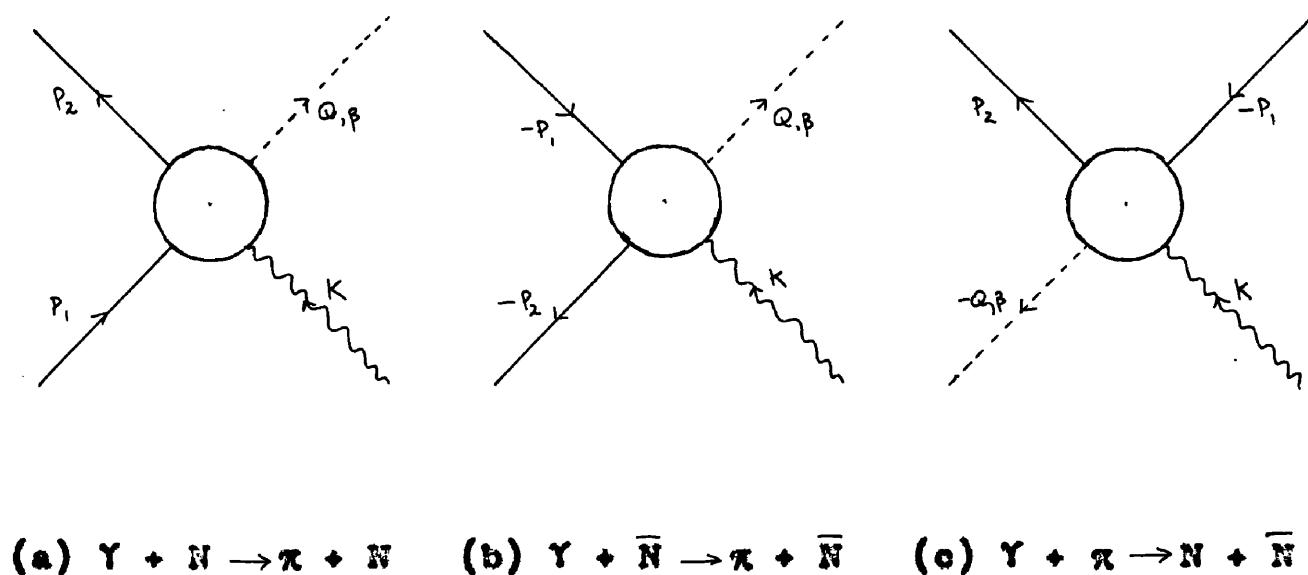


Figure 14.

In particular, we shall consider the photoproduction process. Here

$$s = W^2$$

$$u = N^2 - 2E_2 k - 2qk \cos\theta \quad (\text{IV.2})$$

$$t = \mu^2 - 2\omega k + 2qk \cos\theta$$

where  $\theta$  is the angle given by  $\cos\theta = \frac{(Q \cdot k)}{qk}$ ;  $E_2, E_1$  are the nucleon energies,  $\omega$  is the pion energy, and  $q, k$  are the magnitudes of the final and initial momenta respectively. In terms of  $s$  and  $W$ , we have

$$E_1 = \frac{1}{2W}(s + N^2), \quad E_2 = \frac{1}{2W}(s + N^2 - \mu^2), \quad \omega = \frac{1}{2W}(s - N^2 + \mu^2) \quad (\text{IV.3})$$

$$k = \frac{1}{2W}(s - N^2), \quad q = \frac{1}{2W} \left\{ [s - (N + \mu)^2][s - (N - \mu)^2] \right\}^{1/2}$$

The S-matrix element for the process is

$$S_{fi} = (2\pi)^4 i \delta^4(p_1 + k - p_2 - q) \frac{1}{(2\pi)^6} \left( \frac{N^2}{4E_1 E_2 \omega k} \right)^{1/2} \bar{u}(p_2) T u(p_1)$$

The T-matrix in turn may be expanded in the form

$$T = M_A A(s, u, t) + M_B B(s, u, t) + M_C C(s, u, t) + M_D D(s, u, t), \quad (\text{IV.4})$$

where  $A, B, C, D$  are invariant functions of  $s, u, t$ ,

and

$$\begin{aligned}
 M_A &= i\gamma_5 (\gamma \cdot \varepsilon)(\gamma \cdot \kappa) \\
 M_B &= 2i\gamma_5 \{ (P \cdot \varepsilon)(Q \cdot \kappa) - (P \cdot \kappa)(Q \cdot \varepsilon) \} \\
 M_C &= \gamma_5 \{ (\gamma \cdot \varepsilon)(Q \cdot \kappa) - (\gamma \cdot \kappa)(Q \cdot \varepsilon) \} \\
 M_D &= 2\gamma_5 \{ (\gamma \cdot \varepsilon)(P \cdot \kappa) - (\gamma \cdot \kappa)(P \cdot \varepsilon) - iN(\gamma \cdot \varepsilon)(\gamma \cdot \kappa) \},
 \end{aligned}
 \tag{IV.5}$$

with  $P = \frac{1}{2}(P_1 + P_2)$ .

The isotopic spin decomposition is

$$A^{(s,u,t)} = \delta_{\beta\beta} A^{(+)} + \frac{1}{2} [\tau_\beta, \tau_3] A^{(-)} + \tau_\beta A^{(0)},
 \tag{IV.6}$$

and similarly for  $B, C, D$ . The substitution law then yields the following crossing relations with respect to the interchange of  $s$  and  $u$ :

$$\begin{aligned}
 A^{(+,0)}, B^{(+,0)}, C^{(-)}, D^{(+,0)} & \quad \text{symmetrical} \\
 A^{(-)}, B^{(-)}, C^{(+,0)}, D^{(-)} & \quad \text{antisymmetrical}
 \end{aligned}
 \tag{IV.7}$$

We now wish to derive expressions for the angular momentum eigenamplitudes in terms of the invariant amplitudes  $A, B, C, D$ . We first of all note that the

differential cross-section is given by

$$\frac{d\sigma}{d\Omega} = \frac{q}{k} \left| \sum_s \chi_s^{\epsilon} \chi_s^{\epsilon} \right|^2,$$

where

$$\begin{aligned} \chi_s^{\epsilon} = & i(\underline{\sigma} \cdot \underline{\epsilon}) \chi_1^{\epsilon} + \frac{1}{qk} (\underline{\sigma} \cdot \underline{Q}) \underline{\sigma} \cdot (\underline{k} \times \underline{\epsilon}) \chi_2^{\epsilon} \\ & + \frac{i}{qk} (\underline{\sigma} \cdot \underline{k})(\underline{Q} \cdot \underline{\epsilon}) \chi_3^{\epsilon} + \frac{i}{q^2} (\underline{\sigma} \cdot \underline{Q})(\underline{Q} \cdot \underline{\epsilon}) \chi_4^{\epsilon}. \end{aligned} \quad (\text{IV.8})$$

The  $\chi_s^{\epsilon}$  are related to the  $A, B, C, D$  by

$$F_1 = 4\pi \frac{2W}{(W-N)} \frac{\chi_1^{\epsilon}}{\{(E_1+N)(E_2+N)\}^{1/2}} = A + (W-N)D - \frac{(t-\mu^2)}{2(W-N)}(C-D)$$

$$F_2 = 4\pi \frac{2W}{(W-N)} \left( \frac{E_2+N}{E_1+N} \right)^{1/2} \frac{\chi_2^{\epsilon}}{q} = -A + (W+N)D - \frac{(t-\mu^2)}{2(W+N)}(C-D)$$

$$F_3 = 4\pi \frac{2W}{(W-N)} \frac{\chi_3^{\epsilon}}{\{(E_2+N)(E_1+N)\}^{1/2} q} = (W-N)B + (C-D)$$

$$F_4 = 4\pi \frac{2W}{(W-N)} \left( \frac{E_2+N}{E_1+N} \right)^{1/2} \frac{\chi_4^{\epsilon}}{q^2} = -(W+N)B + (C-D),$$

(IV.9)

and these equations also serve as definitions for the  $F_i$  functions. On the other hand, the  $\chi_s^{\epsilon}$  may be expressed in terms of the multipole amplitudes:

$$Y_1 = \sum_{l=0}^{\infty} [l M_{l+} + E_{l+}] P'_{l+1}(x) + [(l+1) M_{l-} + E_{l-}] P'_{l-1}(x)$$

$$Y_2 = \sum_{l=1}^{\infty} [(l+1) M_{l+} + l M_{l-}] P'_l(x)$$

(IV.10)

$$Y_3 = \sum_{l=1}^{\infty} [E_{l+} - M_{l+}] P''_{l+1}(x) + [E_{l-} + M_{l-}] P''_{l-1}(x)$$

$$Y_4 = \sum_{l=1}^{\infty} [M_{l+} - E_{l+} - M_{l-} - E_{l-}] P''_l(x)$$

The multipole amplitudes  $M_{l\pm}$ ,  $E_{l\pm}$  are functions only of  $s$ ; they refer respectively to transitions initiated by magnetic and electric radiation, leading to final states of orbital angular momentum  $l$  and total angular momentum  $J = l \pm 1/2$ .

From conservation of total angular momentum and parity, one can easily deduce a table for possible transitions:

Angular Momentum			Multipole	Parity (total)
Final (orbital), $l$	Initial (orbital), $L$	Total, $J$		
$l$	$l$	$l - \frac{1}{2}$	Magnetic $2^L$	$(-1)^{L+1}$
$l$	$l-1$	$l - \frac{1}{2}$	Electric $2^L$	$(-1)^L$
$l$	$l$	$l + \frac{1}{2}$	Magnetic $2^L$	$(-1)^{L+1}$
$l$	$l+1$	$l + \frac{1}{2}$	Electric $2^L$	$(-1)^L$

Finally, (IV.10) may be reversed to obtain  $M_{l\pm}, E_{l\pm}$  in terms of the  $\gamma_i$  :

$$M_{l+} = \frac{1}{2(l+1)} \int_{-1}^{+1} dx \left[ \gamma_1 P_l(x) - \gamma_2 P_{l+1}(x) - \frac{1}{(2l+1)} \gamma_3 (P_{l-1}(x) - P_{l+1}(x)) \right] \quad l > 0$$

$$E_{l+} = \frac{1}{2(l+1)} \int_{-1}^{+1} dx \left[ \gamma_1 P_l(x) - \gamma_2 P_{l+1}(x) + \frac{l}{(2l+1)} \gamma_3 (P_{l-1}(x) - P_{l+1}(x)) + \left( \frac{l+1}{2l+3} \right) \gamma_4 (P_l(x) - P_{l+2}(x)) \right] \quad l \geq 0$$

$$M_{l-} = \frac{1}{2l} \int_{-1}^{+1} dx \left[ -\gamma_1 P_l(x) + \gamma_2 P_{l-1}(x) + \frac{1}{(2l+1)} \gamma_3 (P_{l-1}(x) - P_{l+1}(x)) \right] \quad l > 0 \quad \text{(IV.11)}$$

$$E_{l-} = \frac{1}{2l} \int_{-1}^{+1} dx \left[ \gamma_1 P_l(x) - \gamma_2 P_{l-1}(x) - \left( \frac{l+1}{2l+1} \right) \gamma_3 (P_{l-1}(x) - P_{l+1}(x)) - \left( \frac{l}{2l-1} \right) \gamma_4 (P_{l+1}(x) - P_l(x)) \right] \quad l > 1$$

(IV.11), together with (IV.9), yields the required relations between the multipole amplitudes  $M_{\ell\pm}$ ,  $E_{\ell\pm}$  and the invariant amplitudes  $A, B, C, D$ .

However, in order to retain the correct threshold behaviour as  $k^2 \rightarrow 0$  and  $q^2 \rightarrow 0$ , we shall employ redefined amplitudes. As stated before, we shall concentrate on the magnetic and electric dipoles which have  $J = 3/2$ ; that is,  $M_{1+}$  and  $E_{2-}$  respectively. The appropriate redefined amplitudes are

$$\mathcal{M}_{1+} = \frac{W^2 M_{1+}}{kq}, \quad \mathcal{E}_{2-} = \frac{W^2 E_{2-}}{q^2}. \quad (\text{IV.12})$$

Hence we may derive the expressions

$$\mathcal{M}_{1+} = \frac{W^2}{16\pi \{(W-N)^2 - \mu^2\}^{1/2}} \int_{-1}^{+1} dx \left[ F_1 P_1(x) - \frac{q}{(E_2+N)} F_2 P_2(x) - \frac{1}{3} q F_3 (P_0(x) - P_2(x)) \right] \quad (\text{IV.13})$$

$$\mathcal{E}_{2-} = \frac{W^2 (W^2 - N^2)}{16\pi \{(W+N)^2 - \mu^2\}^{1/2} \{(W-N)^2 - \mu^2\}} \int_{-1}^{+1} dx \left[ F_1 P_2(x) - \frac{q}{(E_2+N)} F_2 P_1(x) - \frac{3q}{5} F_3 (P_1(x) - P_3(x)) - \frac{2q^2}{3(E_2+N)} F_4 (P_0(x) - P_2(x)) \right]. \quad (\text{IV.14})$$

2. The Mandelstam representation; analytic properties.

For convenience, we shall denote the amplitudes

$A^{(j)}$ ,  $B^{(j)}$ ,  $C^{(j)}$ ,  $D^{(j)}$  by  $H^{(j)}$ ,  $j=1, \dots, 12$ . We assume that the invariant amplitudes satisfy a Mandelstam representation

$$\begin{aligned}
 H^{(j)}(s, u, t) = \text{Pole terms} &+ \frac{1}{\pi^2} \int_{(N+\mu)^2}^{\infty} \int_{(N+\mu)^2}^{\infty} \frac{h_{12}^{(j)}(s', u')}{(s'-s)(u'-u)} + \frac{1}{\pi^2} \int_{(N+\mu)^2}^{\infty} \int_{t_0}^{\infty} \frac{h_{13}^{(j)}(s', t')}{(s'-s)(t'-t)} \\
 &+ \frac{1}{\pi^2} \int_{(N+\mu)^2}^{\infty} \int_{t_0}^{\infty} \frac{h_{23}^{(j)}(u', t')}{(u'-u)(t'-t)}
 \end{aligned}
 \tag{IV.15}$$

Due to invariance under G-parity, the lower limit  $t_0$  depends on the isotopic spin; for the isotopic vector amplitudes  $^{(+,-)}$ ,  $t_0 = 9\mu^2$ ; whereas for the isotopic scalar amplitudes  $^{(0)}$ ,  $t_0 = 4\mu^2$ . The spectral functions are real, and the boundaries of the regions in which they are non-vanishing, are asymptotic to the lower limits.

The pole terms are more complicated; they correspond to the lowest order uncrossed and crossed nucleon diagrams.

$$A_{\left(\begin{smallmatrix} + \\ 0 \end{smallmatrix}\right)} : \quad \frac{1}{2} g_+ \begin{pmatrix} e_+ \\ e_+ \\ e_+ \end{pmatrix} \frac{1}{(s-N^2)} + \frac{1}{2} g_+ \begin{pmatrix} e_+ \\ -e_+ \\ e_+ \end{pmatrix} \frac{1}{(u-N^2)}$$

$$B_{\left(\begin{smallmatrix} + \\ 0 \end{smallmatrix}\right)} : \quad -\frac{1}{2} g_+ \begin{pmatrix} e_+ \\ e_+ \\ e_+ \end{pmatrix} \frac{1}{(t-\mu^2)(s-N^2)} - \frac{1}{2} g_+ \begin{pmatrix} e_+ \\ -e_+ \\ e_+ \end{pmatrix} \frac{1}{(t-\mu^2)(u-N^2)}$$

$$C_{\left(\begin{smallmatrix} + \\ 0 \end{smallmatrix}\right)} : \quad -\frac{1}{2} g_+ \begin{pmatrix} \mu'_{p_+} - \mu'_{n_+} \\ \mu'_{p_+} - \mu'_{n_+} \\ \mu'_{p_+} + \mu'_{n_+} \end{pmatrix} \frac{1}{(s-N^2)} + \frac{1}{2} g_+ \begin{pmatrix} \mu'_{p_+} - \mu'_{n_+} \\ -(\mu'_{p_+} - \mu'_{n_+}) \\ \mu'_{p_+} + \mu'_{n_+} \end{pmatrix} \frac{1}{(u-N^2)} \quad (\text{IV.16})$$

$$D_{\left(\begin{smallmatrix} + \\ 0 \end{smallmatrix}\right)} : \quad -\frac{1}{2} g_+ \begin{pmatrix} \mu'_{p_+} - \mu'_{n_+} \\ \mu'_{p_+} - \mu'_{n_+} \\ \mu'_{p_+} + \mu'_{n_+} \end{pmatrix} \frac{1}{(s-N^2)} - \frac{1}{2} g_+ \begin{pmatrix} \mu'_{p_+} - \mu'_{n_+} \\ -(\mu'_{p_+} - \mu'_{n_+}) \\ \mu'_{p_+} + \mu'_{n_+} \end{pmatrix} \frac{1}{(u-N^2)}$$

where  $e^2 = \frac{e_+^2}{4\pi} \approx \frac{1}{134}$ ,  $g^2 = \frac{g_+^2}{4\pi} \approx 15$ ,  $\mu'_{p_+} = 1.48 \left(\frac{e_+}{2N}\right)$  and  $\mu'_{n_+} = -1.91 \left(\frac{e_+}{2N}\right)$ .

For fixed  $s$ , the one-dimensional form of the Mandelstam representation (IV.15) is

$$H^{(j)}(s, u, t) = \text{Pole terms} + \frac{1}{\pi} \int_{(N+\mu)^2}^{\infty} du' \frac{H_2^{(j)}(s, u')}{(u'-u)} + \frac{1}{\pi} \int_{t_0}^{\infty} dt' \frac{H_3^{(j)}(s, t')}{(t'-t)}, \quad (\text{IV.17})$$

where

$$H_2^{(j)}(s, u) = \frac{1}{\pi} \int_{(N+\mu)^2}^{\infty} ds' \frac{h_{12}^{(j)}(s', u')}{(s'-s)} + \frac{1}{\pi} \int_{t_0}^{\infty} dt' \frac{h_{23}^{(j)}(u', t')}{(t'+s+u'-2N^2-\mu^2)}$$

$$H_3^{(j)}(s, t) = \frac{1}{\pi} \int_{(N+\mu)^2}^{\infty} ds' \frac{h_{13}^{(j)}(s', t')}{(s'-s)} + \frac{1}{\pi} \int_{(N+\mu)^2}^{\infty} du' \frac{h_{23}^{(j)}(u', t')}{(u'+s+t'-2N^2-\mu^2)} \quad (\text{IV.18})$$

In analogy to the pion-nucleon case,  $H_2^{(j)}$  and  $H_3^{(j)}$  are the

absorptive parts of  $H^{(j)}$  when the variables are in their physical regions for the reactions  $Y + \bar{N} \rightarrow \pi + \bar{N}$ ,  $Y + \pi \rightarrow N + \bar{N}$  respectively, indicated in Figures 14(h), (e).

We may now deduce the analytic properties of the multipole amplitudes in the  $s$ -plane.

(i) We first note that an uncrossed single nucleon diagram is not allowed for  $J = 3/2$  states; the pole term  $\frac{1}{(s-N^2)}$  therefore does not occur in the amplitudes  $M_H$ ,  $E_{2-}$  we are considering.

(ii) We may write

$$u - N^2 = - \left( \frac{s - N^2}{2s} \right) (a + bx)$$

$$t - \mu^2 = - \left( \frac{s - N^2}{2s} \right) (c - bx)$$
(IV.19)

where  $a = (s + N^2 - \mu^2)$ ,  $c = (s - N^2 + \mu^2)$  and  $b = \{ [s - (N + \mu)^2] [s - (N - \mu)^2] \}^{1/2}$ .

Hence one can deduce that the crossed single nucleon term gives rise to a pole at  $s = N^2$  and a cut along the negative real axis  $-\infty \leq s \leq 0$ .

(iii) The  $\frac{1}{(u-t)}$  term gives rise to singularities with branch points at  $s = 0$  and  $s = -\infty$ , as well as those given by the roots of the quadratic equation

$$u' s^2 + [u'^2 - (2N^2 + \mu^2)u' - N^2(N^2 - \mu^2)s] - N^2[(N^2 - \mu^2)u' - N^2(2N^2 - \mu^2)] = 0$$

with  $u' \geq (N + \mu)^2$ . These roots are all real, lying to the left of the point  $s = \frac{N}{(N + \mu)} (N^2 - N\mu - \mu^2)$ . The corresponding cut (a locus of branch points) is

$$-\infty \leq s \leq \frac{N}{(N + \mu)} (N^2 - N\mu - \mu^2) \quad (\text{IV.20})$$

The positive part of this cut (IV.20) corresponds to the physical region for the reaction  $\gamma + \bar{N} \rightarrow \pi + \bar{N}$  (Figure 14(b)) which is directly related to physical photoproduction (Figure 14(a)) by crossing.

(iv) Similarly, the branch points due to  $\frac{1}{(t' - t)}$  occur for  $s = 0$ ,  $s = -\infty$  and for the roots of the quadratic

$$t' s^2 + [t'^2 - (2N^2 + \mu^2)t']s + N^2[(N^2 - \mu^2)t' + \mu^4] = 0,$$

with  $t' \geq 4\mu^2$ . Examination of the discriminant shows that the roots are real provided that  $(t' - \mu^2)(t' - 4N^2) \geq 0$ .

For  $t' \geq 4N^2$ , the roots lie along the negative real axis

$-\infty \leq s \leq 0$ . For  $\mu^2 \leq t' \leq 4N^2$ , the roots are complex and of

the form  $s = \xi + i\eta$ , and it may be easily deduced that

they lie on the loop

$$2\xi(\xi^2 + \eta^2) - (2N^2 + \mu^2)(\xi^2 + \eta^2) - 2N^2(N^2 - \mu^2)\xi + N^4(2N^2 - \mu^2) = 0. \quad (\text{IV.21})$$

This loop is symmetrical about the real  $s$ -axis, and almost coincides with the circle  $|s| = N^2$ . For the range  $4\mu^2 \leq t' \leq 4N^2$ , we only get part of the loop, starting at the points

$$s = (N^2 - \frac{3}{2}\mu^2) \pm \frac{3\mu^2}{2} (N^2 - \mu^2)^{1/2}.$$

The discontinuity across this cut is related by the Mandelstam representation to the absorptive part of the reaction  $\Upsilon + \kappa \rightarrow N + \bar{N}$ , shown in Figure 14(o).

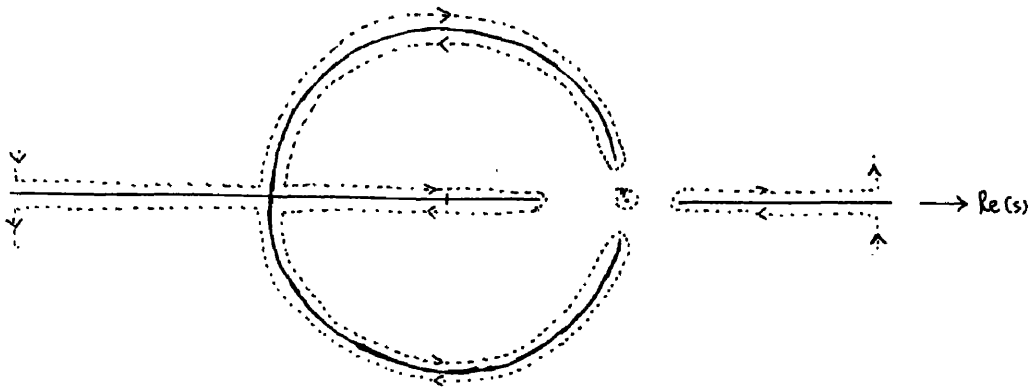


Figure 15

All of these singularities are drawn in Figure 15. We now obtain pole approximations for the various parts.

3. The single nucleon terms.

The single nucleon terms have been set out fully in (IV.16) (for the  $J = 3/2$  states, there are no  $\frac{1}{(S-N^2)}$  terms); they divide very conveniently into two types - contributions arising from the interaction of the photon with the charge and anomalous magnetic moment of the nucleon.

From (IV.9) and (IV.16), we obtain

$$\begin{aligned}
 F_{1,e} &= \frac{C_{e,t}}{(u-N^2)} \\
 F_{2,e} &= -\frac{C_{e,t}}{(u-N^2)} \\
 F_{3,e} &= -\frac{2(W-N)C_{e,t}}{(t-\mu^2)(u-N^2)} \\
 F_{4,e} &= \frac{2(W+N)C_{e,t}}{(t-\mu^2)(u-N^2)} ;
 \end{aligned}
 \qquad
 C_{e,t} = \frac{1}{2}g_t \begin{pmatrix} l_t \\ -l_t \\ l_t \end{pmatrix}
 \qquad
 \text{(IV.22)}$$

and

$$\begin{aligned}
 F_{1,\mu} &= \left[ -(W-N) - \frac{(t-\mu^2)}{(W-N)} \right] \frac{C_{\mu,t}}{(u-N^2)} \\
 F_{2,\mu} &= \left[ -(W+N) - \frac{(t-\mu^2)}{(W+N)} \right] \frac{C_{\mu,t}}{(u-N^2)} \\
 F_{3,\mu} &= \frac{2C_{\mu,t}}{(u-N^2)} \\
 F_{4,\mu} &= \frac{2C_{\mu,t}}{(u-N^2)}
 \end{aligned}
 \qquad
 C_{\mu,t} = \frac{1}{2}g_t \begin{pmatrix} \mu_{t+} - \mu_{t-} \\ -(\mu_{t+} - \mu_{t-}) \\ \mu_{t+} + \mu_{t-} \end{pmatrix}
 \qquad
 \text{(IV.23)}$$

These may now be inserted in (IV.13), (IV.14) for  $\mathcal{M}_H, \mathcal{E}_{2-}$ ; the residues at  $s = N^2$  and the absorptive parts along the negative real axis may then be determined.

For the pole at  $s = N^2$ , the  $\frac{a}{b} \log \left( \frac{a+b}{a-b} \right)$  term (where a,b are as given in (IV.19)) may be evaluated by expanding in powers of  $\frac{b^2}{a^2} = -\frac{\mu^2(4N^2 - \mu^2)}{(2N^2 - \mu^2)^2}$ . However, one cannot do this for  $\frac{c}{b} \log \left( \frac{c+b}{c-b} \right)$  since  $\frac{b^2}{c^2} = -\frac{1}{\mu^2}(4N^2 - \mu^2)$ ; in this case, the appropriate inverse tangent function was taken for the corresponding integral. It may further be noted that  $\mathcal{G}_{2-\mu}^{(s)N}$  does not have a pole at  $s = N^2$ .

The pole approximations were taken as

$$\mathcal{M}_H^{(\pm)}(s)N = \begin{pmatrix} 4.24 \\ -4.24 \\ 2.90 \end{pmatrix} \frac{1}{(s-N^2)} + \begin{pmatrix} 6.1 \\ -6.1 \\ 1.8 \end{pmatrix} \frac{1}{(s+150)} \quad (\text{IV.24})$$

$$\mathcal{G}_{2-}^{(\pm)}(s)N = \begin{pmatrix} 5.55 \\ -5.55 \\ 5.55 \end{pmatrix} \frac{1}{(s-N^2)} + \begin{pmatrix} 0.41 \\ -0.41 \\ -2.15 \end{pmatrix} \frac{1}{(s+150)}$$

4. The crossed-physical photoproduction cut.

As stated previously, the discontinuity across the positive real cut  $0 \leq s \leq \frac{N}{(N+u)} (N^2 - N^2 - u^2)$  can be related by crossing to the absorptive part of the physical photoproduction amplitude. We proceed to calculate the contribution from this cut in a manner similar to that used for the corresponding cut in pion-nucleon scattering.

Resolving (IV.9), we obtain

$$\begin{aligned}
 A(s,x) &= \frac{1}{2W} \left[ (W+N)F_1 - (W-N)F_2 + N(2N^2 - s - u) \left( \frac{F_3}{W-N} + \frac{F_4}{W+N} \right) \right] \\
 B(s,x) &= \frac{1}{2W} [F_3 - F_4] \\
 C(s,x) &= \frac{1}{2W} \left[ F_1 + F_2 + \frac{1}{2}(s-u) \left( \frac{F_3}{W-N} + \frac{F_4}{W+N} \right) \right] \\
 D(s,x) &= \frac{1}{2W} \left[ F_1 + F_2 + \frac{1}{2}(2N^2 - s - u) \left( \frac{F_3}{W-N} + \frac{F_4}{W+N} \right) \right]
 \end{aligned}
 \tag{IV.25}$$

The  $F_i(s,x)$  may be expanded in terms of the multipole amplitudes, as given in (IV.10); this is permissible on the crossed physical photoproduction cut, since it may be proved from the spectral functions that these expansions converge on this cut. We shall further assume that the expansions are dominated by the  $M_{\mu}^{(\pm)}$  amplitude (Chew, Goldberger, Low and Nambu showed that

this amplitude was the dominant one at low energies).

Hence it follows that

$$\begin{aligned}
 F_1 &\approx 4\pi \frac{12s x}{(s-N^2) [(W+N)^2 - \mu^2]^{1/2}} M_{1+}^{(s)} \\
 F_2 &\approx 4\pi \frac{2 [(W+N)^2 - \mu^2]^{1/2}}{kq} M_{1+}^{(s)} \\
 F_3 &\approx -4\pi \frac{6W}{kq [(W+N)^2 - \mu^2]^{1/2}} M_{1+}^{(s)} \\
 F_4 &\approx 0 ;
 \end{aligned}
 \tag{IV.26}$$

and using the replacements  $(t - \mu^2) = (2N^2 - s - u)$ ,  $x = \frac{1}{2kq} (t - \mu^2 + 2\omega k)$ , we derive the formulae

$$\begin{aligned}
 A(s, x) &= \mathcal{G}(s) [3(t - \mu^2) + 2\mu^2 + (W+N)\omega(s)] M_{1+}^{(s)} \\
 B(s, x) &= -3 \mathcal{G}(s) M_{1+}^{(s)} \\
 C(s, x) &= \mathcal{G}(s) \left[ \frac{3}{2} \left( \frac{t - \mu^2}{W+N} \right) + \omega(s) - (W+N) \right] M_{1+}^{(s)} \\
 D(s, x) &= \mathcal{G}(s) \left[ \frac{3}{2} \left( \frac{t - \mu^2}{W+N} \right) + \omega(s) + 2(W+N) \right] M_{1+}^{(s)}
 \end{aligned}
 \tag{IV.27}$$

where  $\mathcal{G}(s) = \frac{4\pi}{kq [(W+N)^2 - \mu^2]^{1/2}}$ ;  $k, q$  and  $\omega$  are given in (IV.3). The isotopic spin superscripts  $\left(\frac{t}{s}\right)$  have been

omitted throughout.

We shall make the additional assumption that it is the  $I = 3/2$  isotopic spin state which is the more important; thus

$$M_{1+}^{(+)}(s) \approx \begin{pmatrix} 2/3 \\ -1/3 \\ 0 \end{pmatrix} M_{1+}^{3/2}(s) \quad (\text{IV.28})$$

The isotopic spin <sup>(6)</sup> amplitude contributes only to  $I = 3/2$ . Chew, Goldberger, Low and Nambu have obtained a formula relating  $M_{1+}^{3/2}(s)$  to the pion-nucleon  $(\frac{3}{2}, \frac{3}{2})$  scattering amplitude  $f_{1+}^{3/2}(s)$ :

$$\frac{M_{1+}^{3/2}(s)}{kq} \approx \frac{(\mu_p - \mu_n)}{2f} \cdot \frac{f_{1+}^{3/2}(s)}{q^2} \quad (\text{IV.29})$$

where  $\mu_p, \mu_n$  are non-rationalised, and  $f^2 = 0.08$ . These approximations (IV.28) and (IV.29) may be substituted into (IV.27), yielding convenient formulae for A, B, C, D.

The contribution from the crossed physical photoproduction cut may be evaluated in a simple manner by introducing the functions

$$H^{(j)}(s, x)^x = \frac{1}{\pi} \int_{(N+1)^2}^{\infty} \frac{dw'}{(w' - w)} \text{Abs } H^{(j)}(w', s) \quad (\text{IV.30})$$

as in the pion-nucleon scattering case; these functions obviously have the correct analytic properties. The required absorptive parts of  $H^{(i)}(w, s)$  may be obtained from (IV.27) and the crossing relations (IV.7). The integrals in (IV.30) are greatly simplified by again using the sharp resonance formula

$$A_{bs} f_{+}^{3/2} = \frac{8\pi W_R}{3} \left(\frac{f}{\mu}\right)^2 q^2 \delta(W^2 - W_R^2).$$

[In his integrals, Ball uses an effective range formula].

Hence we obtain:

$$A_{\rho}^{(\frac{1}{2})}(s)^x = \begin{pmatrix} 2/3 \\ 1/3 \\ 0 \end{pmatrix} k_R q_R \rho_R \left[ 3(2N^2 - u_R - s) + 2\mu^2 + (W_R^2 + N) \omega_R \right] \frac{8W_R^x}{3} \left(\frac{\mu_p - \mu_n}{2f}\right) \left(\frac{f}{\mu}\right)^2 \int_{-1}^{+1} dx \frac{\rho_R(x)}{(u_R - u)}$$

$$B_{\rho}^{(\frac{1}{2})}(s)^x = - \begin{pmatrix} 2/3 \\ 1/3 \\ 0 \end{pmatrix} 3k_R q_R \rho_R \frac{8W_R^x}{3} \left(\frac{\mu_p - \mu_n}{2f}\right) \left(\frac{f}{\mu}\right)^2 \int_{-1}^{+1} dx \frac{\rho_R(x)}{(u_R - u)}$$

$$C_{\rho}^{(\frac{1}{2})}(s)^x = - \begin{pmatrix} 2/3 \\ 1/3 \\ 0 \end{pmatrix} k_R q_R \rho_R \left[ \frac{3}{2} \left( \frac{2N^2 - u_R - s}{W_R^2 + N} \right) + \omega_R - (W_R^2 + N) \right] \frac{8W_R^x}{3} \left(\frac{\mu_p - \mu_n}{2f}\right) \left(\frac{f}{\mu}\right)^2 \int_{-1}^{+1} dx \frac{\rho_R(x)}{(u_R - u)} \quad \text{(IV.31)}$$

$$D_{\rho}^{(\frac{1}{2})}(s)^x = \begin{pmatrix} 4/3 \\ 1/3 \\ 0 \end{pmatrix} k_R q_R \rho_R \left[ \frac{3}{2} \left( \frac{2N^2 - u_R - s}{W_R^2 + N} \right) + \omega_R + 2(W_R^2 + N) \right] \frac{8W_R^x}{3} \left(\frac{\mu_p - \mu_n}{2f}\right) \left(\frac{f}{\mu}\right)^2 \int_{-1}^{+1} dx \frac{\rho_R(x)}{(u_R - u)}$$

The quantities with suffix 'R' have W replaced by  $W_R^*$  in their definitions. (IV.31) may now be substituted into (IV.9) to yield expressions for  $\mathcal{M}_+^{(s)*}$  and  $\mathcal{E}_{2-}^{(s)*}$  from (IV.13), (IV.14).

The crossed cut is shortened slightly as a result of the sharp resonance approximation (as can be seen from the logarithm terms obtained from (IV.31); the limits (positive s) are given by the equations

$$(s-N^2) \left[ (s+N^2-\mu^2) \pm \left\{ [s-(N+\mu)^2][s-(N-\mu)^2] \right\}^{1/2} \right] + 2(W_R^{*2} - N^2)s = 0,$$

and can easily be computed to be

$$0 \leq s \leq 25.4\mu^2 \quad (\text{IV.32})$$

The corresponding pole approximations were found to be

$$\mathcal{M}_+^{(s)*} = \begin{pmatrix} 0.12 \\ 0.06 \\ 0 \end{pmatrix} \frac{1}{(s-25)} \quad (\text{IV.33})$$

$$\mathcal{E}_{2-}^{(s)*} = \begin{pmatrix} 1.66 \\ 0.83 \\ 0 \end{pmatrix} \frac{1}{(s-25)}$$

The negative axis part of the crossed photoproduction

cut is neglected; in order to estimate its contribution, we would need to know the values of the double spectral functions.

### 5. The $\Upsilon\pi$ cut

Very little is known about the process  $\Upsilon + \pi \rightarrow N + \bar{N}$ . However, in this section, an attempt is made to calculate its effect on photoproduction; it is hoped that the results we obtain for the  $\Upsilon\pi$  cut in this section is at least of the correct order of magnitude.

Figure 14(c) for the process  $\Upsilon + \pi \rightarrow N + \bar{N}$  can be derived from the photoproduction process (Figure 14(a)) by making the substitutions

$$P_1 \rightarrow P_1' = -P_1, \quad Q \rightarrow Q' = -Q. \quad (\text{IV.34})$$

In the barycentric system for the reaction, we have

$$\begin{aligned} s &= -(K - P_1')^2 = N^2 - 2Ek' - 2pk' \cos \theta' \\ u &= -(P_2 - K)^2 = N^2 - 2Ek' + 2pk' \cos \theta' \\ t &= -(Q' + K)^2 = (2E)^2 \end{aligned} \quad (\text{IV.35})$$

where  $p, k'$  are the magnitudes of the final and initial momenta respectively,  $E$  is the energy of a final state baryon, and  $\cos \theta' = \frac{1}{pk'} (P_2 \cdot K)$ .  $t$  is the square of the total barycentric energy, and

$$k' = \frac{1}{2\sqrt{t}} (t - m^2), \quad p = \frac{1}{2} (t - 4N^2)^{1/2}, \quad E = \frac{1}{2}\sqrt{t}. \quad (\text{IV.36})$$

The S-matrix element (from (IV.34)) is given by

$$S_{fi} = (2\pi)^4 i \delta^4(p_2 + p'_1 - k - Q') \left( \frac{N^2}{4E_1 E_2 \omega k} \right)^{1/2} \frac{1}{(2\pi)^6} \bar{u}(p_2) T(p'_1, p_2, Q', k) v(p'_1). \quad (\text{IV.37})$$

The differential cross-section is

$$\frac{d\sigma}{dR} = \frac{p}{k'} |\bar{X}_N \mathcal{G} y_N|^2,$$

where

$$\mathcal{G} = \frac{(p_2 \cdot \underline{\epsilon})}{p} g_1 + i \frac{\underline{\sigma} \cdot (p_2 \times \underline{\epsilon})}{p} g_2 + i \frac{(\underline{\sigma} \cdot p_2) p_2 \cdot (\underline{k} \times \underline{\epsilon})}{p^2 k'} g_3 + i \frac{\underline{\sigma} \cdot (\underline{k} \times \underline{\epsilon})}{k'} g_4. \quad (\text{IV.38})$$

The  $g_i$  of (IV.38) are related to the invariant amplitudes

A, B, C, D, and it can be shown that

$$A = \frac{8\pi E}{p^2 k'} [E g_3 + (E-N) g_4]$$

$$B = \frac{2\pi}{k' p E} \left[ 2 g_1 - \frac{E}{p} g_3 - \frac{(E-N)}{p} g_4 \right] \quad (\text{IV.39})$$

$$C = -\frac{4\pi}{p k'} g_2$$

$$D = \frac{4\pi}{p^2 k'} [N g_3 - (E-N) g_4].$$

The discontinuity across the  $\sqrt{s}$  cut can be obtained from the unitarity condition

$$\langle N\bar{N} | T - T^\dagger | \gamma\pi \rangle = \sum_n \langle N\bar{N} | T | n \rangle \langle n | T^\dagger | \gamma\pi \rangle \quad (\text{IV.40})$$

continued analytically from physical energies  $t \geq 4N^2$  to the interval  $4\mu^2 \leq t \leq 4N^2$ . It is assumed that the only important intermediate state in the expansion (IV.40) is a two-pion  $I = 1, J = 1$  state. An expansion can be made for the  $g_i$  in terms of helicity amplitudes, involving the reactions  $\gamma + \pi \rightarrow \pi + \pi$  and  $\pi + \pi \rightarrow N + \bar{N}$ . However, the helicity amplitudes for the latter reaction may be eliminated by re-expressing them in terms of the isotopic-vector electromagnetic form factors  $g_i^V(t)$  of the nucleon. The result of such a calculation (as given by Ball, and by Gourdin, Martin and Lurie) is

$$A_{\text{bs}} A^{\left(\begin{smallmatrix} \pm \\ 0 \end{smallmatrix}\right)}(t) = - \begin{pmatrix} 0 \\ 0 \\ 1 \end{pmatrix} t h(t) g_2^V(t)$$

$$A_{\text{bs}} B^{\left(\begin{smallmatrix} \pm \\ 0 \end{smallmatrix}\right)}(t) = \begin{pmatrix} 0 \\ 0 \\ 1 \end{pmatrix} h(t) g_2^V(t)$$

$$A_{\text{bs}} C^{\left(\begin{smallmatrix} \pm \\ 0 \end{smallmatrix}\right)}(t) = 0$$

$$A_{\text{bs}} D^{\left(\begin{smallmatrix} \pm \\ 0 \end{smallmatrix}\right)}(t) = \begin{pmatrix} 0 \\ 0 \\ 1 \end{pmatrix} h(t) g_1^V(t)$$

(IV.41)

The isotopic spin<sup>(6)</sup> amplitude is the only one which yields a contribution, since invariance under G-parity forbids two-pion states for the<sup>(+,-)</sup> amplitudes.  $h(t)$  is a real function arising from  $\Upsilon + \pi \rightarrow \pi + \pi$ , and Wong<sup>(42)</sup> has shown that an approximate form for it is

$$h(t) = \frac{3\Lambda}{8\sqrt{2} e F_{\pi}(t)} \left( \frac{1+\alpha}{1+\alpha+\beta} \right) \left( \frac{1}{t} + \frac{\beta}{t+\alpha} \right) \quad (\text{IV.42})$$

where  $\alpha = 5$ ,  $\beta = -65$ ,  $F_{\pi}(t)$  is the pion form factor with

$F_{\pi}(t) \simeq 1.08$ .  $\Lambda$  is an arbitrary constant, and Ball has deduced from examination of  $d\sigma(\pi^-)/d\sigma(\pi^+)$  that its magnitude is of the order of  $e$ . However, the helicity amplitude expansions are not valid over the whole of the cut, but only for part of it; it is shown in Appendix C that they are valid on the loop up to at most  $\sim 90^\circ$ .

It is convenient to have  $\delta$ -function approximations for the  $g_i^{\Upsilon}(t)$ ; and these may be derived from (II.43), (II.48) and (II.49) for  $g_i^{\Upsilon}(t)$ ,  $F_{\pi}(t)$  and  $\text{Abs } \Gamma_i(t)$  respectively. Remembering that  $g_i^{\Upsilon}(t)$  is real, we have from (II.43) that

$$g_i^{\Upsilon}(t) = - \left( \frac{e \xi^3}{2E} \right) \frac{\text{Im } \Gamma_i(t)}{\text{Im} \left( \frac{1}{F_{\pi}^*(t)} \right)}$$

from which we immediately obtain

$$g_1^Y(t) \approx 319.9 \frac{ef^2}{\mu} \delta(t-t_R) \quad (\text{IV.43})$$

$$g_2^Y(t) \approx 105.5 ef^2 \delta(t-t_R)$$

The contribution from the near part of the  $\Upsilon\pi$  loop may be found in a simple manner by introducing the functions

$$H^{(j)}(s)^{\delta\pi} = \frac{1}{\pi} \int_{t_1}^{\infty} dt' \frac{\text{Abs } H^{(j)}(t',s)}{(t'-t)} \quad (\text{IV.44})$$

which have the correct analytic properties. Substituting (IV.43) into (IV.40), we obtain from (IV.44)

$$A_{\rho}^{(+)}(s)^{\delta\pi} = - \begin{pmatrix} 0 \\ 0 \\ 1 \end{pmatrix} 105.5 t_R h(t_R) ef^2 \cdot \frac{1}{\pi} \int_{-1}^{+1} dx \frac{P_{\rho}(x)}{(t_R-t)}$$

$$B_{\rho}^{(+)}(s)^{\delta\pi} = \begin{pmatrix} 0 \\ 0 \\ 1 \end{pmatrix} 105.5 h(t_R) ef^2 \cdot \frac{1}{\pi} \int_{-1}^{+1} dx \frac{P_{\rho}(x)}{(t_R-t)}$$

$$C_{\rho}^{(+)}(s)^{\delta\pi} = 0 \quad (\text{IV.45})$$

$$D_{\rho}^{(+)}(s)^{\delta\pi} = \begin{pmatrix} 0 \\ 0 \\ 1 \end{pmatrix} 319.9 h(t_R) \frac{ef^2}{\mu} \cdot \frac{1}{\pi} \int_{-1}^{+1} dx \frac{P_{\rho}(x)}{(t_R-t)}$$

As a result of the  $\delta$ -function approximations (IV.43), the  $\Upsilon\pi$  cut shrinks a little, and for the Frazer-Fulco

$t_e \approx 11.5 \mu^2$ , the loop starts at the points

$$s = 40.04 \pm 19.94 i.$$

The corresponding formulae for  $M_{1+}(s)^{\delta\pi}$  and  $E_{2-}(s)^{\delta\pi}$  may now be obtained from (IV.45), and the pole approximations (for integrations round the near parts of the loop up to  $90^\circ$ ) were found to be

$$\begin{aligned} M_{1+}^{(\pm)}(s)^{\delta\pi} &= \begin{pmatrix} 0 \\ 0 \\ 1 \end{pmatrix} \frac{(0.45 - 1.04i) \Lambda}{s - (33.66 + 15.84i)} + \begin{pmatrix} 0 \\ 0 \\ 1 \end{pmatrix} \frac{(0.45 + 1.04i) \Lambda}{s - (33.66 - 15.84i)} \\ E_{2-}^{(\pm)}(s)^{\delta\pi} &= \begin{pmatrix} 0 \\ 0 \\ 1 \end{pmatrix} \frac{(0.13 + 0.4i) \Lambda}{s - (34.0 + 14.64i)} + \begin{pmatrix} 0 \\ 0 \\ 1 \end{pmatrix} \frac{(0.13 - 0.4i) \Lambda}{s - (34.0 - 14.64i)}. \end{aligned} \tag{IV.46}$$

These are small since  $|\Lambda| \approx e$ .

For the negative real axis and the back part of the loop of the  $\Upsilon\pi$  cut, one would need to know the spectral functions; and therefore they have been omitted from the present considerations.

6. Results.

The  $N/D$  method has again been employed, and the cross-sections for the photoproduction processes  $\gamma + p \rightarrow \pi^0 + p$ ,  $\gamma + p \rightarrow \pi^+ + n$  have been calculated. The differential cross-section for unpolarised photons and nucleons is<sup>43)</sup>

$$\begin{aligned} \frac{d\sigma}{d\Omega} = \frac{q}{k} & \left[ |\psi_1|^2 + |\psi_2|^2 + \frac{1}{2} |\psi_3|^2 + \frac{1}{2} |\psi_4|^2 + \operatorname{Re} \psi_1^* \psi_4 + \operatorname{Re} \psi_2^* \psi_3 \right. \\ & + \cos\theta \left\{ \operatorname{Re} \psi_3^* \psi_4 - 2 \operatorname{Re} \psi_1^* \psi_2 \right\} \\ & - \cos^2\theta \left\{ \frac{1}{2} |\psi_3|^2 + \frac{1}{2} |\psi_4|^2 + \operatorname{Re} \psi_1^* \psi_4 + \operatorname{Re} \psi_2^* \psi_3 \right\} \\ & \left. - \cos^3\theta \operatorname{Re} \psi_3^* \psi_4 \right] \end{aligned}$$

from which the total cross-section may be derived.

The two-channel case, (1)  $\gamma + N$  (2)  $\pi + N$ , was treated first, using the unitarity condition for the inverse of the pion-nucleon scattering amplitude  $\mathcal{G}_{22}^{(s)}$  stated in (II.54). Quantities were taken to only first order in the electromagnetic coupling constant  $e$ ; thus it may be deduced that

$$N_{11}(s) \approx 0$$

(IV.47)

$$g_{12}(s) \approx N_{12}(s) - D_{12}(s) \frac{N_{22}(s)}{D_{22}(s)}$$

$N_{22}(s)$ ,  $D_{22}(s)$  have already been evaluated in Chapter II, so that the problem reduces to determining  $N_{12}(s)$ ,  $D_{12}(s)$ .

In the pion-nucleon scattering case, we worked with the isotopic spin  $I = 3/2, 1/2$  eigenamplitudes. For photoproduction, we therefore carried out the computations first for the amplitudes  $\langle \gamma p | (\pi N)_{3/2} \rangle$  and  $\langle \gamma p | (\pi N)_{1/2} \rangle$ ; from (IV.6), they are related to the  $\begin{pmatrix} + \\ 0 \end{pmatrix}$  amplitudes by

$$\langle \gamma p | (\pi N)_{3/2} \rangle = \sqrt{\frac{2}{3}} [H^{(+)} - H^{(-)}]$$

(IV.48)

$$\langle \gamma p | (\pi N)_{1/2} \rangle = \sqrt{\frac{1}{3}} [H^{(+)} + 2H^{(-)} + 3H^{(0)}]$$

where  $H$  stands here for either  $\mathcal{M}_{1+}^{(s)}$  or  $\mathcal{E}_{2-}^{(s)}$ . The amplitudes of interest can then be found from

$$\langle \gamma p | \pi^0 p \rangle = \sqrt{\frac{2}{3}} \langle \gamma p | (\pi N)_{3/2} \rangle + \sqrt{\frac{1}{3}} \langle \gamma p | (\pi N)_{1/2} \rangle$$

(IV.49)

$$\langle \gamma p | \pi^+ n \rangle = -\sqrt{\frac{2}{3}} \langle \gamma p | (\pi N)_{3/2} \rangle + \sqrt{\frac{1}{3}} \langle \gamma p | (\pi N)_{1/2} \rangle$$

The pole approximations for the pion-nucleon  $I = 3/2, 1/2$  scattering amplitudes are given in Chapter II; (IV.48) indicates the appropriate combinations of the pole terms determined in the present chapter to be taken for the corresponding photoproduction amplitudes.

The experimental cross-sections are drawn in Figure 16; our own results are presented in Figures 17 and 18, corresponding to calculations involving  $M_{1+}^{(s)}$  and  $E_2^{(s)}$  respectively.

The first photoproduction resonance is obtained in Figure 17. The energy at which it occurs is rather low; this is due to the fact that the pion nucleon poles by themselves only produce a low energy scattering resonance (Figure 7(a)). The cross-sections are also larger than the experimental values. As an initial calculation, the  $J = 3/2$ , P-wave  $|(\pi N)_{3/2}\rangle$  state was neglected and only the  $|(\pi N)_{3/2}\rangle$  state taken into account. We see from the Figure that the  $\pi\pi$  pion-nucleon poles help to decrease the cross-sections. Also from the isotopic factors in (IV.49), these cross-sections for the reactions  $\gamma + p \rightarrow \pi^0 + p$  and  $\gamma + p \rightarrow \pi^+ + n$  are in the ratio 2:1. The inclusion of the  $|(\pi N)_{3/2}\rangle$  state reduces this ratio slightly, but not enough to give agreement with experiment. This

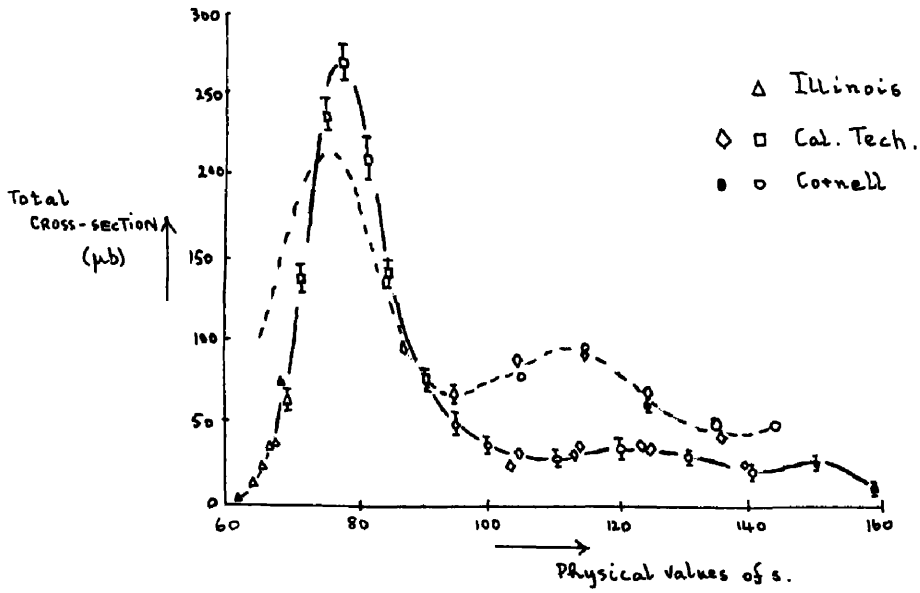
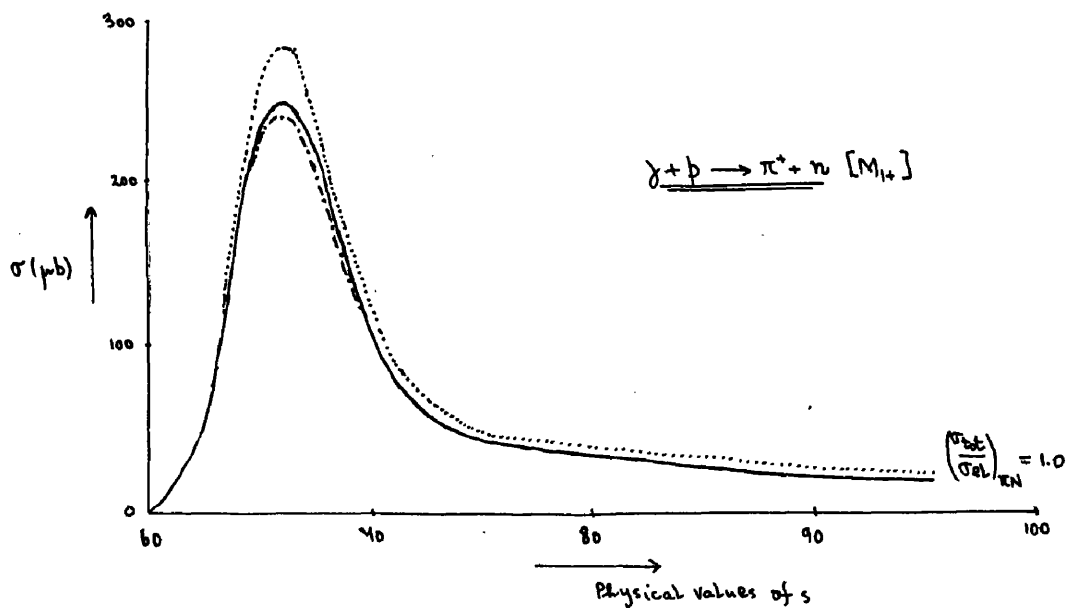
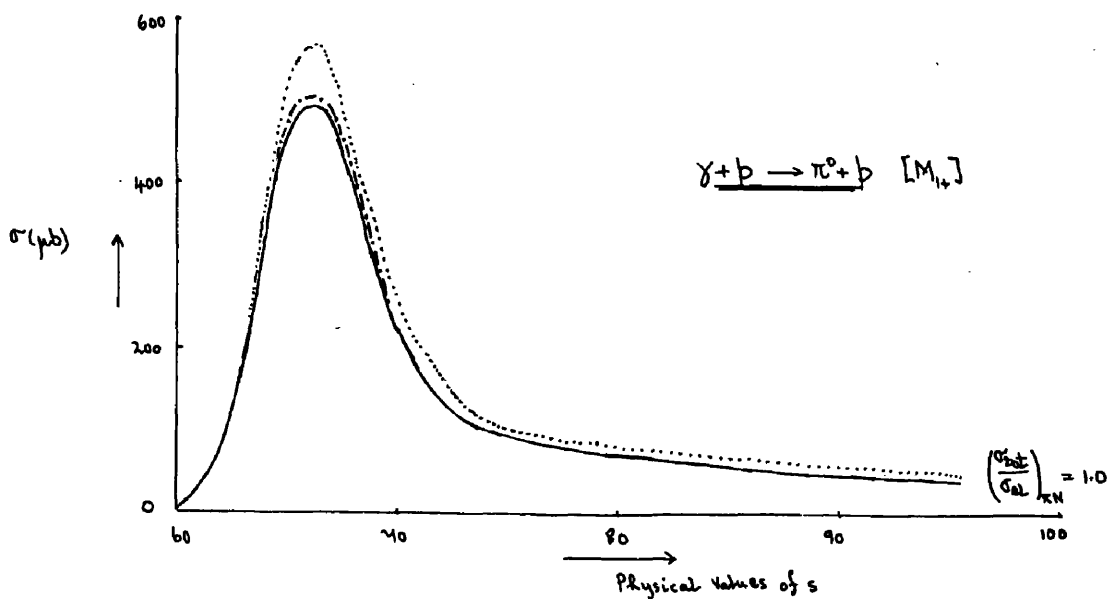


Figure 16.

Experimental results: —  $\gamma + p \rightarrow \pi^0 + p$   
-----  $\gamma + p \rightarrow \pi^+ + n$



**Figure 17**

- ..... Only single nucleon poles of  $|\pi N\rangle_{3/2}$  included
- - - - All poles of  $|\pi N\rangle_{3/2}$  included
- All poles of  $|\pi N\rangle_{3/2}$ ,  $|\pi N\rangle_{1/2}$  included.

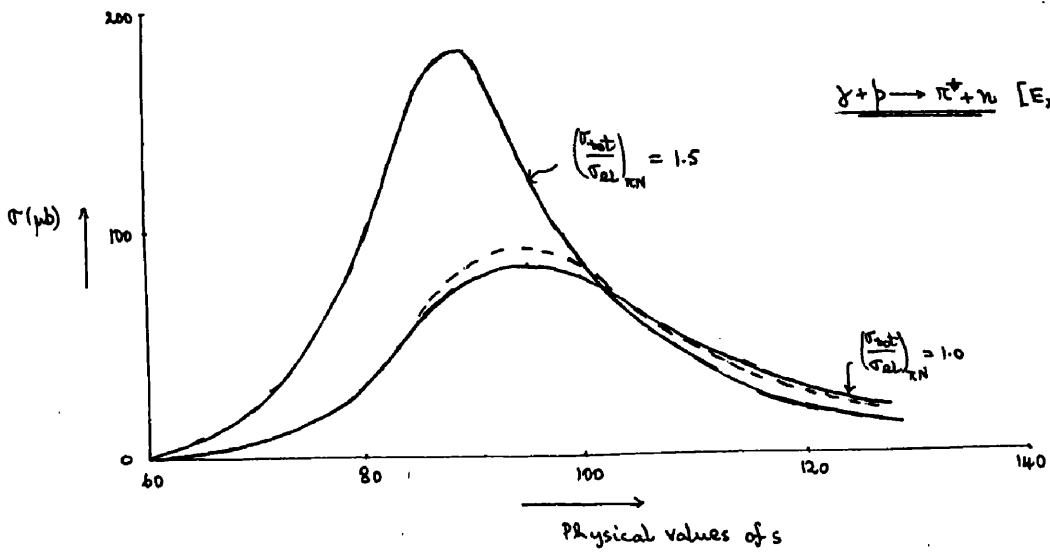
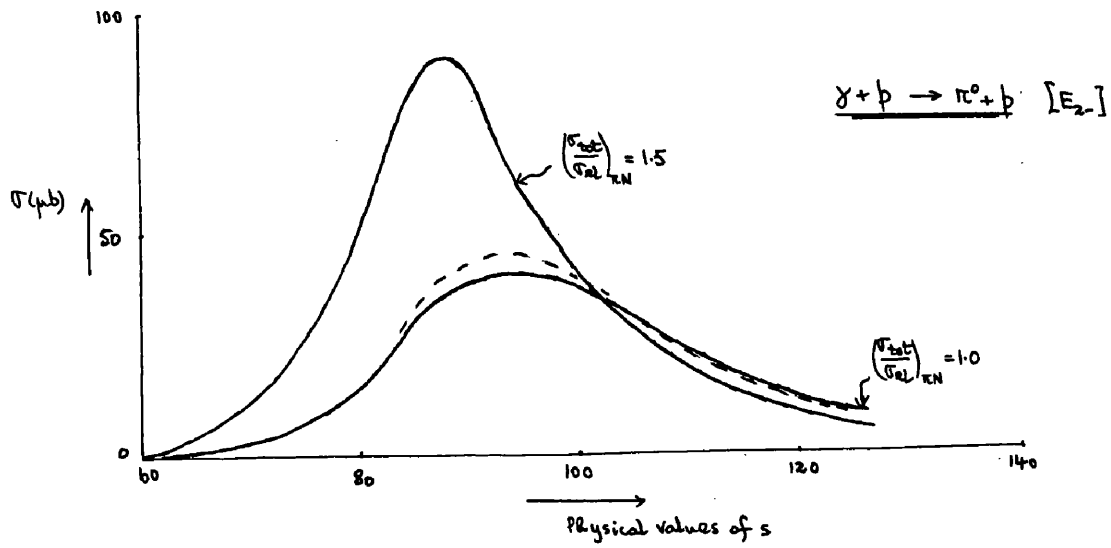


**Figure 18**

- All poles of  $|\pi N\rangle_{1/2}$  included
- All poles of  $|\pi N\rangle_{1/2}$  and  $|\pi N^*\rangle_{1/2}$  included.

would therefore seem to indicate that either we have under-estimated the  $|\pi N)_{1/2}\rangle$  state, or also other multipoles have the effect of reducing the ratio.

The second resonance is obtained in Figure 18. Again, the position is rather low, and the cross-sections large. The resonance is basically due to the dominant effect of the  $J = 3/2$ , D-wave  $|\pi N)_{1/2}\rangle$  state. The ratio 1:2 for the  $\gamma + p \rightarrow \pi^0 + p$ ,  $\gamma + p \rightarrow \pi^+ + n$  cross-sections at these higher energies arises from the isotopic spin factors in (IV.48); the effect of the  $|\pi N)_{1/2}\rangle$  state is small. Increasing  $(\sigma_{tot}/\sigma_{el})_{\pi N}$  above 1.0 causes the resonance to become more peaked, and its position is lowered.

It may be noted that the effect of the  $\gamma\pi$  photo-production cut is small. A range of values for  $\Lambda$  between  $-1.0e$  and  $+1.0e$  were considered; this caused alterations of only 2% and 3% on the  $\gamma + p \rightarrow \pi^0 + p$ ,  $\gamma + p \rightarrow \pi^+ + n$  cross-sections respectively.

Finally, the  $(\pi N^*)_{1/2}$  channel was also included in the calculations for the higher energy cross-sections. The results are indicated in Figures 18(a), (b). Because of their complication, the  $\pi + N^* \rightarrow \pi + N^*$  and  $\gamma + N \rightarrow \pi + N^*$  reactions were omitted.

CHAPTER V - DISCUSSION OF RESULTS

In the previous chapters, a very simple version of the theory has been employed to investigate pion-nucleon scattering and photoproduction up to second resonance energies. By using the various approximations described, we have been able to reproduce most of the qualitative features of the experimental data.

We have firstly considered the  $J = 3/2$ , P- and D-waves of pion-nucleon scattering, resonances being found in the  $I = 3/2$  and  $I = 1/2$  isotopic spin states respectively. In particular, it was noticed that, for the first resonance, the crossed single nucleon terms were the dominant ones, and the  $\pi\pi$  interaction had little effect. On the other hand, for the second resonance, the  $\pi\pi$  interaction played a very significant role, the single nucleon terms by themselves giving small, negative phase shifts  $\delta_2^{1/2}$ .

Since little is known with certainty about the  $\pi\pi$  interaction, our results indicate that some useful information about it might well be gleaned from a detailed study of the D-wave. It would of course be interesting to extend the present treatment to other partial waves, especially to the F-wave to see if it is

possible to obtain the third pion-nucleon resonance. Recently, the energy at which the  $I = 1 = J$   $\pi\pi$  resonance is thought to occur has increased<sup>45)</sup>, and the value favoured at the moment is  $t_R \approx 29\mu^2$ , as compared to the Frazer-Fulco  $t_R \approx 11.5\mu^2$  taken here. Obviously further calculations related to the work of this thesis, as well as for other partial-waves, should be made with this higher value of  $t_R$ . The  $I = 0 = J$   $\pi\pi$  state should also be included, since more data about this state is now becoming available.

The  $\pi N^*$  channel is rather difficult to handle, both because of the algebraic complication and also because the reactions involved do not satisfy a Mandelstam representation. However, we have shown by taking only the Born terms of  $\pi + N \longrightarrow \pi + N^*$  that the  $\delta_{2-}^{1/2}$  pion nucleon phase shift is certainly enhanced. Since we have already evaluated the coupling parameter for the  $\pi NN^*$  vertex, it should be possible to incorporate in addition the Born terms of the reaction  $\pi + N^* \longrightarrow \pi + N^*$  which is naturally involved in the matrix  $N/D$  method.

The results obtained in pion photoproduction depend to a great extent on those for pion-nucleon scattering; resonances in the photoproduction cross-section appear

as consequences of the corresponding scattering resonances, and this has been shown by our work on the  $J = 3/2$ , magnetic and electric dipole amplitudes. In addition, it was found that the  $\pi\pi$  pion-nucleon poles reduced the height of the first resonance photoproduction peaks, while variation of the constant  $\Lambda$  arising from the reaction  $\Upsilon + \pi \rightarrow \pi + \pi$  produced changes of only a few percent.

Again, further study should be devoted to other multipole amplitudes over all energies. In particular, one would like to determine the cause of the discrepancy (mentioned in Chapter IV) in the ratio of the first resonance peaks for the reactions  $\Upsilon + p \rightarrow \pi^0 + p$  and  $\Upsilon + p \rightarrow \pi^+ + n$ , and also which state (or states) gives rise to the third photoproduction resonance.

Our method has been greatly restricted by the lack of knowledge about various sections of the left-hand cuts, and we were unable to estimate their contributions. One would hope that it will not be too long before sufficient information is known about the double spectral functions themselves, when both pion-nucleon scattering and photoproduction may be solved by means of a complete theory.

ACKNOWLEDGMENTS

The author would like to express his gratitude to Dr. R.G. Moorhouse for his guidance, encouragement and assistance throughout the whole of this thesis.

He also wishes to thank Professor J.C. Gunn for his interest in the problem, and for the use of the facilities in the Department of Natural Philosophy.

The numerical calculations were carried out in two hundred hours or so on the university D.E.U.C.E. computer, and the author fully appreciates the co-operation of the maintenance staff of the Computing Department.

Finally, he gratefully acknowledges the receipt of a Studentship from the Department of Scientific and Industrial Research.

APPENDIX A - USEFUL INTEGRALS

We here set out a number of elementary integrals involving Legendre polynomials, and which are relevant to the thesis.

$$\int_{-1}^{+1} dx \frac{P_0(x)}{(a+bx)} = \frac{1}{b} \log \left( \frac{a+b}{a-b} \right)$$

$$\int_{-1}^{+1} dx \frac{P_1(x)}{(a+bx)} = \frac{1}{b} \left[ 2 - \frac{a}{b} \log \left( \frac{a+b}{a-b} \right) \right]$$

$$\int_{-1}^{+1} dx \frac{P_2(x)}{(a+bx)} = -\frac{3a}{b^2} + \frac{1}{2b} \left( \frac{3a^2}{b^2} - 1 \right) \log \left( \frac{a+b}{a-b} \right)$$

$$\int_{-1}^{+1} dx \frac{P_3(x)}{(a+bx)} = \frac{1}{b} \left[ \left( \frac{5a^2}{b^2} - \frac{4}{3} \right) - \frac{a}{2b} \left( \frac{5a^2}{b^2} - 3 \right) \log \left( \frac{a+b}{a-b} \right) \right]$$

$$\int_{-1}^{+1} dx \frac{P_4(x)}{(a+bx)} = \left( \frac{55a}{12b^2} - \frac{35a^3}{4b^4} \right) + \frac{1}{8b} \left( 35 \frac{a^4}{b^4} - 30 \frac{a^2}{b^2} + 3 \right) \log \left( \frac{a+b}{a-b} \right)$$

APPENDIX B

ON THE ANALYTICITY OF PARTIAL WAVE AMPLITUDES  
FOR UNSTABLE PARTICLES IN PERTURBATION THEORY

1. Introduction

In this appendix, we consider two-particle scattering processes of the type  $a + b \rightarrow c + d$ , in which one of the outgoing particles is unstable in the sense that an external stability condition<sup>48),49)</sup> is violated. If one considers the analytic properties of scattering amplitudes in terms of Feynman diagrams, as for example in Figure 19, then the external stability condition is

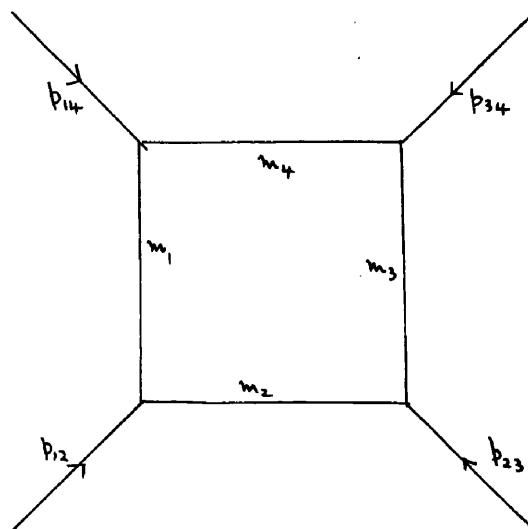


Figure 19

said to be violated at the (14) vertex, say, if  $|p_{14}|^2 > (m_1 + m_4)^2$ .

Such a situation might occur, for example, in the wide-angle pair production of electrons by photons on protons, as in Figure 20. For sufficiently high energy of the incident photon  $\gamma_1$ , an electron-positron pair may be produced by a virtual photon  $\gamma_2$  whose 4-momentum squared is large enough to violate an external stability condition in the proton Compton scattering amplitude.

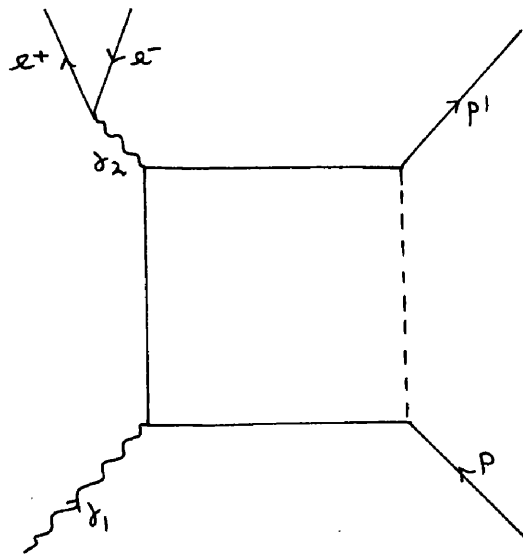
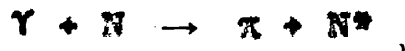
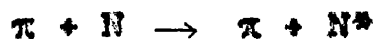


Figure 20

Another situation is in the consideration of the

production of particles using an isobar model  $N^*$ <sup>54</sup>),  
as in



where  $N^*$  subsequently decays into a nucleon and a pion. For these amplitudes (which are of course important in the rest of the thesis), the external stability condition may be violated at the  $N^*$  corner of a graph.

In § 2 (for completeness), we write down briefly some essential expressions and the equations of the surfaces of possible singularity for the scattering amplitude corresponding to the fourth order loop diagram in Figure 19. There is also a discussion of the physical sheet and of the contours of integration. In § 3, we investigate the behaviour of the scattering amplitude on these surfaces, and finally in § 4 describe the singularities of the corresponding partial wave amplitudes.

## 2. The scattering amplitude and Landau surfaces.

The scattering amplitude for the fourth order loop diagram in Figure 19 can be written (apart from a constant) in the form:

$$Y_\epsilon = \lim_{\epsilon \rightarrow 0^+} \int_0^1 \dots \int_0^1 d\alpha_1 \dots d\alpha_4 \frac{\delta(1 - \sum \alpha_i)}{[D_1(\alpha_i; p_{jk}) - i\epsilon]^2} \quad (\text{B.1})$$

where

$$D_1(\alpha_i; p_{jk}) = \sum_{i=1}^4 \alpha_i m_i^2 - \sum_{i < j} \alpha_i \alpha_j p_{ij}^2, \quad (\text{B.2})$$

and we have taken  $p_{13} = p_{12} + p_{23}$ ,  $p_{24} = p_{23} + p_{34}$ . It is more convenient<sup>48),49)</sup> to introduce the quantities

$y_{ij}$  ( $= y_{ji}$ ) defined by the equations

$$p_{ij}^2 = m_i^2 + m_j^2 - 2m_i m_j y_{ij} \quad \text{for } i \neq j \quad (\text{B.3})$$

$$y_{ii} = 1;$$

and to change the integration variables to  $x_i$ , given by

$$x_i = \frac{\alpha_i m_i}{\sum_{j=1}^4 \alpha_j m_j} \quad (\text{B.4})$$

The amplitude  $Y_\epsilon$  then reduces to the simple form:

$$Y_\epsilon = \lim_{\epsilon \rightarrow 0^+} \int_0^1 \dots \int_0^1 dx_1 \dots dx_4 \frac{N(x_i) \delta(1 - \sum x_i)}{[D(x_i; y_{jk}) - i\epsilon]^2}, \quad (\text{B.5})$$

where

$$D(x_i; y_{jk}) = \sum_{i,j=1}^4 x_i x_j y_{ij} \quad (B.6)$$

Let us suppose that the quantities  $y_{12}, y_{23}, y_{34}$  all satisfy both internal and external stability condition, while  $y_{14}$  violates an external stability condition; that is

$$-1 < y_{12}, y_{23}, y_{34} < +1, \quad y_{14} < -1. \quad (B.7)$$

$y_{13}$  and  $y_{24}$  are the variables in the theory; by (B.3), they are directly proportional to the more familiar energy-squared variables,  $s$  and  $t$ .

As can be seen directly from (B.2), the amplitude  $\mathcal{F}_\epsilon$  defined in (B.1) and (B.5) (with  $y_{13}, y_{24}$  in their real physical scattering regions) is precisely the Feynman amplitude, which is obtained by associating a small negative imaginary part to each  $m_i^2$  ( $i=1, \dots, 4$ ), the squares of the internal masses. So long as  $\epsilon \neq 0$ , the contours of integration may be taken along the real  $x_i$ -axes, and the integral in (B.5) is well-defined. However,  $\mathcal{F}_\epsilon$  may become singular in the limit as  $\epsilon$  tends

to zero, due<sup>63)</sup> to either an end-point singularity or a coincident singularity (pinching the contour) in each of the integrations.

As a consequence of  $\gamma_{14} < -1$ , all of the contours of integration in (B.5) may no longer be taken as real when  $\varepsilon$  is put equal to zero. For if  $\chi_2 = \chi_3 = 0$ , we find immediately that D vanishes at the points

$$\chi_1 = \frac{1}{2} \pm \frac{1}{2} \left( 1 - \frac{2}{1-\gamma_{14}} \right)^{1/2}, \quad \chi_4 = \frac{1}{2} \mp \frac{1}{2} \left( 1 - \frac{2}{1-\gamma_{14}} \right)^{1/2}; \quad (\text{B.8})$$

and it is important to note that D vanishes at these points for all values of the variables  $\gamma_{13}, \gamma_{24}$ . These points obviously do not pinch their respective contours, and so they may be avoided by deforming these contours off the real axes. This deformation must be carried out in such a way that  $\gamma_{\mathcal{E}}$  remains the physical scattering amplitude. By finding the zeros of the denominator in (B.5) with  $\chi_2 = \chi_3 = 0$  and  $\varepsilon \neq 0$ , and observing their movement as  $\varepsilon \rightarrow 0$ , we may deduce that, when  $\varepsilon = 0$ , the  $\chi_+$  and  $\chi_-$  contours are of the form indicated in Figure 21.

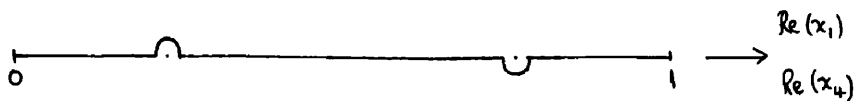


Figure 21

Also, the amplitude  $\gamma_e$  may be extended outside the physical scattering regions by continuing analytically in the variables  $y_{13}, y_{24}$ ; this constitutes the physical sheet<sup>50</sup>). In our subsequent investigations, we shall therefore consider the multi-sheeted function  $F(y_{13}, y_{24})$  defined by

$$F = \int_0^1 \dots \int_0^1 dx_1 \dots dx_4 \frac{N(x_i) \delta(1 - \sum_i x_i)}{[D(x_i; y_{ik})]^2}, \quad (\text{B.9})$$

where the  $x_1^-, x_4^-$  contours are as indicated in Figure 21, and the  $x_2^-, x_3^-$  contours are real; and determine in particular the singularities of  $F$  on its physical sheet.

It can easily be shown that  $F$  is certainly on its physical sheet when  $y_{13}, y_{24}$  both have small negative imaginary parts. Expanding  $D$ , we have

$$\begin{aligned} D(x_i; y_{13} - i\epsilon', y_{24} - i\epsilon') &= 2x_1 x_3 y_{13} + 2x_2 x_4 y_{24} \\ &+ \left[ \sum_{i=1}^4 x_i^2 + 2(x_1 x_2 y_{12} + x_2 x_3 y_{23} + x_3 x_4 y_{34} + x_4 x_1 y_{14}) \right] \\ &- 2i\epsilon' (x_1 x_3 + x_2 x_4), \end{aligned} \quad (\text{B.10})$$

and here the  $y_{13}, y_{24}$  on the right hand side are assumed to be in their physical regions.

With all the  $x_i$  real and so  $(x_1 x_3 + x_2 x_4)$  positive,

(B.10) obviously gives the Feynman denominator, as in (B.5). However, the factor  $(x_1 x_3 + x_2 x_4)$  can vanish in the four cases  $x_1 = x_2 = 0$ ,  $x_1 = x_4 = 0$ ,  $x_3 = x_4 = 0$  and  $x_2 = x_3 = 0$ . For the first three of these cases, it is easy to show that (B.10) reduces to a positive quantity (again giving the correct Feynman limit as  $\epsilon'$  tends to zero); for example, for  $x_1 = x_2 = 0$ , (B.10) becomes

$$x_3^2 + x_4^2 + 2x_3 x_4 \gamma_{34} = 1 - 2(1 - \gamma_{34}) x_3 (1 - x_3)$$

by eliminating  $x_4$  (using  $\sum_i x_i = 1$ ), and this has the positive minimum value of  $\frac{1}{2}(1 + \gamma_{34})$ ; similarly for the second and third cases. The fourth case,  $x_2 = x_3 = 0$ , corresponds precisely to the situation where we have the small contour deformations discussed above. Eliminating  $x_4$ , say, and putting  $x_1 = \xi + i\eta$  (where  $\eta$  is small, and  $\xi$  is in a neighbourhood of the points in (B.8)), we find that (B.10) contains the imaginary part

$$-2i(1 - \gamma_{14})(1 - 2\xi)\eta \quad ; \quad (\gamma_{14} < -1)$$

For the lower deformation,  $\xi < \frac{1}{2}$  and  $\eta > 0$ , while for the upper deformation,  $\xi > \frac{1}{2}$  and  $\eta < 0$ . Thus at each of the deformations, (B.10) still possesses a small negative

imaginary part, and so again is the correct Feynman denominator. (This is of course what we would have expected, since these contour deformations were in fact chosen to correspond to the Feynman limit).

Hence when  $y_{13}$  and  $y_{24}$  approach their real axes from their lower half-planes,  $F$  becomes identical with the Feynman amplitude  $\mathcal{F}$  and is therefore on its physical sheet.

The surfaces on which  $F$  may be singular, are given by the vanishing of the determinant and principal minors of the matrix  $\mathcal{D}$  :

$$\mathcal{D} = \begin{pmatrix} 1 & y_{12} & y_{13} & y_{14} \\ y_{12} & 1 & y_{23} & y_{24} \\ y_{13} & y_{23} & 1 & y_{34} \\ y_{14} & y_{24} & y_{34} & 1 \end{pmatrix} \quad (\text{B.11})$$

Explicitly, the equations of these surfaces are:

$$y_{13} = \pm 1, \text{ and } y_{24} = \pm 1 \quad ; \quad (\text{B.12})$$

$$\begin{aligned}
 L_4^\pm & : \quad y_{13} = y_{12} y_{23} \pm \left\{ (1 - y_{12}^2)(1 - y_{23}^2) \right\}^{1/2} \\
 L_2^\pm & : \quad y_{13} = y_{14} y_{34} \pm \left\{ (1 - y_{14}^2)(1 - y_{34}^2) \right\}^{1/2} \\
 L_3^\pm & : \quad y_{24} = y_{12} y_{14} \pm \left\{ (1 - y_{12}^2)(1 - y_{14}^2) \right\}^{1/2} \\
 L_1^\pm & : \quad y_{24} = y_{23} y_{34} \pm \left\{ (1 - y_{23}^2)(1 - y_{34}^2) \right\}^{1/2};
 \end{aligned}
 \tag{D.13}$$

and

$$\Delta(y_{ij}) \equiv \det \mathcal{D} = 0.
 \tag{D.14}$$

It will be noticed that, since  $y_{14} < -1$ , the surfaces  $L_2^\pm$  and  $L_3^\pm$  are complex. In Figure 22, we have drawn a typical curve  $\Gamma$  corresponding to the real solutions  $(y_{13}, y_{24})$  of the equation (D.14). ( $y_{13} = \pm 1$  and  $y_{24} = \pm 1$  are asymptotes to  $\Gamma$ ;  $L_4^\pm$  and  $L_1^\pm$  are the horizontal and vertical tangents respectively).

A picture of the surface  $\Sigma_1$  which connects the various parts of  $\Gamma$  and which arises from the complex conjugate roots of (D.14), may be obtained by using the usual search-line technique<sup>49</sup>).

We must now investigate whether  $F$  is singular or regular on the surfaces (D.12), (D.13) and (D.14) on its physical sheet.

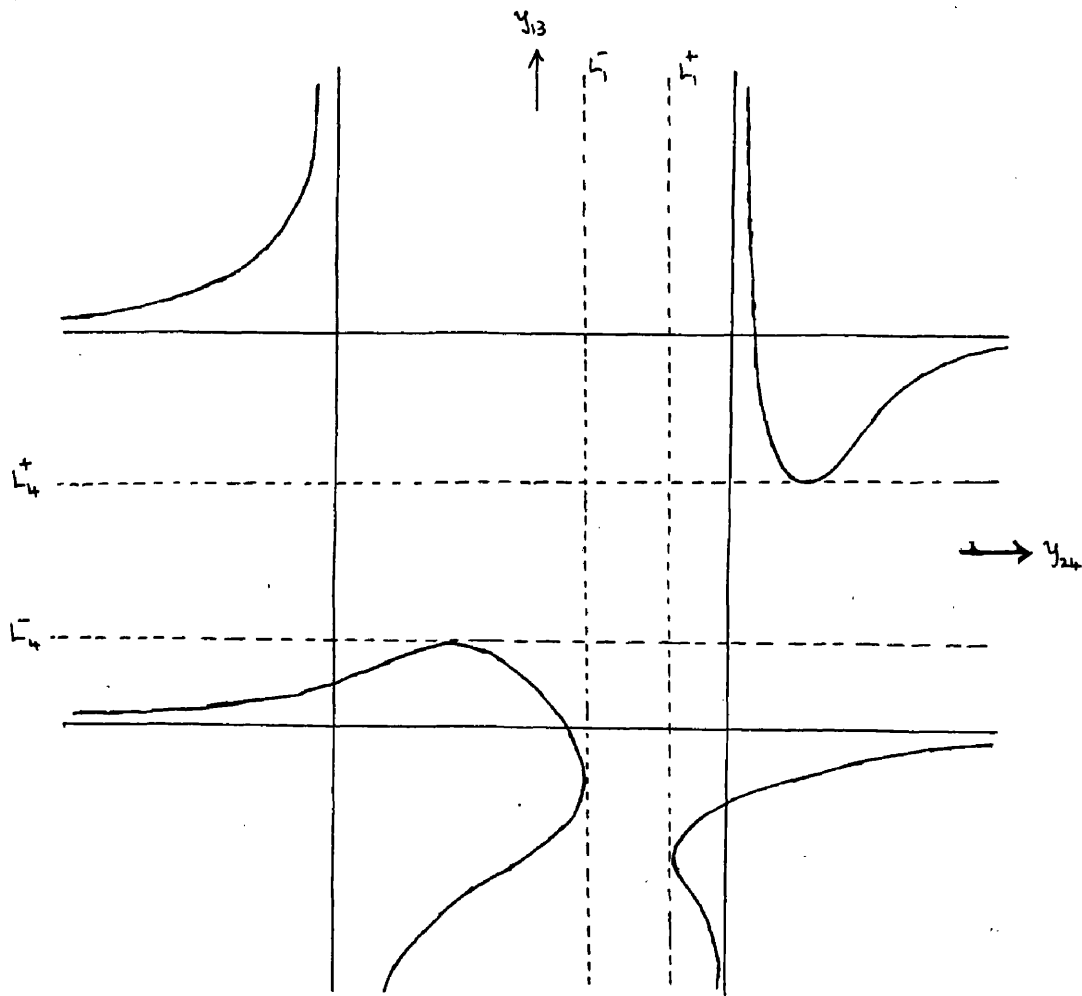


Figure 22.

3. The singularities of F.

One method<sup>51)</sup> of determining the singularities of a scattering amplitude is to perform an analytic continuation in the (real) external masses from a region

of known analyticity to a more extensive region containing the desired values of the external masses, and to observe the gradual development of the Landau surfaces. However, if one attempts to make a continuation in one of the external masses through the point where an external stability condition is violated, a singularity is found at that point. This may cause the sudden appearance and disappearance of singularities on the physical sheet of  $F$ , and so invalidates the above method.

The procedure adopted in this appendix is to consider the analytic continuation from a region  $\mathcal{R}$  which has

$\text{Im } y_{13} < 0$ ,  $\text{Im } y_{24} < 0$  (regular for the physical sheet of  $F$ ), up to and on to each of the various Landau surfaces (B.12), (B.13) and (B.14) separately.

For the surfaces  $y_{13} = \pm 1$ , we firstly note that we can continue analytically from  $\mathcal{R}$  up to neighbourhoods of these surfaces without needing to deform the contours of integration (other than the small deformations indicated in Figure 21, of course) since we can go by a route along which  $D$  does not vanish. Further, on these surfaces (which correspond to  $\alpha_2 = \alpha_4 = 0$ ),  $D$  reduces to

$$D = 1 + 2\alpha_1(1 - \alpha_1)(y_{13} - 1),$$

where we have eliminated  $x_3$  by the  $\delta$ -function in (B.5). As  $x_1$  varies along its contour from 0 to 1 (Figure 21), we see that  $D$  is always positive if  $y_{13} = +1$ , but vanishes (two coincident roots) at the point  $x_1 = \frac{1}{2}$  if  $y_{13} = -1$ . ( $D$  certainly does not vanish on the complex parts of the  $x_1$ -contour, since  $D$  acquires a non-zero imaginary part there). These roots pinch the contour (as may be shown by taking  $y_{14}$  slightly greater than  $-1$ ). Thus  $F$  is regular on the surface  $y_{13} = +1$ , but singular on the surface  $y_{13} = -1$ .

Similarly  $F$  is regular on  $y_{24} = +1$ , but singular on  $y_{24} = -1$ .

It may likewise be seen that no further contour deformations are necessary to reach the real tangential surfaces  $L_1^\pm, L_4^\pm$ , and in fact  $F$  is regular on these four surfaces provided that the conditions

$$y_{12} + y_{23} \geq 0, \quad y_{23} + y_{34} \geq 0 \quad (\text{B.15})$$

are satisfied. For example, on  $L_4^\pm$  (which correspond to  $x_4 = 0$ ),  $D$  reduces to

$$D = x_1^2 + x_2^2 + x_3^2 + 2x_1x_2y_{12} + 2x_2x_3y_{23} + 2x_1x_3y_{13},$$

with  $\alpha_1 + \alpha_2 + \alpha_3 = 1$ . For  $\alpha_1$  real, Karplus et al.<sup>48)</sup> have shown that this D can be expressed as a positive definite quadratic form ( $\gamma_{ij} > -1 \sim L_4^\pm$ ) if the first of the conditions (B.15) holds. For complex  $\alpha_1 = \xi + i\eta$ , where  $\xi$  is in the neighbourhood of the points in (B.8), D can be written (eliminating  $\alpha_3$ , say) in the form

$$D = (ax_2^2 + bx_2 + c) + i\eta(dx_2 + e).$$

For D to vanish, both its real and imaginary parts must vanish simultaneously. However, the resulting quadratic and linear equations in  $\alpha_2$  are not consistent, and so D is non-zero also in the complex parts of the  $\alpha_1$ -contour. Therefore, because of the non-vanishing of D, F is regular on  $L_4^\pm$ ; and similar arguments apply for  $L_1^\pm$ . It may be noted that the conditions (B.15) are not really very restrictive, and are certainly satisfied for the examples mentioned in §1 of this appendix (in fact,

$\gamma_{12}, \gamma_{23}, \gamma_{34}$  are all positive there).

Similar results of regularity do not hold, however, on all of the complex tangential surfaces  $L_2^\pm, L_3^\pm$ <sup>64)</sup>, as may be deduced from the investigations of Landshoff and Treiman<sup>65)</sup> who considered the reduced vertex diagram

to which these surfaces correspond; they showed that, whereas  $L_2^-, L_3^-$  are regular,  $L_2^+, L_3^+$  are singular. That  $F$  is regular on  $L_2^-, L_3^-$  follows from the fact that we may easily continue analytically from  $R$  up to and on to these surfaces without  $D$  vanishing. However, in order to go from the region  $R$  (which has  $\text{Im } y_{13} < 0, \text{Im } y_{24} < 0$ ) to a neighbourhood of  $L_2^+$ , say, (which has  $\text{Im } y_{13} > 0$ ), we must pass through the real point where  $\text{Im } y_{13} = 0$ , and  $D$  can vanish for a point on the previously chosen integration contours. This singularity may nevertheless be avoided by further deforming these contours; this can certainly be done, since we are not yet on any of the Landau surfaces and these are the only surfaces where we may have unavoidable singularities. Thus we must continually deform the contours as we enter the upper half  $y_{13}$ -plane and approach  $L_2^+$  until, when we finally reach  $L_2^+$ , the contours can retreat no further and are pinched by coincident singularities. Hence we are unable to continue  $F$  analytically from  $R$  on to  $L_2^+$ , or similarly on to  $L_3^+$ .  $F$  is therefore singular on  $L_2^+, L_3^+$  on its physical sheet.

Just as for the real tangents  $L_1^\pm, L_4^\pm$  we may continue from  $R$  up to the real curve  $\Gamma$  without further contour

deformation. For the behaviour of  $F$  on  $\Gamma$ , the method of Fowler et al.<sup>66)</sup> was used:  $D$  vanishes on  $\Gamma$  at the points  $x_i$  ( $i=1, \dots, 4$ ) given by

$$\frac{x_1}{\Delta_1^k} = \frac{x_2}{\Delta_2^k} = \frac{x_3}{\Delta_3^k} = \frac{x_4}{\Delta_4^k} \quad \text{for any } k \text{ (} k=1, \dots, 4 \text{)} \quad (\text{B.16})$$

where  $\Delta_j^i$  is the cofactor of  $y_j$  in the expansion of  $\Delta \equiv \det \mathcal{D}$ . Since all the cofactors in (B.16) are real, and  $\sum x_i = 1$ , it may be deduced that (B.16) is satisfied only when the  $x_i$  ( $i=1, \dots, 4$ ) are real. Therefore, since the allowed real values of the  $x_i$  in (B.5) are only positive, we must determine the region  $R$  in the real  $y_{13}, y_{24}$  plane (Figure 22) where the cofactors in (B.16), regarded as functions of  $y_{13}$  and  $y_{24}$ , have the same sign.

It is convenient here to take  $k=2$  because, for  $y_{14} < -1$ ,  $\Delta_2^2$  is negative for all real  $y_{13}, y_{24}$ . The regions where the other three cofactors are negative can easily be obtained, and it is found that no part of  $\Gamma$  lies in the intersection ( $R$ ) of these regions. Therefore  $D$  does not vanish anywhere on  $\Gamma$  for the allowed positive values of the  $x_i$ -variables of integration; and thus

$F$  is regular both on  $\Gamma$  and also on that part of  $\Sigma_1$  sprouting out along  $\Gamma$ .

However,  $F$  is not regular on the whole of  $\Sigma_1$ : it is singular on that section which is separated off from the rest of  $\Sigma_1$  by the branch cut joining the points of contact of  $L_2^+$  and  $L_3^+$  with  $\Sigma_1$ . (The 1-dimensional branch cut on this 2-dimensional surface  $\Sigma_1$ , which lies in the 4-dimensional  $y_{13}^-$ ,  $y_{24}^-$  space, divides  $\Sigma_1$  into two separate sections).

The singularities of the scattering amplitude  $F$  are therefore the real threshold singularities at  $y_{13} = -1$ ,  $y_{24} = -1$ , and complex singularities at values of  $y_{13}$ ,  $y_{24}$  corresponding to  $L_2^+$ ,  $L_3^+$  and the above singular section of  $\Sigma_1$ . The presence of these complex singularities invalidates a Mandelstam representation for  $F$ .

4. The singularities of the partial wave amplitudes

The singularities of the partial wave amplitudes of  $F$ :

$$f_\ell(s) = \int_{-1}^{+1} d(\cos\theta) F(s, \cos\theta) P_\ell(\cos\theta)$$

are slightly simpler than those of  $F$  itself, as a result

of the theory of Taylor and Warburton<sup>67)</sup>. They showed that, in the case when all the stability conditions are satisfied, the partial wave amplitudes do not possess complex singularities due to the singular parts of  $\zeta_1$ , since these singularities depend on the internal masses squared  $m_i^2$  only as differences. By a slight extension of their argument, the same is true even when an external stability condition is violated; and  $f_2(s)$  has no complex singularities arising from the singular section of  $\zeta_1$ .

In Figure 23, we have indicated a typical cut s-plane

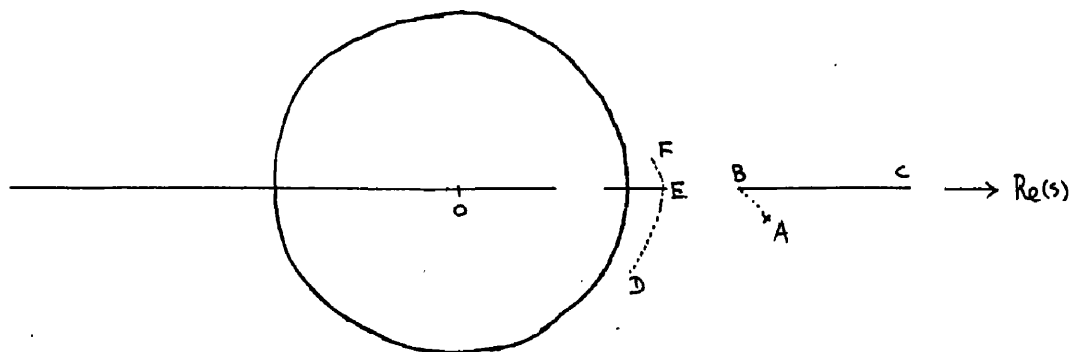


Figure 23.

for  $f_2(s)$ . Besides the usual physical cut and the u-, t-cuts, there are branch cuts arising from  $L_2^+$ ,  $L_3^+$ .

The cut due to  $L_2^+$  starts at the complex point A, and may be taken so that it joins up with the physical cut BC. The surface  $L_3^+$  produces a similar cut in the t-plane, and this becomes the cut DEF (the locus of branch points) shown in the s-plane. However, it may be remarked that these latter branch cuts from  $L_2^+$ ,  $L_3^+$  are not directly related to any physical process, and so it is no longer easy to determine the discontinuities across them. It also seems very difficult at present to see what new singularities will be introduced into the above s-plane from higher order perturbation diagrams.

APPENDIX C.

VALIDITY OF LEGENDRE POLYNOMIAL EXPANSIONS

The convergence of the Legendre polynomial expansions in the complex  $s$ -plane is investigated with the use of the following theorem:

If  $F(z)$  is analytic inside an ellipse with foci at  $z = \pm 1$ , then it can be expanded in a Legendre series

$$F(z) = \sum_l a_l P_l(z) \quad \text{within the ellipse.}$$

We shall consider first the  $\Upsilon\pi$  cut for which  $4\mu^2 \leq t \leq 4N^2$ . The region of convergence of the Legendre polynomial expansions used is limited by the singularities of  $H_3^{(j)}(s, t')$  in the complex  $\cos \theta'$ -plane. From (IV.35), we have

$$y(t, s) = \cos \theta' = \frac{-1}{2k\rho} (s - N^2 + 2kE) = - \frac{2\sqrt{E} (s + \frac{1}{2}t - N^2 - \frac{1}{2}\mu^2)}{(t - \mu^2)(t - 4N^2)^{1/2}}, \quad (\text{C.1})$$

where of course  $t$  is the square of the energy for the process  $\Upsilon + \pi \rightarrow N + \bar{N}$ .

The expression for  $H_3^{(j)}(s, t')$  is given in (IV.18) :

$$H_3^{(j)}(s, t') = \frac{1}{\pi} \int_{(N+\mu)^2}^{\infty} ds' \frac{h_{13}^{(j)}(s', t')}{(s' - s)} + \frac{1}{\pi} \int_{(N+\mu)^2}^{\infty} du' \frac{h_{23}^{(j)}(u', t')}{(u' + s + t' - 2N^2 - \mu^2)} \quad (\text{C.2})$$

It can be shown from crossing that the two terms in (C.2) produce singularities which lie symmetrically about the origin in the  $y$ -plane. Singularities arise when the spectral functions are non-zero and the denominators vanish; let  $s_{bc}(t)$  be the smallest value of  $s$  for which this happens. Then the corresponding singularities in the  $y$ -plane from the two terms of  $H_3^{(j)}$  are

$$y(t, s_{bc}) = \pm i \frac{2\sqrt{t} \left( s_{bc}(t) + \frac{1}{2}t - N^2 - \frac{1}{2}\mu^2 \right)}{(t - \mu^2)(4N^2 - t)^{3/2}} \quad (C.3)$$

These singularities limit the size of the ellipse in which a Legendre polynomial expansion is valid (Figure 24).

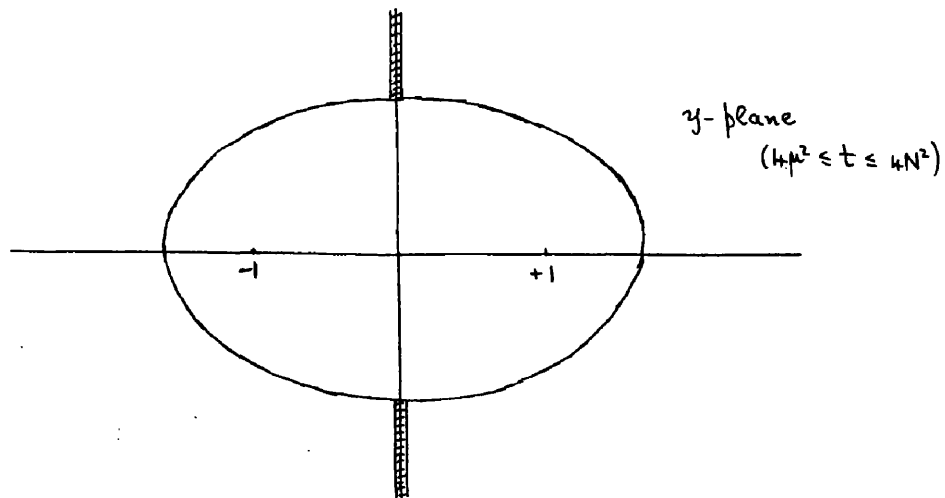


Figure 24.

To find an approximate solution, let us take the ellipse as an infinite strip<sup>41)</sup>. Thus the condition that  $\gamma$  lies within the strip is

$$|\operatorname{Im} \gamma| \leq \frac{2\sqrt{t} \left( S_{B,c}(t) + \frac{1}{2}t - N^2 - \frac{1}{2}\mu^2 \right)}{(t - \mu^2)(4N^2 - t)^{1/2}},$$

and from (C.1), this becomes

$$\left| \operatorname{Re}(s) + \frac{1}{2}t - N^2 - \frac{1}{2}\mu^2 \right| \leq S_{B,c}(t) + \frac{1}{2}t - N^2 - \frac{1}{2}\mu^2. \quad (\text{C.4})$$

Now let us take  $s$  complex and on the  $\gamma\pi$  cut; it is approximately of the form  $s \approx N^2 e^{i\phi}$ . Thus the condition (C.4) reduces to

$$\sin^2 \phi/2 \leq \frac{1}{2N^2} \left( S_{B,c}(t) + t - N^2 - \mu^2 \right). \quad (\text{C.5})$$

The minimum of  $(S_{B,c}(t) + t)$  can be determined from the boundaries of the spectral functions as drawn by Ball, and it is found to be  $\approx 96.3 \mu^2$  at  $t \approx 12\mu^2$ . Hence we deduce from (C.5) that a Legendre polynomial expansion is valid on the  $\gamma\pi$  cut for  $|\phi| \lesssim 90^\circ$ .

Similar investigations can be made for the negative real axis part of the  $\gamma\pi$  cut, and also for the crossed photoproduction cut.

## REFERENCES

- 1) H. Yukawa, Proc. Phys.-Math. Soc. Japan, 17, 48 (1935)
- 2) See "Quantum Electrodynamics" (Dover), ed. by  
J. Schwinger.
- 3) J.M. Jauch and F. Rohrlich "The Theory of Photons and  
Electrons".
- 4) G.F. Chew and F.E. Low Phys. Rev. 101, 1570 and 1579  
(1956)
- 5) R. Kronig J. Opt. Soc. Ann. 12, 547 (1926)
- 6) H.A. Kramers Atti Congr. intern. fis., como, 2, 543  
(1927)
- 7) R. Kronig Physica 12, 543 (1946)
- 8) N.G. Van Kampen Phys. Rev. 89, 1072 (1953), Phys. Rev.  
91, 1267 (1953).
- 9) F. Rohrlich and R.L. Gluckstern Phys. Rev. 86, 1 (1952)
- 10) M. Gell-Mann, M.L. Goldberger and W. Thirring, Phys.  
Rev. 95, 1612 (1954)
- 11) M.L. Goldberger Phys. Rev. 99, 979 (1955)
- 12) H. Lehmann, K. Symanzik and W. Zimmermann, Nuovo Cim.  
1, 205 (1955)
- 13) H.L. Anderson, W.C. Davidson and U.F. Kruse Phys. Rev.  
100, 339 (1955).
- 14) V. Haber-Schaim Phys. Rev. 104, 1113 (1956)

- 15) A. Salam Nuovo Cim. 2, 424 (1956)  
A. Salam and W. Gilbert Nuovo Cim. 2, 607 (1956).  
J.C. Polkinghorne Nuovo Cim. 4, 216 (1956)
- 16) G.F. Chew, M.L. Goldberger, F.E. Low and Y. Nambu  
Phys. Rev. 106, 1337 (1957).
- 17) G.F. Chew, M.L. Goldberger, F.E. Low and Y. Nambu  
Phys. Rev. 106, 1345 (1957).
- 18) M.L. Goldberger, Y. Nambu and R. Oehme Ann. Phys.  
2, 226 (1957)
- 19) G.F. Chew, R. Karplus, S. Gasiorowicz and  
F. Zachariasen Phys. Rev. 110, 265 (1958)  
P. Federbush, M.L. Goldberger and S.B. Treiman  
Phys. Rev. 112, 642 (1958).
- 20) P.J. Matthews and A. Salam Phys. Rev. 110, 565 (1958)
- 21) E. Corinaidesi Nuovo Cim. 4, 1605 (1956).  
N.N. Bogoliubov and A.A. Logunov Nucl. Phys. 5, 383  
(1957)  
M.L. Goldberger and S.B. Treiman Phys. Rev. 110, 1178  
(1958), Phys. Rev. 111, 354 (1958).  
Nuovo Cim. 2, 451 (1958).
- 22) N.N. Khuri Phys. Rev. 107, 1148 (1957).  
A. Klein and C. Zemach Ann. Phys. 7, 440 (1959)
- 23) G.F. Chew Phys. Rev. 112, 1380 (1958).

- 24) P. Cziffra and H. Moravcsik U.C.R.L. 8707 (1959).
- 25) J.G. Taylor, H. Moravcsik and J. Uretsky Phys. Rev. 111, 689 (1959).
- 26) K. Symanzik Phys. Rev. 105, 743 (1957).
- 27) N.N. Bogoliubov, D.M. Medvedev and M.K. Polivanov  
"Problems of the Theory of Dispersion Relations"
- 28) H. Drehermann, R. Oehme and J.G. Taylor Phys. Rev. 109, 2178 (1958)
- 29) H. Lehmann Nuovo Cim. Suppl. 14 177 (1959)
- 30) F.J. Dyson Phys. Rev. 110, 1460 (1958).
- 31) S. Mandelstam Phys. Rev. 112, 1344 (1958); Phys. Rev. 115, 1741 and 1752 (1959).
- 32) G.F. Chew U.C.R.L. 9289.
- 33) G.F. Chew and S. Mandelstam Phys. Rev. 119, 467 (1960).
- 34) G.F. Chew, S. Mandelstam and H.P. Noyes Phys. Rev. 119, 478 (1960).
- 35) M. Cini and S. Fubini Ann Phys. 10, 352 (1960).
- 36) J.W. Moffat Phys. Rev. 121, 926 (1961).  
D.H. Bransden and J.W. Moffat Phys. Rev. Lett. 6,  
708 (1961), Nuovo Cim. 21, 505 (1961).
- 37) G.F. Chew U.C.R.L. 9701.
- 38) G.F. Chew and S.C. Fratschi Phys. Rev. 123, 1478 (1961)

- 39) W.R. Frazer and J.R. Fulco Phys. Rev. 117, 1603 (1960)  
Phys. Rev. Lett. 2, 365 (1959), Phys. Rev.  
117, 1609 (1960).
- 40) W.R. Frazer and J.R. Fulco Phys. Rev. 119, 1420 (1960)
- 41) S.C. Frautschi and J.D. Walecka Phys. Rev. 120,  
1486 (1960).
- 42) H.S. Wong U.C.R.L. 9251.
- 43) J.S. Ball U.C.R.L. 9172.
- 44) J. Dowcock, W.N. Cottingham and D. Lurie Nuovo Cim.  
16, 918 (1960), Nuovo Cim. 19, 142 (1960).  
Phys. Rev. Lett. 5, 386 (1960).  
D. Amati, E. Leader and B. Vitale Nuovo Cim. 17, 68  
(1960), Nuovo Cim. 18, 409 (1960), Nuovo Cim.  
18, 458 (1960).  
M. Gourdin, D. Lurie and A. Martin, Nuovo Cim. 18,  
933 (1960).  
M. Gourdin and A. Martin Nuovo Cim. 16 78 (1960),  
Nuovo Cim. 17, 224 (1960).
- 45) E. Pickup, D.K. Robinson and E.O. Salant Phys Rev.  
Lett. 5, 192 (1961).
- 46) S.W. MacDowell Phys. Rev. 116, 774 (1959).  
F. Ferrari, G. Frye and M. Pusterla Phys. Rev. 123,  
308 and 315 (1961).  
R.G. Moorhouse Nuovo Cim. 20, 123 (1961).

- 47) J. Dowcock and A. Martin Nuovo Cim. 14, 516 (1959).  
R. Blankenbecler, M.L. Goldberger, N.N. Khuri and  
S.B. Treiman Ann Phys. 10, 62 (1960).
- 48) R. Karplus, C.N. Sommerfield and E.H. Wichmann  
Phys. Rev. 111, 1187 (1958); Phys. Rev. 114  
376 (1959).
- 49) J. Tarski J. Math. Phys. 1, 149 (1960).
- 50) R.J. Eden Phys. Rev. 119, 1763 (1960); Phys. Rev.  
121, 1567 (1961).
- 51). P.V. Landshoff, J.C. Polkinghorne and J.C. Taylor  
Nuovo Cim. 19, 939 (1961).  
R.J. Eden, P.V. Landshoff, J.C. Polkinghorne and  
J.C. Taylor Phys. Rev. 122, 307 (1961).
- 52) L.D. Landau Kiev Conference (1959).
- 53) See, for example, Rochester Conference Report (1960).
- 54) S.J. Lindenbaum and R.H. Sternheimer Phys. Rev. 109,  
1723 (1958).  
R.F. Peierls Phys. Rev. 118, 325 (1960); Phys. Rev.  
Lett 5, 166 (1960).
- 55) J.D. Bjorken Phys. Rev. Lett. 4, 473 (1960).
- 56) J. Hamilton and T.D. Spearman Ann Phys. 12, 172 (1961)
- 57) W.D. Walker, W.D. Shephard and J. Davis Phys. Rev.  
118 1612 (1960).

- 58) W. Rarita and J. Schwinger Phys. Rev. 60, 61 (1941).
- 59) S. Kusaka Phys. Rev. 60, 61 (1941).
- 60) See J.M. Blatt and V. Weisskopf "Theoretical Nuclear  
Physics".
- 61). A.W. Hendry Nuovo Cim. (to be published)
- 62) Y. Fujii Progr. Theor. Phys. 24, 1013 (1960).
- 63) R.J. Eden Proc. Roy. Soc. A210, 388 (1952).  
J.C. Polkinghorne and G.R. Screation Nuovo Cim. 15,  
289 (1960).
- 64) J.C. Polkinghorne (private communication). The  
author would like to thank Dr. Polkinghorne  
for pointing this out, and also for  
enlightening correspondence.
- 65) P.V. Landshoff and S.B. Treiman Nuovo Cim. 19, 1249  
(1961).
- 66) M. Fowler, P.V. Landshoff and R.W. Lardner Nuovo Cim.  
17, 956 (1960).
- 67) J.G. Taylor and A.E.A. Warburton Phys. Rev. 120,  
1506 (1960).